Titre: Title:	Controlled drug release from porous co-continuous polymer blends
Auteur: Author:	Zhenyu Xiang
Date:	2008
Type:	Mémoire ou thèse / Dissertation or Thesis
Référence: Citation:	Xiang, Z. (2008). Controlled drug release from porous co-continuous polymer blends [Mémoire de maîtrise, École Polytechnique de Montréal]. PolyPublie. https://publications.polymtl.ca/8237/

UNIVERSITÉ DE MONTRÉAL

CONTROLLED DRUG RELEASE FROM POROUS CO-CONTINUOUS POLYMER BLENDS

ZHENYU XIANG

DÉPARTMENT DE GÉNIE CHIMIQUE

ÉCOLE POLYTECHNIQUE DE MONTRÉAL

MÉMOIRE PRÉSENTÉ EN VUE DE L'OBTENTION

DE DIPLÔME DE MAÎTRISE ÈS SCIENCES APPLIQUÉES

(GÉNIE CHIMIQUE)

NOVEMBRE 2008

Your file Votre référence
ISBN: 978-0-494-48939-0
Our file Notre référence
ISBN: 978-0-494-48939-0

UNIVERSITÉ DE MONTRÉAL

ÉCOLE POLYTECHNIQUE DE MONTRÉAL

Ce mémoire intitulé :

CONTROLLED DRUG RELEASE FROM POROUS CO-CONTINUOUS POLYMER BLENDS

présenté par : ZHENYU Xiang

en vue de l'obtention du diplôme de : Maîtrise ès sciences appliquées

a été dûment accepté par le jury d'examen constitué de :

Mme HOEMANN Caroline, Ph.D., président

M. FAVIS Basil, Ph.D., membre et directeur de recherche

M. BUREAU Martin, Ph.D., membre

ACKNOWLEDGEMENTS

I would like to give my great thanks to my academic supervisor, Prof. Basil. D. Favis, who has created a scientific and amiable laboratory environment for all his students. I wish to thank Prof. Favis for his genius advices and directions on my research as well as the financial support for completion of this degree.

Dr. Pierre Sarazin has given me tremendous help in my research. I wish to give him many thanks for continuous help and valuable advice on my work, and being a great friend in the lab.

Thanks my jury members, Prof. Coroline Hoemann and Dr. Martin Bureau for sharing their wisdom and giving advices during my preparation of this thesis.

Special thanks to Dr. Mike Bushmann for offering equipments in his lab.

Mrs. Suzie Poulin, Mrs. Julie Tremblay and Mr. Eric from Department of Physics and Department of Biomedical Engineering, have helped in the training and arrangements of XPS, UV spectrometer and SEM. Without their help, this project won't be able to finish on time.

And plus the technicians in Department of Chemical Engineering: Carol Panchaud, Daniel Dumas, Gino Robin, Jacque Beausoleil, Jean Huard, Martine Lamarche, Melina Hamdine and Robert Delisle, thanks for all the help and conveniences you offered me in my work.

I would also send my sincere thanks to the fellow students who have graduated or are still pursuing their degrees. I wish I could list all the helps and friendship I enjoyed in

my two years here. However, it could be such a long list, which itself would be a chapter in this thesis. They not only help me on my research, but also offer great friendship which means a lot to me these days. If I list all of their names, two pages may not be enough here. What I remember is that with their friendship and support, I have a wonderful time while I am far away from my home country.

At last, but for sure not the least, I would like to give my special thanks to my families and relatives, who are very understanding and supportive in my study aboard in this country, and help me see this world differently, encourage me to face difficulties and most importantly, cherish and enjoy life. I am very thankful and feel myself lucky enough to have you all in my life.

RÉSUMÉ

La libération de médicaments consiste à administrer un composé pharmaceutique dans un corps vivant pour obtenir un effet thérapeutique. La livraison de médicaments contrôlée, qui atteint le même effet d'une façon contrôlée, est devenue très prometteuse dans de nombreuses disciplines. Comparé au système thérapeutique conventionnel, un système de livraison contrôlée de médicaments offre de nombreux avantages, tels que la livraison ciblée du médicament, une concentration constante du médicament, moins d'effets secondaires, moins d'administrations répétées du médicament, une efficacité améliorée de celui-ci et un meilleur confort pour le patient. L'objectif final de la livraison contrôlée de médicament (controlled drug release) est de libérer les substances thérapeutiques d'une façon contrôlable, permettant ainsi une livraison continue sur une longue période.

Les matériaux polymères poreux sont largement étudiés dans divers domaines et on les retrouve aussi dans les applications biomédicales. Ils peuvent être utilisés comme échafaudages dans le domaine du génie tissulaire, et aussi comme substrat pour des dispositifs pour la libération de médicaments. Différentes techniques de fabrication permettent de préparer ces matériaux poreux, dont le volume de porosité, les dimensions et la distribution des pores sont ajustés pour l'application visée. Les mélanges de polymères dont les phases sont co-continues se sont avérés être une méthode reproductible pour concevoir des structures polymères poreuses adaptées pour la livraison de médicaments. Cette technique offre un large contrôle des

caractéristiques du matériau poreux telles que la fraction volumique de pores et la taille de pore.

L'objectif de ce projet était d'améliorer les propriétés de livraison contrôlée d'une structure poreuse dérivé d'une mélange de polymère co-continue.

Ce travail a démontré qu'il était possible de mieux contrôler la libération instantanée initiale et d'accroître la durée totale de livraison de la BSA.

Deux stratégies ont été utilisées: la déposition à la surface interne de polyélectrolytes couche par couche et la fermeture partielle de la porosité à la surface externe de la structure. Un substrat poreux de polylactide (PLA) ayant une taille de pore moyenne de 1.5 μm, a été utilisé comme dispositif de livraison d'une substance modèle. Ce substrat a été obtenu par l'extraction sélective de la phase PS d'un mélange PLA/PS dont les phases étaient co-continues. L'aire de surface interne et les dimensions des pores ont été déterminées par la méthode BET d'adsorption d'azote et par analyse d'image. L'albumine de sérum bovin (BSA) a été sélectionnée comme substance modèle pour l'étude de la libération contrôlée. La protéine a été chargée dans les substrats poreux en suivant un protocole de cycles haute pression/vide. Il a été montré que la solution de BSA pénétrait dans tous les pores du substrat. Les substrats poreux de PLA avec 0, 3 et 5 couches de polyélectrolytes et avec une surface externe ouverte à 100, 12 et 2% ont été étudiés séparément et en combinant les deux types de modifications. Des essais de libération in vitro ont permis de déterminer le profil de livraison de l'albumine de sérum bovin (BSA) via la spectrophotométrie UV. Il a été

démontré que, bien que les deux effets soient importants, la modification de la surface interne prédomine dans le contrôle du taux de libération. Quand la modification avec 5 couches de polyélectrolytes est combinée avec une surface ouverte externe du substrat de 2% (échantillon L5C), la synergie est dramatique, présentant alors une libération instantanée initiale 5 fois plus faible pour les deux premières heures et une livraison totale 123 fois plus longue que celle obtenue avec l'échantillon de référence (100% d'ouverture externe, surface interne non modifiée). À la fin de l'essai, l'échantillon L5C a libéré 89% de la masse totale de BSA chargée, indiquant un haut niveau d'interconnectivité des micro-canaux dans le PLA poreux. Le mécanisme de livraison pour ce système est clairement contrôlé par la diffusion, avec des gradients de concentration bien définis, tels que mesurés par XPS, suivant la direction de la libération et cela, aussi bien pour l'échantillon ayant sa surface externe 100% ouverte et a surface interne modifiée (L0) que pour l'échantillon ayant uniquement une extrémité ouverte (L5E). Ces effets indiquent un mécanisme de diffusion combiné avec une interaction sorption/désorption de la BSA avec le substrat de PLA.

ABSTRACT

Drug delivery refers to the administration of a pharmaceutical compound into a living body to achieve a therapeutic effect. Controlled drug delivery, which achieves the same effect in a controlled fashion, has raised significant interest from multiple disciplines. Compared to a conventional therapeutic system, a controlled drug release system offers many advantages, such as stabilized plasma drug concentration, fewer side effects, less repeat drug administrations, improved drug efficacy and patient compliance. The ultimate goal of controlled drug release is to release therapeutic agents in a controllable manner, achieving sustained release over an extended time period.

Porous polymer materials are widely used in various fields including biomedical applications. They can be used as scaffolds for tissue engineering, and also as a substrate for drug delivery devices. Different fabrication techniques have been used to prepare porous polymer materials varying in porosity, pore-size and its distribution, which meet different requirements of various applications. Polymer blends with a co-continuous morphology via immiscible binary polymer blending has been shown to be a reproducible route to fabricate porous polymer materials for drug delivery. This technique offers wide control over the morphology of the porous material including porosity and pore-size.

The objective of this work is to improve the burst release and final drug release times from porous devices derived from co-continuous polymer blends.

This work has demonstrated that it is possible to exercise a wide range of control over both the initial burst release and the final drug release times from porous PLA devices derived from co-continuous polymer blends. Two strategies were used, a layer-by-layer polyelectrolyte surface deposition approach on the porous PLA surface and the application of a partially closed-cell protocol. A PLA porous substrate with a pore-size of 1.5 μm, derived from a PLA/PS blend via selective solvent extraction of PS phase, was used as the drug delivery device. The surface area and pore dimensions were examined via BET nitrogen adsorption and image analysis. Bovine serum albumin (BSA) was used as a model drug for the controlled drug release study. The protein is loaded into the porous substrates following a high-pressure-vacuum loading protocol. Studies of the accessibility of BSA solution to the micropores was carried out and showed a full solution penetration into the porous device. Porous PLA substrates with 0, 3 and 5 layers of polyelectrolyte and with open areas of 100%, 12 % and 2% were studied both separately and in combination. In vitro release tests were performed to study the release profile of BSA from the devices via UV spectrophotometry. It is shown that, while both are important, surface modification is more dominant in controlling the release rate than the partially closed cell approach. When a 5 polyelectrolyte layer surface modification of the PLA and a partially closed cell approach (2 % open area) are combined, in the L5C sample, the synergy is dramatic with a 5 times reduction in the first two hour burst release amount and a total release time which is extended by 123 times as compared to the

100% open cell, surface unmodified, reference sample. The L5C sample ultimately releases 89% of the total BSA loaded demonstrating the high level of interconnectivity of the micro channels in the porous PLA. The mechanism of release in this system is clearly diffusion controlled with well defined concentration gradients, as measured by XPS, observed in the direction of release for both the 100% open cell system (L0) and the surface modified, partially closed sample with one end open (L5E). These effects point towards a diffusion mechanism combined with a sorption/desorption interaction of the BSA with the modified PLA surface.

CONDENSÉ EN FRANÇAIS

1. La livraison contrôlée de médicaments

La livraison contrôlée de médicaments s'est rapidement développée dans les dernières décennies. Ce nouveau centre d'intérêt implique les technologies de multiples disciplines telles que la biologie, la chimie, la science des matériaux et le génie chimique.

Les médicaments les plus avancés impliquent des protéines et des gènes qui requièrent une administration efficace et une libération contrôlable afin que le patient en bénéficie pleinement. La prise conventionnelle de médicaments fait face à de nombreux défis, tel qu'un effet moindre lorsque le médicament est dégradé ou désactivé dans l'environnement gastro-intestinal. Elle doit être plus fréquente et cause inévitablement des fluctuations de concentration du médicament dans le plasma sanguin tout en ne permettant pas de cibler le site d'activité du médicament, son taux de libération, une bioactivité spécifique et sa durée d'action. Les techniques de libération contrôlée ont pour objectif de résoudre un certain nombre de ces problèmes, en libérant et en maintenant les concentrations de médicament à un niveau thérapeutique actif, et d'ainsi améliorer l'efficacité du médicament et de réduire les effets secondaires toxiques. Comme le médicament est libéré avec une plus grande efficacité, il est possible de réduire la fréquence d'administration et aussi de minimiser l'inconfort du patient. À cette fin, les substances thérapeutiques

devraient être libérées de manière contrôlable, permettant une libération continue sur une longue période de temps. On trouve de tels systèmes de libérations contrôlés sous forme de microparticules, nanoparticules, hydrogels, implants, etc., qui peuvent être ingérés oralement, injectés par intraveineuse, inhalés ou agir au contact de la peau. La question clé est de concevoir un substrat ou échafaudage convenable, qui pourra efficacement agir avec les molécules thérapeutiques.

2. Les dispositifs poreux en polymère biodégradable

Les dispositifs polymères sont de bons candidats comme biomatériaux en raison de leurs propriétés physico-chimiques. Ils ont été fortement étudiés pour la libération contrôlée depuis les années 70. Bénéficiant de leurs excellentes propriétés mécaniques, ainsi que de leur biocompatibilité et leur biodégradabilité, ces polymères ont été appliqués comme sutures, implants et systèmes de libération de médicaments. Ces systèmes se décomposent généralement via une dégradation hydrolytique et l'érosion de la matrice polymère. Le taux de biodégradation ou de bioérosion dépend essentiellement de la structure, du poids moléculaire et de la cristallinité du polymère. Le taux de libération du médicament peut être contrôlé en agissant sur la diffusion de celui-ci à travers la matrice polymère et / ou en modifiant le comportement du polymère pour se dégrader. Les propriétés de biodégradation du matériau, son interaction avec les molécules actives et l'environnement spécifique déterminent le profil de libération pour le dispositif.

Le polylactide (PLA) est parmi les polymères biodégradables les plus intensivement étudiés. Les matériaux poreux métalliques et de polymères ont montré leur potentiel dans le développement de dispositifs biomédicaux. Les propriétés telles que le volume de porosité, la taille de pore et la distribution en taille de pore sont essentielles. Ces paramètres sont dépendants des matériaux et des techniques de fabrication et doivent être correspondre à l'application visée. Précédemment, il a été démontré que les structures poreuses issues de mélanges binaires de polymères immiscibles dont les phases sont co-continues présentaient des propriétés prometteuses comme systèmes de libération de médicaments. Deux polymères immiscibles sont mélangés à l'état fondu pour créer une morphologie entièrement co-continue. Ensuite, une structure ayant une porosité continue peut être obtenue par l'extraction sélective de l'une des phases polymères. Les propriétés du substrat poreux découlent de celles du mélange de polymères et ces dernières peuvent être contrôlées de manière précise via différents paramètres tels que la composition du mélange, la rhéologie des polymères et les conditions du procédé de mise en œuvre à l'état fondu.

Des dispositifs poreux obtenus via cette technique possèdent une aire de surface interne très grande et une taille de pore contrôlable.

L'hydrophobie du PLA peut constituée une limitation importante pour son application dans le domaine biomédical. C'est pourquoi plusieurs techniques de modifications de surface ont été étudiées pour résoudre cet inconvénient :

modifications de l'état physique, implantations ioniques, traitements plasma et auto-assemblages couche par couche (LbL). Parmi celles-ci, le dépôt couche-par-couche est très adapté pour la modification de la surface de matériaux tridimensionnels complexes, dont la surface est difficilement accessible par d'autres techniques.

L'objectif de ce projet est d'améliorer la libération instantanée initiale et la libération continue de médicaments dans des substrats poreux issus de mélanges de polymères co-continus. Nous avons appliqué deux stratégies : 1) le dépôt de polyélectrolytes couche-par-couche sur les surfaces internes de la structure poreuse; 2) la fermeture partielle des pores à la surface externe du substrat dans le but de diminuer la libération instantanée initiale et de prolonger la période de libération de la substance. L'influence de divers paramètres sur le profil de livraison ont été examinés, tels que le nombre de couches de polyélectrolytes et l'aire ouverte à la surface externe de la structure poreuse. La spectrométrie de photoélectrons X (XPS) a été utilisée pour étudier les mécanismes de livraison de notre substrat.

Le matériau polymère poreux utilisé dans cette étude a été obtenu à partir d'un mélange binaire de polymères présentant une morphologie co-continue, dont une phase était extraite. Des systèmes binaires spécifiques peuvent être choisis, caractérisés par des propriétés rhéologiques et des conditions de mise en oeuvre appropriées, telles que la température et la durée de recuit statique. Cette technique permet de fabriquer des matériaux poreux dont la taille de pore varie de moins d'un micron jusqu'à des centaines de microns.

Dans cette étude, le polylactide (PLA) et le polystyrène (PS) ont été choisis pour fabriquer le mélange. Ils ont été mélangés à une fraction volumique de 50% à 200°C pendant 7 minutes. Après refroidissement et séchage des cylindres ayant une longueur de 3.5-4.5 mm et un diamètre de 3 mm ont été découpés. La phase PS a été sélectivement extraite avec du cyclohexane. La continuité de la phase PS dans le mélange a été calculée par gravimétrie après l'extraction et le séchage, indiquant une continuité supérieure à 90%.

La morphologie de la structure poreuse a été examinée par microscopie électronique à balayage (SEM), par la méthode BET d'adsorption d'azote et l'analyse d'image (IA). Avant l'extraction au cyclohexane, les échantillons pour l'analyse microscopique ont été microtomés afin de préparer une surface plane quasi parfaite. Les micrographies du SEM ont été analysées (IA) pour obtenir la taille moyenne des pores. La méthode BET d'adsorption d'azote donne une mesure précise de l'aire de surface et du diamètre des pores pour un matériau poreux tridimensionnel. Les matériaux PLA poreux préparés possèdent un diamètre de pore de 1.5 μm et une aire de surface interne de 1.53 m^2/g.

L'albumine de sérum bovin (BSA) a été choisie comme substance modèle. La BSA a été chargée dans le dispositif poreux en suivant un protocole préétabli de haute pression – vide. Après le chargement, les échantillons étaient rincés dans de l'eau désionisé Milli-Q pour enlever la protéine liée sur la surface extérieure du dispositif avant le séchage sous vide. Comparée à d'autres techniques d'encapsulation de

médicaments, cette méthode introduit la substance pharmaceutique après la préparation du dispositif. Ainsi la substance ne subit pas les conditions du procédé de fabrication et sa bioactivité est préservée. Des études ont été effectuées pour examiner l'efficacité de chargement et la pénétration de la solution de BSA dans la structure poreuse. Dans les conditions du protocole de chargement, la solution de BSA peut pénétrer dans l'échantillon poreux et accéder à tous les micropores.

La spectroscopie UV-Visible a servi à suivre la libération in vitro de la BSA chargée dans nos dispositifs poreux. Le dispositif poreux chargé de BSA a été placé dans une cellule UV remplie de 3 ml d'eau désionisée Milli-Q, puis incubé à 37°C avec une agitation verticale de 5 tour/min pour assurer une distribution homogène de la BSA libérée à l'intérieur de la cellule UV. À chaque intervalle prédéterminé de temps, la concentration de BSA à l'intérieur de la cellule a été mesurée par le spectromètre et ainsi, la quantité cumulée de BSA libérée a été calculée à partir de la concentration en BSA et du volume d'eau résiduelle à l'intérieur de la cellule UV, en utilisant une courbe d'étalonnage du signal UV en fonction de la concentration de BSA. Pour le dispositif poreux non modifié, plus de 90% de la BSA a été libérée dans les deux premières heures, et a par la suite atteint un pourcentage cumulatif de libération de 97.3% BSA en quatre heures.

Afin de réduire cette libération initiale quasi instantanée et prolonger la durée de libération, le dépôt couche-par-couche de polyélectrolytes à la surface interne et la fermeture partielle de la surface externe du dispositif ont été effectués. Pour obtenir

une surface externe partiellement fermée, un substrat PLA poreux a été plongé très brièvement dans du chloroforme, un solvant du PLA, afin de fermer les pores de la surface externe en formant une peau. Ensuite, une partie de cette peau a été enlevée pour laisser apparaître la porosité. Sous cette peau, la structure poreuse originale est préservée. L'épaisseur de cette peau peut être contrôlée par la durée d'immersion du substrat dans le chloroforme. Dans notre étude, nous avons obtenu une peau de 70 ± 20 μm en 5 secondes. Cette stratégie a permis d'obtenir des échantillons dont 12% et 2% de la surface externe est ouverte (respectivement en découpant l'une des extrémités du cylindre, et en coupant un coin du cylindre). Comparé à l'échantillon 100% ouvert, ceux ouverts à 12% et 2% ont permis de réduire fortement la libération initiale par respectivement 38% et 52% et d'augmenter la durée nécessaire pour libérer totalement la BSA à 9 heures et 30 heures. La surface externe partiellement fermée contribue à la libération contrôlée en limitant la surface disponible pour la libération et en augmentant ainsi la tortuosité à travers le dispositif pour que la BSA diffuse à l'extérieur.

Le dépôt couche-par-couche est une technique utile pour modifier la surface des polymères, particulièrement dans un substrat poreux tridimensionnel. Le dépôt couche-par-couche de polyélectrolytes change les propriétés de la surface interne du substrat. Un polycation interagit plus fortement avec une BSA négativement chargée, par rapport à la surface non modifiée de PLA. Dans notre étude, 3 ou 5 couches de polyélectrolytes ont été déposées sur la surface interne. de polyélectrolyte ont été

déposés sur poreux, en suivant le même protocole de chargement que pour la BSA. Le PDADMAC et le PSS ont été choisis comme polyanion et polycation. Les 3 ou 5 couches – alternativement polyanion, polycation – ont permis de garder le PDADMAC comme dernière couche. Après ces dépôts, la BSA a été chargée sur la couche de PDADMAC. Le suivi de la libération de BSA in vitro révèle que les 3 et 5 couches de polyélectrolytes ont pu réduire la libération initiale respectivement de 51% et 65%, et d'allonger le durée de libération à 32 heures et 96 heures. Les couches de polyélectrolytes contribuent à la libération contrôlée en améliorant l'affinité de la surface de PLA pour la BSA.

En combinant ces deux stratégies, nous avons pu atteindre une durée totale de libération de 17 jours. Cette synergie est remarquable, avec une libération 5 fois plus faible de BSA au cours des deux premières heures et une durée totale de libération 123 fois plus longue que celle de l'échantillon de référence (porosité ouverte, pas de modification couche-par-couche). Bien que les deux stratégies soient intéressantes, l'effet de la modification de surface couche-par-couche est prépondérant. La spectroscopie de photoélectrons X a permis d'examiner la distribution de BSA à l'intérieur du dispositif poreux pour l'échantillon de référence et l'échantillon modifié avec 5 couches de polyélectrolytes avec seulement une extrémité du cylindre ouverte. Initialement, la BSA est distribuée de façon homogène dans l'échantillon de référence. Pour les deux échantillons, on constate que le mécanisme de livraison pour ce système est clairement contrôlé par la diffusion, avec des gradients de concentration

bien définis suivant la direction de la libération. Ces effets indiquent un mécanisme de diffusion combiné avec une interaction sorption/désorption de la BSA avec le substrat de PLA.

TABLE OF CONTENT

ACKNOWLEDGEMENTS IV

RÉSUMÉ VI

ABSTRACT IX

CONDENSÉ EN FRANÇAIS XII

TABLE OF CONTENT XXI

LIST OF FIGURES XXVII

LIST OF TABLES XXXI

LIST OF APPENDICES XXXI

LIST OF ABBREVIATIONS AND SYMBOLS XXXIII

CHAPTER 1_INTRODUCTION 1

1.1 Controlled Drug Release 1

1.2. Porous Devices Derived from Biodegradable Polymer 2

CHAPTER 2_LITERATURE REVIEW 6

2.1 Drug delivery 6

2.1.1 Introduction 6

2.1.2 Controlled Drug Delivery 6

2.1.4 Drug Release Mechanisms 9

2.1.4.1 Diffusion-controlled Drug Delivery System 9

2.1.4.2 Degradation-controlled Drug Delivery System 12

2.1.4.3 Swelling-controlled Drug Delivery System 13

2.2 Porous Device 16

2.2.1 Fiber Bonding 17

2.2.2 Solvent Casting and Particulate Leaching 18

2.2.3 Melt Molding 20

2.2.4 Gas Foaming 21

2.2.5 Electrospinning 22

2.2.6 Freeze Drying 23

2.3 Biodegradable Polymers 25

2.3.1 Introduction 25

2.3.2 PLA 26

2.3.3 PGA 29

2.3.4 PLGA 29

2.3.5 Degradation and Erosion Mechanism 32

2.3.5.1 Factors Influencing Degradation Rate 33

2.4 Co-continuous Morphology of Polymer Blends.....37

2.4.1 Co-continuous Morphology.....38

2.4.2 Morphology Control.....42

2.4.2.1 Influence of Volume Fraction on the Morphology.....43

2.4.2.2 Influence of Viscosity Ratio on the Morphology.....43

2.4.2.3 Influence of Interfacial Tension on the Morphology.....44

2.4.2.4 Influence of Processing Conditions on the Morphology.....46

2.5 Surface Modification of Polymer.....50

2.5.1 Introduction.....50

2.5.2 Layer-by-Layer (LbL) Electrostatic Self-Assembly (ESA).....51

CHAPTER 3 EXPERIMENTAL METHODOLOGY.....66

3.1 Materials.....67

3.3 Preparation and Characterization of Porous Device.....68

3.3.1 Solvent Extraction and Extent of Continuity.....68

3.3.2 Microtomy and Microscopy Surface Characterization.....69

3.3.3 Pore-size and Surface Area Determination via BET.....70

3.4 High Pressure-Vacuum Loading Apparatus and Loading Efficacy Calculation.....72

3.5 Modification of the Porous Devices 75

3.5.1 Layer-by-Layer Surface Deposition of Polyelectrolytes into Porous PLA 76

3.5.1.1 Preparation of Polyelectrolyte Solution.....77

3.5.2 Partially Closed-Cell Morphology 77

3.6 In Vitro BSA Release Test.....78

3.6.1 Preparation of Standard BSA Solutions 80

3.7 Protein Distribution Study.....84

CHAPTER 4 CONTROLLING BURST AND FINAL DRUG RELEASE TIMES FROM POROUS POLYLACTIDE DEVICES DERIVED FROM CO-CONTINUOUS POLYMER BLENDS 86

4.1 Article Presentation.....86

4.2 Controlling Burst and Final Drug Release Times from Porous Devices Derived from Co-continuous Polymer Blends 89

4.2.1 Abstract.....89

4.2.2 Introduction 90

4.2.3. Experiments 98

4.2.3.1 Materials 99

4.2.3.1 Blend Preparation 99

4.2.3.2 Solvent Extraction and Extent of Continuity 100

4.2.3.3 Microtomy and Microscopy Surface Characterization 101

4.2.3.4 Pore-size and Surface Area Determination via BET 101

4.2.3.5 High- Pressure Loading Apparatus 102

4.2.3.6 Layer-by-Layer Surface Deposition of Polyelectrolytes into Porous PLA 103

4.2.3.7 Close-cell and Partially Closed Morphology 105

4.2.3.8 In Vitro BSA Release Studies 106

4.2.3.9 Protein Distribution Study via X-ray Photoelectron Spectroscopy (XPS) 106

4.2.4 Results and Discussion 108

4.2.4.1 Porous Device Morphology 108

4.2.4.2 BSA Loading Effects 109

4.2.4.3 Surface Modification via Layer-by-layer Technique 111

4.2.4.4 Partially Closed-Cell Strategy 113

4.2.4.5 In-Vitro Release of BSA from Partially Closed Cell Porous Devices. 117

4.2.4.6 Combined Effect of PLA Surface Modification and a Partially-Closed Structure on Release 123

4.2.4.7 Study of Protein Distribution inside the Sample via XPS 130

4.2.4.8 Mechanism of Release 136

4.2.5. Conclusion 138

CHAPTER 5_GENERAL DISCUSSION AND CONCLUSIONS 140

5.1 General Discussion 140

5.1.1 Effect of Partially Closed-Cell Strategy on BSA Release Profile 140

5.1.2 Effect of LbL Surface Modifications on BSA Release Profile 141

5.1.3 Combined Effect of Two Modification Strategies 141

5.1.4 Release Mechanism Study 142

5.1.5 Future Work 142

5.2 Conclusions 147

REFERENCE 148

APPENDIX 173

LIST OF FIGURES

Figure 2.1 Controlled drug delivery and traditional drug delivery 7

Figure 2.2 Schematic illustration of the mechanism of drug release from diffusion-controlled drug delivery system 10

Figure 2.3 Schematic illustration of the mechanism of drug release from degradation-controlled drug delivery system..... 13

Figure 2.4 Schematic representation of the relationship between diffusion controlled, degradation controlled and swelling controlled biodegradable polymeric systems 14

Figure 2.5 Polymerization route to polylactide acid 27

Figure 2.6 Chemical structure of poly(lactic acid) (PLA) 28

Figure 2.7 Chemical structure of poly(glycolic acid) (PGA) 29

Figure 2.8 Synthesis and chemical structure of poly(lactic-co-glycolic acid)..... 30

Figure 2.9. Schematic representations of erosion mechanisms..... 33

Figure 2.10 Schematic representation of immiscible binary polymer blends..... 39

Figure 2.11 Schematic relationship between polymer volume fraction and continuity 40

Figure 2.12 Effect of annealing temperature on binary blends morphology (show the pore-size and distribution)..... 48

Figure 2.13 Effect of annealing time on binary blends morphology (show the

pore-size and distribution) 48

Figure 2.15 Schematic representation of aminolysis and layer-by-layer self-assembly process with oppositely charged polyelectrolytes on an aminolyzed PLLA membrane surface. 54

Figure 2.16 Advancing contact angle as a function of the layer number of PSS and chitosan. Odd numbers represent films with PSS as the outermost layer, whereas even number films have chitosan as the outermost layer.....55

Figure 2.17. SFM images (tapping mode) of the PLLA surface. 57

Figure 2.18 Schematic illustration of the modification of the PLLA substrates. 57

Figure 2.19 Water contact angles of the PLLA surfaces treated by PAH solution at different pH values (taken from Lin et al. 2006). 58

Figure 2.20 Water contact angles as a function of treatment time of the PLLA surfaces treated with PAH solution at pH=11.2. 59

Figure 2.21 Contact angles of the PAH/PSS multilayer assembly: layers of odd numbers have PAH as the outermost layer; layers of even numbers have PSS as the outermost layer (layer zero is the virgin PLLA).....59

Figure 2.22 Schematic representation of the first proposed buildup process of human serum albumin (HAS) layers on films terminating with poly(allylamine hydrochloride) (PAH). 63

Figure 2.23 Schematic representation of the second proposed model to explain the buildup process of thick HSA films on PEM terminating with PAH. 64

Figure 3.1 Experimental Summary 66

Figure 3.2 Schematic presentation of high-pressure-vacuum loading protocol..... 73

Figure 3.3 Porous sample inside test tube, with sample holder keeping its position..... 74

Figure 3.5 Calibration curve of BSA concentration in water, measured via UV at 280 nm 83

Figure 3.6 Arrangement of spots for XPS test, showing also the sample dimension..... 85

Figure 4.1 Experimental process 98

Figure 4.2 Mass of BSA loaded into samples with lengths from 2 to 6 mm. 109

Figure 4.3 Deposited polyelectrolyte mass as a function of the number of layers deposited by the LbL approach. 112

Figure 4.4 SEM images showing the porous PLA devices..... 114

Figure 4.5 SEM images showing porous PLA in closed-cell form 116

Figure 4.6 Effect of a partially closed-cell structure on the drug release for unmodified porous PLA samples 119

Figure 4.7 Relationship between open surface area and release profiles characteristics..... 122

Figure 4.8 Effect of number of polyelectrolyte layers on the drug release 123

Figure 4.9 Effect of a partially closed-cell structure (one-end open) on the drug release for modified porous PLA samples 126

Figure 4.10 Effect of a partially closed-cell structure (one-corner open) on the drug release for surface modified porous PLA samples 128

Figure 4.11 Effect of surface modification and partially closed-cell strategy 129

Figure 4.12 BSA distribution inside the unmodified porous template with open-cell 131

Figure 4.13 BSA distribution inside the one-end opened porous template with 5 layers of polyelectrolyte surface deposition 134

LIST OF TABLES

Table 3.1 Characteristic Properties of the Materials 67

Table 3.2 Preparation of BSA solutions of standard concentrations 82

Table 3.3 UV spectrophotometer readings for standard BSA solutions 83

Table 4.1 Characteristic Properties of the Materials 99

Table 4.2 BSA Release from PLA Substrates 118

Table B.1 Sample series 176

LIST OF APPENDICES

APPENDIX A LOADING BSA AND POLYELECTROLYTES INTO POROUS DEVICE 173

APPENDIX B SAMPLE SERIES 176

APPENDIX C EXPLANATION OF BURST RELEASE 177

LIST OF ABBREVIATIONS AND SYMBOLS

3-D	Three-dimensional	σ	Interfacial tension
$\Delta\pi$	Osmotic pressure difference	η	Viscosity
ΔG_{mix}	Gibbs free energy of mixing	k	Boltzmann constant
ΔH_{mix}	Enthalpy of mixing	LbL	Layer-by-layer
ΔP	Hydrostatic pressure difference	ρ	Density
ΔS_{mix}	Entropy of mixing	P	Pressure
AFM	Atomic force microscopy	PAH	Poly(allylamine hydrochloride)
APD	Atmospheric pressure discharges	PBS	Phosphate buffer solution
BET	Brunauer, Emmett, and Teller	PDADMAC	Poly(diallyldimethylammonium chloride)
BSA	Bovine serum albumin	PEG	Poly(ethylene glycolide)
c	Concentration	PEI	Poly(ethyleneimide)
CS	Chondroitin sulfate	PEO	Poly(ethylene-oxide)
φ	Volume fraction	PGA	Poly(glycolic acid)
ϵ	Permittivity	PLA	Poly(lactic acid)
ECM	Extracellular matrix	PLGA	Poly(lactic-co-glycolic acid)
ESA	Electrostatic self-assembly	PLLA	Poly(L-lactic acid)
FDA	Food and Drug Administration	PSS	Poly(sodium 4-styrenesulfonate)
FDM	Fused deposition modeling	$\dot{\gamma}$	Shear rate
GAG	Glycosaminoglycan	RF	Radio frequency
GI	Gastro intestine	SEB	Styrene-ethylene-butylenes
HDPE	High density polyethylene	SEBS	Styrene-ethylene-butylenes-styrene
IA	Image Analysis	SEM	Scanning electron Microscopy
IEP	Isoelectronic polint		

T_g	Glass transition temperature	UV	Ultra Violet
T_m	Melting temperature	XPS	X-ray photoelectron spectroscopy
L0	Samples with no PE layers and 100% open surface area	L0E	Samples with no PE layers and 12% open surface area
L0C	Samples with no PE layers and 2% open surface area	L3	Samples with 3 PE layers and 100% open surface area
L3E	Samples with 3 PE layers and 12% open surface area	L3C	Samples with 3 PE layers and 2% open surface area
L5	Samples with 5 PE layers and 100% open surface area	L5E	Samples with 5 PE layers and 12% open surface area
L5C	Samples with 5 PE layers and 2% open surface area		

CHAPTER 1

INTRODUCTION

1.1 Controlled Drug Release

Controlled drug release has developed rapidly in recent decades. It has become an area of interest, involving technology from multidisciplines including biology, chemistry, material science and chemical engineering.

Advanced drugs like proteins and genes require effective administration and controllable release to derive optimum benefits. Conventional drug administration faces many challenges such as huge drug loss due to the degradation and deactivation of drug molecules in the harsh environment of the gastrointestinal tract. It requires frequent administration of drugs and inevitably causes fluctuation of drug concentration in plasma as it does not allow for site specificity and control over release rate, drug bioactivity and its duration. The controlled drug release technique aims to solve the problems by protecting and transporting pharmaceutical agents to specific sites, local releasing and maintaining drug concentration at a therapeutic effective level, hence it can improve the drug efficacy, and reduce toxic side effects. As drugs are delivered with greater efficacy, it allows to reduce the administration frequency and minimize patients' discomfort. To achieve this, the pharmaceuticals should be released in a controllable fashion, which results in sustained release over

an extended time period. Controlled drug release systems are used in the form of microparticles, nanoparticles, hydrogel, implants, etc., and can be administrated via oral ingestion, intravenous injection, inhalation and transdermal route. A key issue in controlled drug release is to construct a suitable substrate or scaffold, which can effectively interact with drug molecules.

1.2. Porous Devices Derived from Biodegradable Polymer

Polymer devices designate to be good candidates as biomaterial due to their chemical and physical properties. They have been actively used for drug delivery ever since 1970s. Benefiting from their mechanical property, biocompatibility and biodegradability, biodegradable polymers become favorable in biomedical uses such as sutures, implants and drug delivery system. Many biodegradable polymers can degrade in vivo and without producing any harmful side-products. Many researchers have focused on its biomedical applications. Drug delivery systems derived from biodegradable polymer, in general, break down via the hydrolytic degradation and erosion of the polymer matrix. The biodegradation or bioerosion rate basically depends on the structure, molecular weight, and crystallinity of the polymer. The drug release rate can be controlled by manipulating its diffusion through the polymer matrix, and/or the degradation behaviors of the polymer. Biodegradation properties of the material, together with its interaction with drug molecules, and surrounding environment, determine the drug release profile from the device.

Poly(lactic acid) (PLA) is among the most extensively used biodegradable polymers, which can be metabolized by the body thus causes few side effect and require no retrieval of the device after administration.

Porous materials made of metals and polymers have shown their potential in developing biomedical devices. The properties such as porosity, pore-size and its distribution are essential to porous materials. These parameters depend on specific material and fabrication technique, and fit in the requirement from various applications. Porous substrates derived from immiscible binary polymer blends with co-continuous morphology were proved as a route to fabricate drug delivery and controlled release systems. Two immiscible polymers are blended to create fully co-continuous structure, and a highly interconnected porous structure can be obtained by selective extraction of one polymer phase. Properties of the porous substrates, which refer to the phase properties in the polymer blends, can be highly controlled via different parameters such as blends composition, polymer rheology property and processing conditions. Porous devices obtained via this technique possess large internal surface area and controllable pore-size, which is promising in drug delivery application.

The surface properties of PLA, such its poor hydrophilicity, can be a limitation for its biomedical application due to the consequent poor protein and cell attachments. Hence many surface modification techniques, have been employed to solve this problem, including physical entrapment, ion implantation, plasma treatment and

layer-by-layer (LbL) electrostatic self-assembly. Among these techniques, LbL best suits for surface modifications of polymer material with complex three dimensional structure, which is not easily accessible for other modification techniques.

The objective of this work was to fabricate scaffolds with a sustained drug release rate with possible elimination of bust release.

General objectives for this study:

1. To control burst and final drug release times from porous devices derived from co-continuous polymer blends
2. To investigate the mechanism of release from these systems

Specific objectives of this research:

1. To study the effect of partially closed-cell strategy with different open surface area available for drug release on the BSA release profile.
2. To study the effect of LbL surface modification strategy with different number of polyelectrolyte layers on the BSA release profile.
3. To study the combined effect of a closed-cell strategy and LbL surface modification on drug release
4. To investigate the protein distribution inside porous substrate and study the drug release mechanism using XPS.

This thesis is arranged into four chapters. The first chapter gives an introduction and background information referring to this work. It reviews the drug delivery technique and porous materials, describes candidate biopolymers and fabrication methods, and

discusses the possible routes to modify polymer surface and the protein adsorption onto solid surface. Chapter 2 presents the fabrication and characterization of the porous substrate, protein loading protocol, the modification of the porous device and the in vitro release test, as well as the study of protein distribution. The third chapter discusses about the drug release profile of all sample made, with/without surface modification. Finally chapter 4 gives a general conclusion of the work and shares some ideas for future work.

CHAPTER 2

LITERATURE REVIEW

2.1 Drug delivery

2.1.1 Introduction

Drug delivery is a common term that refers to the delivery of pharmaceutical compounds and drugs to a human or animal body. The delivery method by which a drug is administered inside the body has a significant effect on its efficacy. The goal of drug delivery systems is not only to deliver a drug into the body, but at the ideal local concentration with the minimum number of doses (Langer, 1990). This makes the successful delivery of therapeutic agents to the targeted tissue a crucial factor in effective treatment of most medical conditions. In the past two decades, controlled drug delivery systems as a novel route to deliver pharmaceutics with high efficiency, have attracted a lot of focus and attention.

2.1.2 Controlled Drug Delivery

Two of the most common drug delivery methods are oral administration and intravenous injection, which we call as conventional drug delivery. Drugs for conventional drug delivery normally appear as tablets for oral administration or

medication for intravenous injection. For both methods, the drug must overcome many factors in order to retain its efficacy.

Oral administration is painless and convenient while injection is painful and requires sterile needles and training. However, both methods suffer significant therapeutic limitations as both two drug delivery forms administer the entire dose of a drug in one shot, which results in a high or even toxic drug concentration in the plasma, which then falls down below its minimum therapeutic effective concentration, thus another dose is required. This is called, a sawtooth release profile, shown as a dashed line in Fig. 2.1 (adapted from Rhine et al. 1980; Santini et al. 2000; Edlund and Albertsson, 2002).

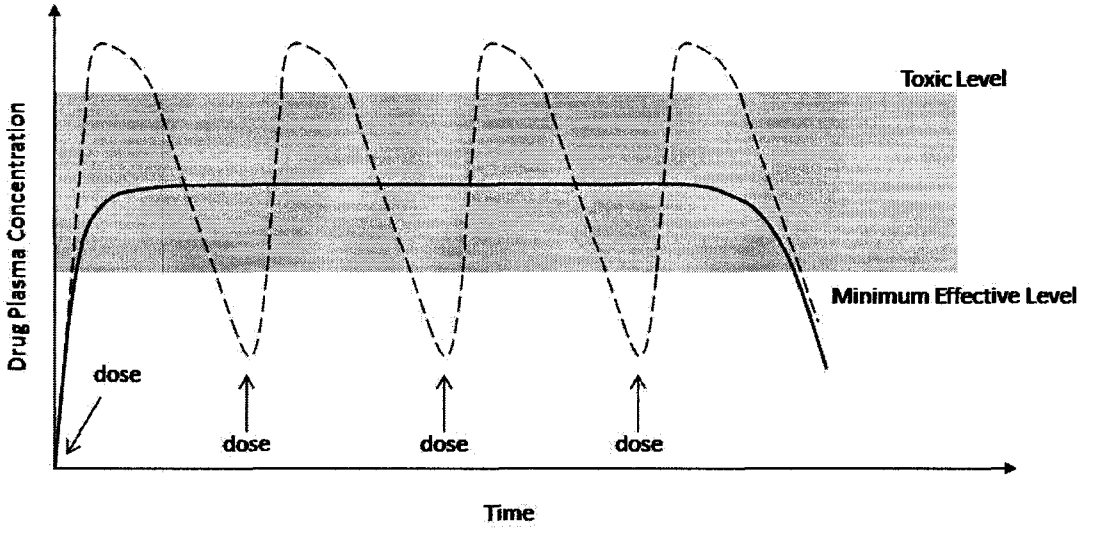

Figure 2.1 Controlled drug delivery and traditional drug delivery (adapted from Rhine et al. 1980; Santini et al. 2000; Edlund and Albertsson, 2002)

This figure shows the drug plasma concentration of controlled release (plot in solid

line, shows one administration), compared to traditional delivery (plot in dashed line, shows four repetitive administrations). Additional doses are necessary for traditional administration and the drug plasma concentration rises to the toxic level and falls below the minimum effective level during each cycle. While during the same period, controlled drug release, which indicates continuous drug release profile consistent with zero-order kinetics, maintains a constant therapeutic concentration in the plasma. Frequent repetitive administrations, daily or more often, have to be followed in order to maintain the drug concentration at the minimum therapeutic effective level, due to the high rate of metabolism and/or degradation of the drug in the body, which in return leads to strong fluctuation of the drug concentration in the body. This may cause undesirable side effects and decreases the effectiveness of the drug. In the case of drugs with low therapeutic indices, which indicate how close the levels of toxic and therapeutic drug levels are, such a sawtooth release profile become more problematic.

Compared to conventional drug delivery, controlled drug release aims to achieve a sustained release of pharmaceutics over an expanded time period, which results in a relatively constant drug concentration in plasma. Controlled drug delivery has several advantages over conventional delivery, including 1) improved drug efficacy; 2) minimization of harmful side effects; 3) maintenance of drug levels within a therapeutically effective range; and 4) lower administrations frequency resulting in improved patient compliance (Breimer, 2003).

In addition to the temporal control of the drug release, spatial control of highly potent drugs such as anticancer drugs, can localize the effect of the drugs only in the target area, while preventing any systemic side effects in the unwanted area. Such a technique targets drug molecules to specific tissues and therefore require lower systemic concentrations to achieve the required concentration in the diseased tissue. It helps to decrease the possibility of exposing healthy tissue to high drug concentrations, sometimes at levels toxic to healthy cells. As a comparison, conventional drug administration (e.g., oral, intravenous, intramuscular) cannot be controlled or targeted to body compartments where the drug is required (Kostarelos, 2003).

2.1.4 Drug Release Mechanisms

Controlled drug delivery system can be divided into different categories, based on their drug release mechanisms: diffusion-controlled drug delivery system, degradation-controlled drug delivery system and osmotic-controlled drug delivery system.

2.1.4.1 Diffusion-controlled Drug Delivery System

The diffusion mechanism has been employed for many controlled release devices. In the case of a diffusion control system, the drug can be surrounded by a polymer barrier (reservoir system) or it may be uniformly distributed throughout the polymer matrix (monolithic system). As shown in Figure 2.2, drug release is controlled by

transport of the drug through the polymer membrane or matrix with dissolution liquid, from where the drug is embedded (Alderborn, 2002; Langer and Peppas, 2003).

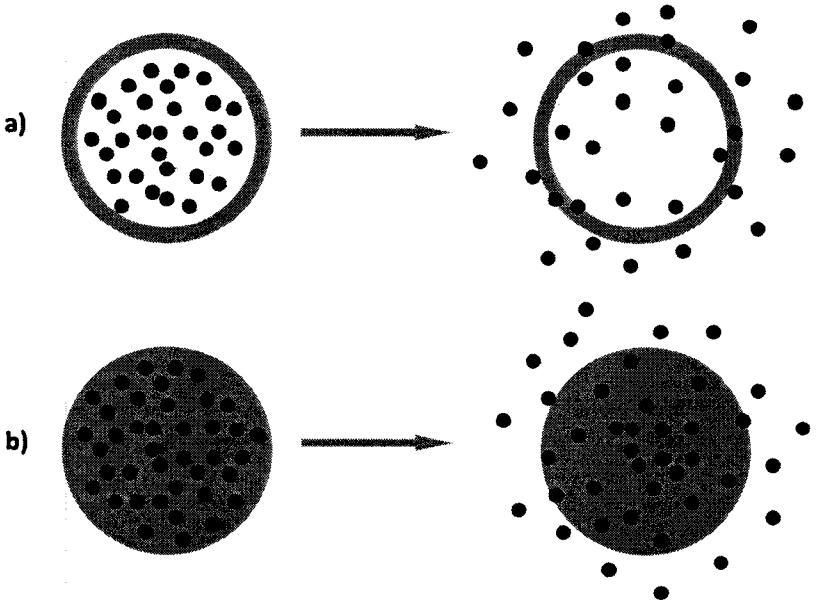

Figure 2.2 Schematic illustration of the mechanism of drug release from diffusion-controlled drug delivery system. a) and b) show reservoir system and monolithic system, respectively (adapted from Alderborn, 2002)

In general drugs in the diffusion controlled system are released in two steps: 1) diffusion medium diffuses into the system and dissolve the drug thus establish a concentration gradient of dissolved drug with higher drug concentration inside the drug delivery system; 2) the dissolved drugs diffuse out through the membrane or liquid filled pores following the concentration gradient. The drug release profiles can be obtained via solving Fick's second low of diffusion, giving appropriate boundary conditions:

$$\frac{\partial C}{\partial t} = \nabla \cdot (D\nabla C)$$

where C and D are drug concentration in the polymer and diffusion coefficient, respectively. The concentration gradient over the diffusion distance, the diffusion area, the diffusion distance and the diffusion coefficient of the drug in the diffusion medium, all play a role in determining the drug diffusion rate (Alderborn, 2002).

The reservoir system consists of a reservoir layer encapsulated by a non-degradable, hydrophobic layer. Its diffusion is controlled by how easily drug molecules can pass through the membrane. The diffusion kinetics is represented as the diffusion coefficient of a specific drug in a specific type of polymer membrane. Diffusion through the membrane can take place through liquid-liquid pores, or through the solid phase that forms the membrane. As the diffusion distance in this system remains constant, the drug release rate remains constant as long as a constant drug concentration gradient is maintained. The membrane based systems are limited to certain molecules and membrane materials. However, the pores of the typically used membranes are not big enough to allow transportation of large molecules such as proteins. Besides, hydrophobicity of the membrane material can also slow down the delivery rate.

In the other case, matrix types of delivery systems, with the same polymer as the ones used in the membrane system, are often used, where drugs are dissolved or dispersed uniformly throughout the entire volume of the matrix. When the matrix device is exposed to dissolution liquid, the dissolution liquid penetrates inside, the

solid drugs embedded are dissolved and then diffuse through the polymer network. The interface between dissolved and non-dissolved zones moves from the surface of the device into the center. At the dissolving interface the solubility concentration of the drug remains constant. Drug solubility in the polymer matrix, drug solubility in the dissolution liquid, porosity and tortuosity of the drug release system, can effectively affect the drug release profile. Typically, the cumulative release percentage of the drug from the matrix type device is proportional to the square root of time. (Paul and McSpadden, 1976)

2.1.4.2 Degradation-controlled Drug Delivery System

A degradation controlled drug delivery system involves chemical reactions leading to polymer degradation when the polymer comes in contact with the release medium or microorganisms. Then the drugs encapsulated inside the polymer matrix can be released readily with the degradation process, as shown in Figure 2.3. As drugs release from the degraded polymer matrix, they also diffuse out of the drug delivery system. Thus the release mechanism is not only controlled by the chemical degradation of the polymers, but also by the diffusion process (Shah et al. 1992).

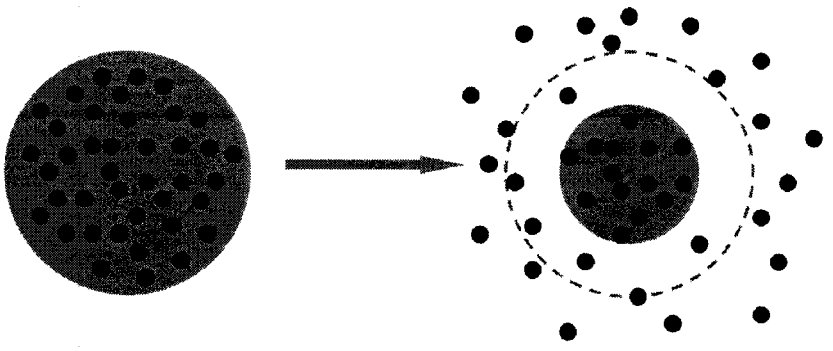

Figure 2.3 Schematic illustration of the mechanism of drug release from degradation-controlled drug delivery system (adapted from Alderborn, 2002).

The polymer degradation process can be modulated by the selection of polymer with certain structure and surface properties. PLA, PLGA, poly(anhydrides), poly(ortho esters), and poly(amino acids) are amongst the most commonly used polymers for the degradation based delivery systems. Depending on where the degradation occurs, from the surface inwards, or homogeneously throughout the polymer matrix, these polymers follow two degradation/erosion mechanisms, namely surface erosion and bulk erosion. As the most popular material, the PLGA degradation based delivery systems were developed in various forms: film, enveloped form, and particle form (Yolles and Sartori, 1980). For more information about biodegradation of the polymer, we discuss in details in the following section.

2.1.4.3 Swelling-controlled Drug Delivery System

When water penetrates into the matrix of a hydrophilic polymer, the matrix swells due to the disentanglement and dissolution of the polymer. This characteristic is also used in controlled drug delivery systems, as the drug diffusion coefficient in the swelled region is much higher than that in the unswelled glassy region. In this case, the drug release behavior is controlled by the polymer matrix relaxation and dissolution, combined with drug diffusion in the polymer matrix (Harland et al. 1988).

Besides all the mechanisms discussed above, mechanical energy and electrical

energy are also employed in limited cases as release energy (Heilmann, 1984). In fact, in most drug release systems, one or more drug release mechanism may take place at the same time. The drug release from a polymeric device is determined by the time scale of three processes: drug and water diffusivity, polymer swelling and polymer erosion (Gopferich, 1996).

The relationship between these three processes is shown schematically in Figure 2.4:

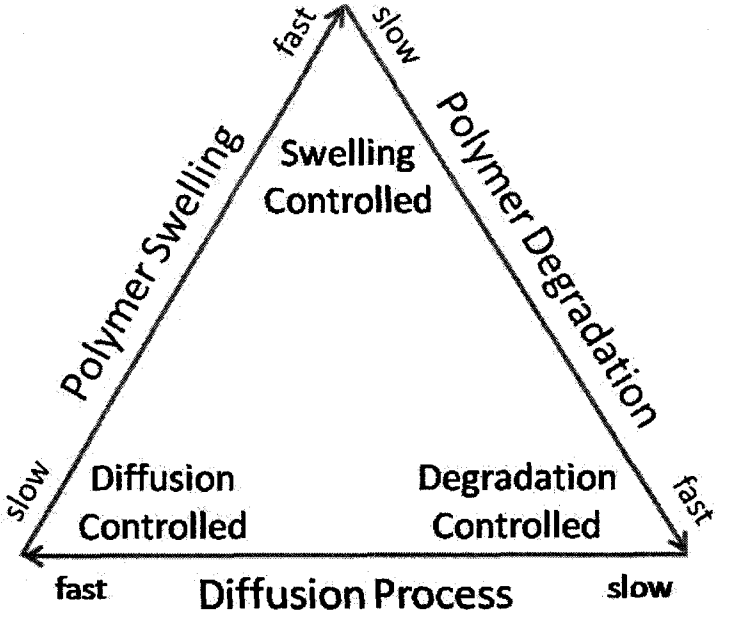

Figure 2.4 Schematic representation of the relationship between diffusion controlled, degradation controlled and swelling controlled biodegradable polymeric systems, (taken from Gopferich, 1996)

If erosion is slower than the diffusion process, the drug will be released by diffusion. If diffusion of water into the polymer is faster than degradation but slower than polymer relaxation, the drug release is controlled potentially by swelling. The drug

release is erosion controlled only if degradation is the fastest process. For many polymers, the three processes have similar rates and they all contribute to the drug release rate. The sequence of events, mechanism and time of degradation is highly dependent on the geometry of the degrading device.

Although different drug release mechanisms make it impossible to precisely predict the drug release fashion from certain drug delivery systems, yet there are several parameters that can affect drug release rate in general, including drug loading, device porosity and tortuosity, material intrinsic dissolution rate, etc.

2.2 Porous Device

The ideal scaffold should have a suitable pore size and high internal surface area for specific applications. It should also be suitable to incorporate bioactive molecules. In order to achieve this, many porous materials have been investigated and studied for controlled drug delivery, including silica, ceramic, and various polymer materials (Bryne et al. 2000; Grayson et al. 2003; Lai et al. 2003; Santiti et al. 1999; Slowing et al, 2007;). Most of these porous materials are used as reservoir devices, utilizing their void volume to house the therapeutics. The large surface area of porous material provides a convenient means by which enhanced drug loading and/or surface modification can take place to improve its properties. Here in this study we focus on the fabrication techniques for porous polymer materials.

One of the concerns of fabricating porous polymer materials is that the technique applied should prepare porous materials from various polymers while protecting the incorporated drugs or other bioactive molecules during the processing There are various established fabrication methods of porous polymer materials, including fiber bonding, solvent casting and particulate leaching, melt molding, gas foaming, electrospinning, freeze-drying, etc. as discussed below. The properties of the scaffold such as pore size, porosity, biocompatibility, drug release rate, degradation rate and mechanical strength are essential and they are all affected by the manner of fabrication. However, none of these techniques meets all the requirements imposed

above. Porous scaffolding techniques generally create either a completely random geometry or only spherical pores. Most techniques involve the application of harsh conditions such as heat and pressure to the polymer or dissolving it in an organic solvent to mold the material into its desired shape. The excessive use of organic solvents may impose possible toxicity due to residual solvents in the porous polymer. While each method presents distinct advantages and disadvantages, the appropriate technique must be selected to meet the requirement for specific application.

2.2.1 Fiber Bonding

In order to improve the mechanical properties of a single fiber and prepare porous scaffolds, fibers can be bound together at their intersections. This technique is called fiber bonding (Cima et al. 1991). In this procedure, two biocompatible polymers are used. Fibers of polymer I are arranged and bonded together at their contact points by melting. Prior to heat treatment, Polymer II, which has a higher melting temperature than Polymer I, is dissolved in an organic solvent (non-solvent for polymer I) and cast over the fibers and then dried under vacuum in order to remove the solvent. Polymer II casting is applied here to protect the fibers of Polymer I and prevent its structure from collapsing at elevated temperatures.

Heat treatment is applied to bond the fibers. The processing temperature falls between the melting temperature of Polymer I and II. After that, Polymer II is dissolved and removed from the fiber surface. The first example of this technique

was introduced by Mikos et al., who used PGA as Polymer I, PLLA as Polymer II and methylene chloride as a solvent of PLLA. Mooney et al. further developed this technique by applying rotational movement during the spraying and arrangement of the fibers, which contributed to decrease the randomness of the final products and narrow the pore size distribution.

This technique was the first technology that formed randomly connected fiber network structures. It is simple and easy to carry out. And the scaffolds made by this method have high area to volume ratio and high porosity, which is suitable to enhance cell attachment. However, this technique is limited to certain polymer and solvent systems and it can only prepare porous materials without any further control on the micro-structure that possesses acomplex three dimensional structure. And, as the diameter of the fibers cannot be adjusted during processing, the pore-size and porosity in the final product are uncontrollable.

2.2.2 Solvent Casting and Particulate Leaching

This technique improves the control over pore-size and scaffold porosity by choosing a porogen with desirable size.

The porogen (usually salt particles) is sieved to ensure a narrow size-distribution prior to following treatments. A biocompatible polymer is dissolved into a solvent (non-solvent of the porogen), and then the porogen is mixed with the solution containing polymer to give a good dispersion. The whole mixture (solution) is cast

into a container and the solvent is allowed to evaporate. The residues are removed by further vacuum drying and the polymer is solidified. This prepares a polymer composite with the porogen well dispersed inside the polymer matrix. A solvent of the porogen is used to dissolve and leach out the porogen from the composite. This solvent is usually water, which cannot dissolve polymer. After removing of the porogen, spare space is formed inside the polymer matrix, with the same size of the porogen.

This technique can prepare polymer porous materials with specific a pore-size, porosity and also surface-to-volume ratio, by choosing proper polymer-porogen-solvent combination and adjusting the fabrication parameters , the type, amount, and size of porogen. The pores inside the porous material can be isolated or interconnected, depending on the amount of the porogen, if well dispersed in the system. The first example was reported by Mikos et al. in 1994 using both PLLA and a PLGA polymer matrix with salt particles dispersed inside (Mikos et al. 1994). Other systems with different polymer matrix or porogens were also reported (Hacker et al. 2003; Holy et al. 1999).

Further development of this technique involves the control of the crystallinity of the polymer matrix by annealing the polymer matrix before particulate leaching. This technique is able to prepare highly interconnected porous materials with good control on the pore structure compared to previous ones. Plus, it requires a small amount of polymer to prepare porous materials. However, the incomplete leaching remains a

problem. Furthermore, the porous materials prepared by solvent casting are usually brittle which may limit their applications. Other polymers, including copolymer and polymer blends, can be introduced to solve this problem (Wake et al. 1996).

2.2.3 Melt Molding

This technique also requires the preparation of a polymer solution with porogen well dispersed inside as in the particulate leaching technique. However, instead of solvent evaporation right after the formation of the composite, the solution is poured into a mold with the required shape and the system is heated above the polymer melting temperature (T_m, for semicrystalline polymers) or glass transition temperature (T_g, for amorphous polymers), which allows the polymer chains to rearrange. After this, the composite is removed from the mold. It is cooled in an aqueous medium where the porogen can dissolve and leach out, thus forming the porous structure in the polymer matrix (Robert et al. 2000). In some cases, bioactive materials such as gelatin were used as porogen or part of the porogen, however, high processing temperature cause stability issues in these bioactive materials. This technique uses molds and porogens to create porous materials with complex three dimensional micro-structures. Compared to solvent casting, it provides more control of the final product via molding pressure and demolding techniques.

To improve the randomly shaped porous structures created by the method mentioned above, micro-molding techniques have been developed to allow a more precise

control over the micro-geometry in biodegradable polymers. Micro-molds were prepared by photolithography and etching techniques to give precisely defined structures. The geometrical patterns of the micro-molds were transferred to target polymers by various molding techniques. However, most of the micro-molding techniques are limited to the production of two-dimentional micro-geometries. Some other micro-molding techniques, such as 3-D printing, lamination of two-dimensional micro-patterned layers, and fused deposition modeling (FDM), were developed to from more precisely defined three-dimensional networks of micro-structures in tissue scaffolds (Kim, et al, 1998; Vozzi, et al. 2002; Zein, et al. 2002).

2.2.4 Gas Foaming

In this technique, polymer disks (PLGA, for example) are firstly formed by compression. After compression, the polymer disks are treated with high-pressure CO_2. The subsequent pressure decrease to ambient levels leads to the nucleation and formation of pores in the polymer matrix from the CO_2 gas (Mooney et al.1996b). Via controlling the maximum pressure loaded and the pressure reduction rate, this pore size can be controlled.

This technique is free of organic solvent in preparing the porous material and thus decreases the biocompatibility issue for the implants. However, there is an issue about the influence of high pressure on the structure and bioactivity of the bioactive agents incorporated in the system. And the porous material made using gas foaming

lacks mechanical properties because of the irregular pore structures inside the polymer matrix. Besides, the porous structure only exits inside the polymer bulk without opening to the surface, hence the materials need further fabrication. By incorporating another technique such as particulate leaching, this problem can be solved and it gives porous structure with pores opened to the material surface (Harris et al. 1998).

2.2.5 Electrospinning

Derived from the electrostatic spraying for polymer coating, the electrostatic fiber spinning, or electrospinning, finds its use in the preparation of polymer porous materials. In this technique the polymer dissolved in solution is forced through a charged metal capillary at a constant spraying rate. The electrostatic field between the capillary and the collecting plate helps to assemble the fine fibers on the plate where the solvent evaporates and form the porous material.

There are many parameters to control namely the pore size, porosity, and fiber thickness of the final products, including polymer-solvent combination, solution concentration, capillary diameter, ejection rate, electrostatic field voltage, distance between the capillary and the collecting plate, cooling temperature and even the material of the plate. Compared to fiber bonding, electrospinning puts few limitations on the polymer system and many biocompatible polymers can be used in this technique to prepare polymer porous materials (Yoshimoto et al. 2003). However,

due to its fiber nature, the final products still lack mechanical properties.

2.2.6 Freeze Drying

In this technique a desired polymer is dissolved in an organic solvent. Water is added to the solution and external forces are applied to emulsify the water, which is immiscible with the polymer solution, in the system. The emulsion is then poured into a metal container or mold and quenched in liquid nitrogen. After quenching, the polymer scaffold is freeze dried to remove water and solvent, thus a leaving porous structure inside the polymer matrix (Robert et al. 2000).

Highly interconnected porous scaffold structures can be obtained by this method. This technique can be applied to various biocompatible polymers including PLA, PGA and PLGA. By dissolving water-soluble drugs in the water phase during preparation, drugs can be incorporated into the porous materials fabricated, showing the potential of this technique in developing drug delivery systems (Hsu et al. 1997; Yannas et al. 1980). However, it can only prepare porous materials with limited pore sizes.

Other fabrication methods of porous polymer materials include phase separation, in situ polymerization, membrane lamination, etc. (Bryant and Anseth, 2001; Hua et al. 2002; Mooney et al. 1994).

In this group we have developed a novel fabrication method to prepare polymer porous material with highly controllable porosity and pore-size varying from

submicron dimensions to hundreds of microns. It can also be applied to most biocompatible polymers. This technique will be discussed in detail in the following section.

2.3 Biodegradable Polymers

2.3.1 Introduction

The material used for biomedical applications is a key issue in the development of novel medical treatments. Controlled drug delivery systems, which aim for the sustained release of a drug at a constant rate, are mostly fabricated using polymers with good biodegradability and biocompatibility. They are required to be non-toxic materials and offer easy control of the degradation behavior.

Biodegradability describes the controlled or predictable degradation of material in vivo. While some materials may be designed as a permanent implant, an optimal drug delivery system can degrade and dissolve inside the body, then be depleted by human body, requiring no retrieval of the device after the drugs has been released. This avoids surgical costs and improves patient compliance. In tissue engineering, the degradation rate of the scaffold can be adjusted to match the rate of tissue regeneration. In this case, new tissue formation can effectively replace the material.

A large number of biodegradable polymers provide promising results for biomedical applications. They were first approved for medical use by the FDA in the 1960s and have been extensively studied and used (Brannon-Peppas et al. 1997; Gilding and Reed, 1979; Middleton and Arthur. 1998; Uhrich et al. 1999). Since their successful development in 1970, synthetic biodegradable polymers have become popular materials in biomedical applications. The biodegradability of the materials, in

addition to their customized physical and chemical properties make them good candidates for implantable bio-medical devices. They have found use in different clinical applications in the form of implantable orthopedic devices (Middleton and Arthur, 2000) and controlled drug delivery systems (Chasin and Langer, 1990). Nowadays hetero chain polymers, which refer to polymers that have atoms other than carbon, such as oxygen and nitrogen, in their backbones, are widely applied. Polyesters including (lactide acid) (PLA), poly(glycolic acid) (PGA) and their copolymers (PLGA) are amongst the most widely-used, FDA approved, biodegradable polymers (Cam et al. 1996; Kulkarni et al, 1996).

2.3.2 PLA

Poly(lactic acid) or polylactide (PLA) is a biodegradable polyester than can be synthesized from natural sources such as starch. It has been reported that PLA is prepared via three methods: direct condensation/coupling of lactic acid, azeotropic dehydration condensation of lactic acid (as shown in Fig. 2.5) and ring opening polymerization of the cyclic lactide dimer, with the last one as the most general approach for production of high molecular weight PLA (Drumright et al. 2000).

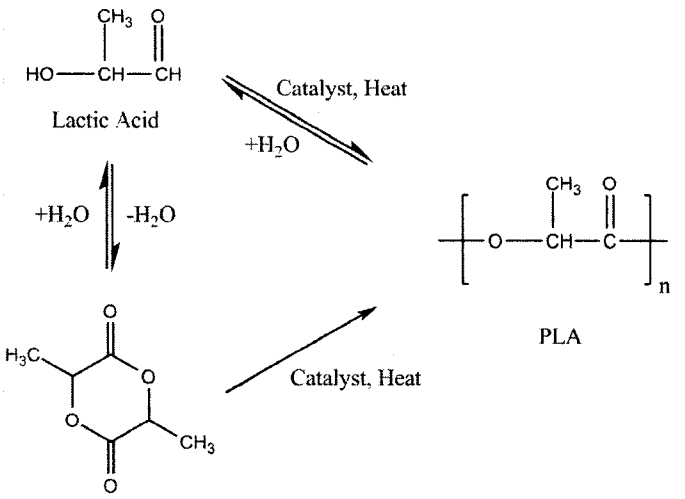

Figure 2.5 Polymerization route to polylactide acid

Lactic acid (2-hydroxypropionic acid, $CH_3CHOHCOOH$) is the simplest hydroxyl acid with an asymmetric carbon atom. Depending on the pendant methyl group in the molecule, there are in two optically active configurations of lactic acid isomer, the L(+) and D(-) isomers, and their blend DL isomer. After synthesis, these isomers form PLLA, PDLA and PDLLA, respectively. PLLA is a semi-crystalline, optically active stereoregular polymer and PDLA is an amorphous, optically inactive racemic polymer, while PDLLA is a blend of the two (Lewis, 1990).

In general, PLA is a semi-crystalline polymer. Its architecture and molecular weight determines its crystallinity, the mechanical properties and the processing temperature. The degradation behavior of PLA also depends on its crystallinity. PLLA shows higher crystallinity and due to the steric interactions between methyl groups and water molecules, PLA is more hydrolytically stable and has a slower degradation rate

as compared to PDLLA, typically requiring more than 2 years to be completely absorbed (Bersma et al. 1995; Middleton and Arthur, 1998). It has a melting point (T_m) of 175 °C and a glass transition temperature (T_g) of 65 °C. PLA shows high tensile strength, high modulus and low elongation (Garlotta, 2002). It is very soluble in organic solvents such as chloroform. Figure 2.6 shows the chemical structure of PLA. The high biocompatibility and non-toxic by-products of degradation present PLA as an ideal material for implantable drug delivery systems.

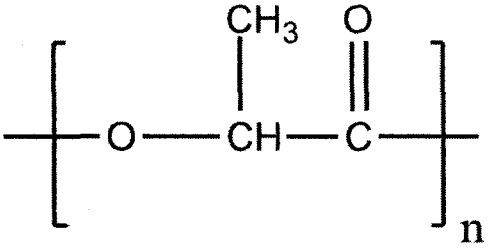

Figure 2.6 Chemical structure of poly(lactic acid) (PLA)

PLA can be processed by many industrial scalable processing techniques including molding, foaming and bleding. It is approved by the Food and Drug Administration for its intended use in fabricating articles used in food industry and biomedical application including drug delivery devices and hard tissue scaffolds. The most common use of PLA in drug delivery has been in the form of drug-loaded microspheres (Ehtezazi et al. 2000; Wagenaar and Muller, 1994).

2.3.3 PGA

PGA is also a crystalline biodegradable polymer. Figure 2.7 shows its chemical structure. Its crystallinity (reported in the range of 35-75%) is higher than PLA as it lacks the methyl side groups of PLA. High crystallinity leads to tight packing in PGA structure, giving PGA some specific physical and chemical properties such as its insolubility in most organic solvents.

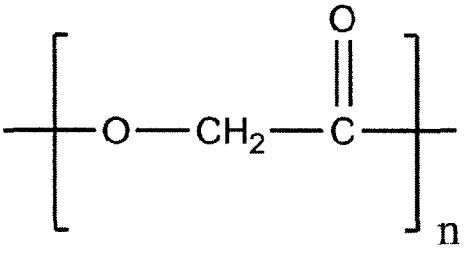

Figure 2.7 Chemical structure of poly(glycolic acid) (PGA)

2.3.4 PLGA

Blocks of PLA and PGA have been synthesized to form the linear amorphous biodegradable copolymer poly(lactide-co-glycolide) (PLGA). PLGA can be synthesized by random ring-opening copolymerization of these two different monomers. Figure 2.8 shows the synthesis and chemical structure of PLGA (taken from (Middleton et al. 2000).

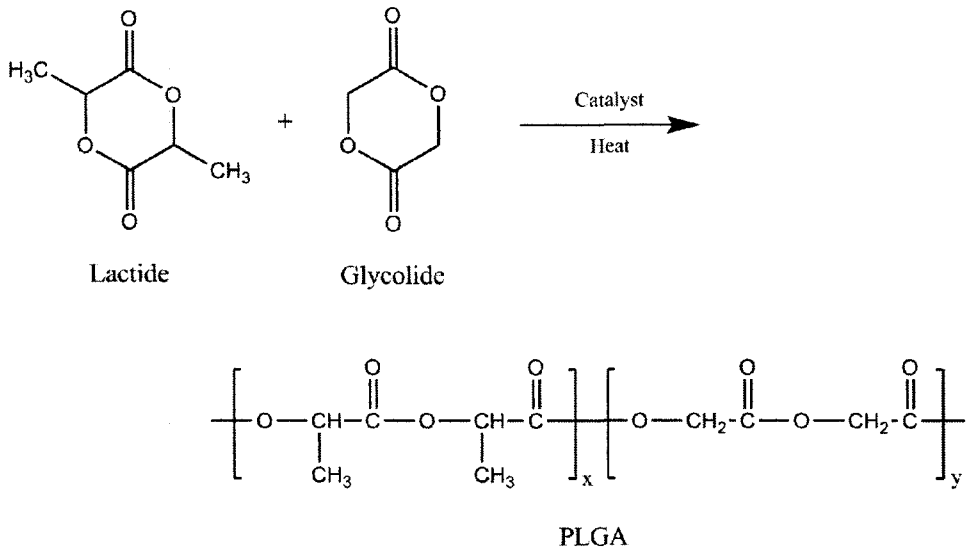

Figure 2.8 Synthesis and chemical structure of poly(lactic-co-glycolic acid)

The ratio of lactide and glycolide copolymers plays an important role in determining the properties of the final material. Its physical and chemical characteristics strongly depend on these two composites and their monomer ratio. For example, depending on the crystallinity of PLA composite, PLGA prepared from PLLA and PGA are crystalline copolymers, and those from P-D,L-LA and PGA are amorphous (Lewis, 1990).

Most forms of PLGA are amorphous in nature, and exhibit a glass transition temperature in the range of 45-60 °C. By increasing the glycolic acid percent in the copolymer and/or increasing molecular weight, the glass transition temperature (T_g) of PLGA increases correspondingly (Jamshidi, 1988).

Lactic acid is more hydrophobic than glycolic acid and hence PLGA with high

molecule percents of PLA is more hydrophobic, less crystalline and degrades slower than PLGA with more PGA blocks. The degradation rate of PLGA also depends on the PLA:PGA ratio and increases with an increase in the percentage of glycolide copolymer (Anderson et al. 1997). However, PLGA 50:50 is an exception to the rule and shows the fastest degradation rate (1-2 months) amongst all forms of PLGA, PLA and PGA.

As the degradation behavior of PLGA can be adjusted by the PLA:PGA ratio, the release of incorporated drug molecules can also be controlled. Besides its high biocompatibility and tunable physical properties, PLGA has been the most popular polymer used in resorbable implants and sutures, tissue engineering scaffolds and micro- and nanospheres for drug delivery and imaging (Kohn and Lenger, 1996; Kumar et al. 2001). The end products of PLGA degradation are lactic and glycolic acids, which are metabolized by the body. FDA-approved drug delivery devices using PLGA such as Nutropin Depot®, Trekstar Depot® and Zoladex®, has already been introduced into the market for treating cancer and hormone deficiencies.

2.3.5 Degradation and Erosion Mechanism

Polymer degradation refers to the chain scission process that breaks polymer chains down to oligomers and finally into monomers (Gopferich, 1996). The degradation of the polymer matrix can play a crucial role in the drug release profile.

Biodegradable polymers degrade either by the activity of biological agents such as enzymes, or by the hydrolytic cleavage in the backbone of the polymers, producing monomer and other low molecular weight degradation products. The most important mode of degradation for polymers used for drug delivery is chemical degradation, in which hydrolysable bonds between monomers are cleaved. The performance of hydrolyzable biodegradable polymers is primarily dependent on their erosion mechanisms (Gopferich, 1997).

Mechanisms for erosion have been proposed which mainly include surface or heterogenous erosion, and bulk or homogenous erosion (Gopferich, 1996). Both mechanisms cause material loss from the polymer bulk and in most cases both two mechanisms usually happen stimutaneously and compete with each other (Auras et al. 2004). Surface erosion occurs when the polymer degradation is faster than diffusion of water. In this case, the dimension of the polymer device gradually decreases during the degradation process. While bulk erosion occurs when the diffusion of water into the polymer is faster than degradation. In this case, the dimension of the polymer device remains constant even till the last stage of degradation. Enzymatic

degradation occurs only at the polymer surface, while non-enzymatic hydrolysis can occur throughout the polymer's bulk because water can diffuse through the amorphous regions of the polymer. The surface and bulk erosion processes are shown schematically in Figure 2.9 (adapted from Gopferich, 1996).

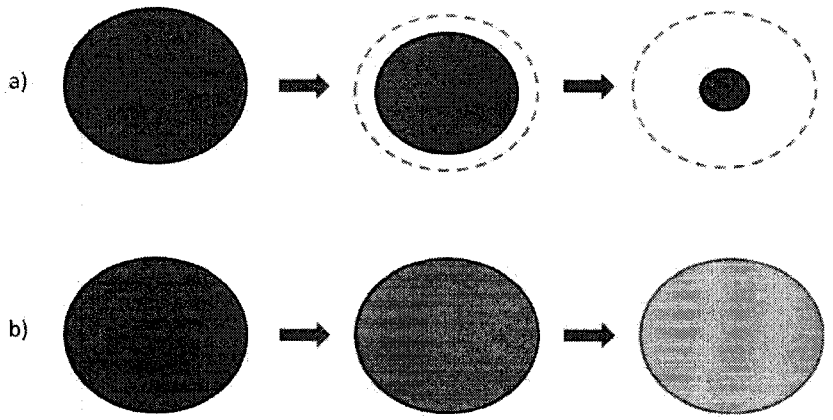

Figure 2.9. Schematic representations of erosion mechanisms. a) surface erosion and b) bulk erosion. The dashed lines show the original device dimensions (adapted from Gopferich, 1996).

Polymer degradation, assisted by either hydrolysis or enzymes, is typically characterized by a change in morphology and reduction of polymer mass.

2.3.5.1 Factors Influencing Degradation Rate

The biodegradation rate of a biodegradable polymer depends on many factors, which can be basically categorized into two groups: environmental factors and the nature of

the polymer. The environmental factors include water, pH value and temperature. Polymers need water for the hydrolysis process. Some plastics, such as PLA, will not biodegrade without prior hydrolysis. Water is also a requirement of microorganisms to grow. In general the hydrolysis reaction is more likely to take place in a moisture-rich environment. As the degradation products of biodegradable polymer are mostly acids, they will lead to a pH value change in the exposure environment close to where the biodegradation process takes place. Poor diffusion and depletion of acids after being produced causes accumulation of acids, which influences the rate of the hydrolysis reaction, or the activities of living organisms (Siepmann et al. 2004; Klose et al. 2006). A decrease in pH is possible to cause an increase in polymer degradation (autocatalysis), if the polymer degradation can be catalyzed by protons.

Temperature plays another significant role in controlling polymer biodegradation since both hydrolysis reaction rates and microbial activity increase as temperature increases. However, for microorganisms when the temperature is too high they may lose their viability.

Polymer factors that influence degradation include the polymer structure, molecular weight, and crystallinity (Cam et al. 1996; Winzenburg et al. 2004). Polymer backbone structure and its side groups determine its flexibility. The biodegradable polymer should be conformationally flexible to move and rotate its atoms and chemical bonds, which offers easy access for the water molecules in the hydrolysis

process. In enzyme-catalyzed biodegradation, polymers with high flexibility can adjust easily to fit into the active reaction sites of enzymes. All these result in an increased degradation rate. Furthermore, since biodegradation can also be an enzymatic reaction, it is very specific to chemical bonds and the structures of particular functional groups. Atoms other than carbon in the polymer backbone make the polymers susceptible to hydrolysis and therefore can make them susceptible to biodegradation.

Water can only diffuse through the amorphous regions of the polymer and hydrolytic reactions are controlled in part by the rate of water diffusion into the polymer bulk in the amorphous regions. For example, PLGA with higher percent of PLA, which is less crystalline than PGA regions, tends to degrade faster due to a more rapid hydrolysis process.

It is also reported that there is upper limit of molecular weight at which microorganisms can degrade the polymer surface (Chandra and Rustgi, 1998). This value varies for different polymers. For example, PLA with a molecular weight above 20,000 Daltons is considered to be difficult to degrade by microorganisms (Auras et al. 2004).

Besides all these polymer characteristics, the size and shape of the device are also considered as a factor affecting its degradation rate. Other conditions being the same, polymers with a higher surface to volume ratio will degrade faster than those with

low ones, as they expose more polymer chains to the external environment for hydrolysis and enzymatic degradation takes place. The best example is the nano-device. Due to its small dimension and higher surface to volume ratio, nanoparticles degrade faster than the micro-devices. Device dimension also plays a critical role in determining the diffusion rate of the degradation products, which as discussed above, will change the micro-environment close to where degradation takes places. (Siepmann et al. 2004).

Though hydrolysis and enzyme-assisted degradation take place, most degradable polymers used for drug delivery and medical applications are bulk eroding polymers. Their degradation is mostly caused by the hydrolytic cleavage of the ester bond and the penetration of water into the bulk is much faster than the polymer degradation.

2.4 Co-continuous Morphology of Polymer Blends

Polymer blends are physical mixtures of two or more structurally different polymers. Polymer blending has been studied and used to develop new polymeric materials for several decades, as the product from polymer blending combines the properties of its components. (Paul and Bucknall, 2000; Utracki, 1989.). Compared to the synthesis of new monomers and the development of new polymerization routes, polymer blending is usually cheaper and less time-consuming.

The immiscibility of two polymers is mainly a thermodynamic issue resulting from the unfavourable mixing enthalpy and low mixing entropy due to the nature of the polymers (Olabishi, 1979).

$$\Delta G_{mix} = \Delta H_{mix} - T \cdot \Delta S_{mix} \tag{2.2}$$

The entropy of mixing ΔS_{mix} is a function of the molecular sizes being mixed. Due to the high molecular weight of polymers, ΔS_{mix} is negligible. The enthalpy of mixing ΔH_{mix} depends on the energy change associated with the changes in nearest neighbor contacts during mixing and it is positive in most polymer blends systems, as polymer blending is usually endothermic in nature. Thus the free energy of mixing is also positive. The polymers with a positive mixing free energy of mixing are immiscible polymers. Blending of these immiscible polymers leads to heterogeneous system with dual or multi phases. Here in this chapter we discuss binary polymer blends system only.

2.4.1 Co-continuous Morphology

Generally in an immiscible binary blend system, the volume composition and the viscoelastic properties of the two polymers determine the type of the morphology. Most of the dual phase blends consist of a dispersed phase of one component which disperses in the matrix phase of the other component, which is continuous throughout the system. This morphology is called droplet/matrix morphology. Polymer with higher volume composition in the blends tends to form the matrix phase (major phase) and then encapsulate the other polymer with lower volume composition, which then forms the dispersed phase (minor phase). Given the same concentration, the component with higher fluidity tends to encapsulate the component with higher viscosity. The drop/matrix type morphology usually appears when the minor phase (dispersed phase) is at low volume faction.

Furthermore, depending on polymer systems, there is an intermediate region where no clear dispersed phase and matrix phase can be identified as both components form a continuous phase. These two phases interpenetrate with each other throughout the bulk of the blend, as shown as Figure 2.10.

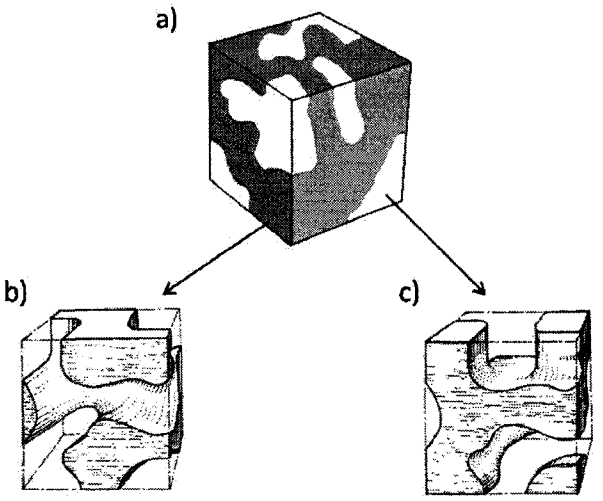

Figure 2.10 Schematic representation of immiscible binary polymer blends

The black and white parts in Figure 2.10a) represent two polymers. Figure 2.10b) and 2.10c) show the structure for each polymer phase after the extraction of the other phase from the co-continuous binary polymer blends like the one shown in Figure 2.10a) (Gregen et al. 1996).

At this point, the continuity of each phase reaches 100%. The blend system with this morphology is called a co-continuous blend. This phenomenon is known as co-continuity, or dual phase continuity. The term continuity is usually defined as the volume of minor phase involved in the continuous path divided by the total volume of the minor phase.

Figure 2.11 a) schematically shows the transition from droplet/matrix morphology to co-continuous morphology.

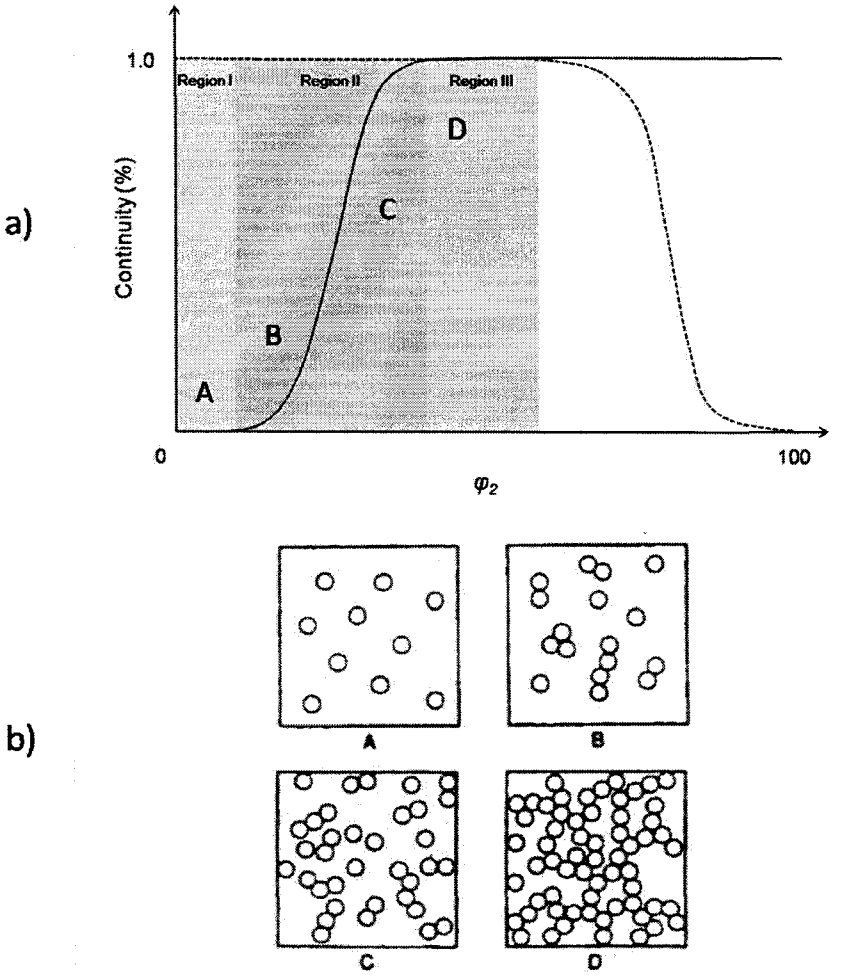

Figure 2.11 Schematic relationship between polymer volume fraction and continuity (b is taken from Hsu and Wu, 1993)

In Figure 2.11 φ is the volume fraction and 1 and 2 indicate two immiscible polymers 1 and 2. Solid line shows the continuity of polymer 2 and the dashed line shows that of polymer 1. When polymer 2 is at a very low concentration (region I), it is well dispersed as droplets in the matrix phase of polymer 1. These droplets are isolated hence the continuity of polymer 2 is very close to 0%. Meanwhile, the continuity of polymer 1 is 100%. When the concentration of polymer 2 increases, it begins to take

more space in the binary system and some of the droplets begin to coalesce, which results in a gradual increase in the continuity of polymer 2, even if it is still a dispersed phase (region II). When the concentration of polymer 2 increases to a certain level, its continuity reaches 100%, while at the same time continuity of polymer 1 also maintains at 100%, indicating both polymers are fully interconnected through a continuous pathway. The blend system reaches the dual phase continuity region (region III) where both polymer 1 and 2 can be considered as matrix phases. Further increasing the polymer 2 concentration, phase inversion takes place, and polymer 1 loses its 100% continuity and becomes the dispersed phase while polymer 2 maintains as the matrix phase. Here phase inversion refers to a transition composition at which a dispersed phase becomes a continuous phase, while the originally continuous phase becomes dispersed. The concentration window of dual phase continuity region depends on specific system of immiscible binary polymer blends.

Co-continuous morphology development undergoes the transition from one minor phase dispersed in another matrix to dual phase continuity. This transition process can be explained by percolation theory, as shown in Figure 2.11b (taken from Hsu and Wu, 1993).

At the beginning, particles of polymer of minor phase (represented as circles) are disconnected and separated from each other (A). As the volume fraction of minor phase increases, these particles progressively start to connect with each other, leading

to an increasing continuity (B and C), and finally continuity is established throughout the whole bulk (D).

Blends with a co-continous morphology benefit from the properties of both polymer phases. Due to their potential to develop advanced materials for applications in many fields, such as conductive polymer and impact resistance materials, polymer blends systems with co-continuous morphology have been intensively studied (Cook et al. 1996; Gubbels et al. 1994; Hourston et al. 1996; Levon et al. 1993; Tchoudakov et al. 1996).

2.4.2 Morphology Control

Previously in research works from our group, we have carried out many studies on the fundamental mechanism of polymer blending and morphology control, especially the co-continuous morphology (Li et al. 2002; Sarazin and Favis, 2003; Yuan and Favis, 2004; Sarazin and Favis, 2005). It has been shown that the morphology parameters including the phase size, phase shape and its distribution, can be influenced and further controlled by a wide range of factors. Theoretical and experimental studies indicate that in a dual-phase immiscible polymer blend system, volume fraction (composition), rheological properties of the components, interfacial tension and processing conditions including shear rate, processing time and annealing time after blending, play important roles in determining the morphological structures of polymer blends (David, 1993; Favis, 1992).

2.4.2.1 Influence of Volume Fraction on the Morphology

As mentioned in the last section, depending on various binary polymer systems, the co-continuous morphology appears at different ranges of volume fraction of one component. In order to obtain a co-continuous morphology, both components of the blends system must reach a sufficient quantity to form continuous phase. In order to control the phase size, other factors, such as interfacial tension, rheological properties and processing parameters, should be considered.

2.4.2.2 Influence of Viscosity Ratio on the Morphology

The viscosity of the polymer material indicates how it can spread and disperse during the blending process. A polymer with high viscosity resists changing its phase shape or being broken up. It has the tendency to be encapsulated by the polymer with lower viscosity. Viscosity ratio has strong influence on the phase size (Avgeropoulos et al. 1976).

The phase size increases as the viscosity ratio increases, which mean greater viscosity differences between the two components. Viscosity and viscosity ratio affect the morphology and the composition at the phase inversion point (Favis and Chalifoux, 1988; Jordhamo et al. 1986).

Several researchers had proposed some equations in order to quantitatively explain the relationship between the blend composition and component viscosity at the point where the phase inversion takes place (Miles et al. 1988):

$$\frac{\varphi_1}{\varphi_2} = \frac{\eta_1(\dot{\gamma})}{\eta_2(\dot{\gamma})} \tag{2.3}$$

where φ is the volume fraction and $\eta(\dot{\gamma})$ is the viscosity under shear rate of $\dot{\gamma}$. 1 and 2 indicate two polymers.

Later in 1990s, Ho et al. revised the equation by adding an exponential factor of 0.29 at the side of viscosity ratio (Ho et al. 1990).

$$\frac{\varphi_1}{\varphi_2} = 1.22 \left(\frac{\eta_1(\dot{\gamma})}{\eta_2(\dot{\gamma})}\right)^{0.29} \tag{2.4}$$

Both models predict that the less viscous polymer has a stronger tendency to become the continuous phase. However, the value of the phase inversion point predicted from these theoretical equations does not match well with the experimental results as all of them neglected the influence of the classical parameters governing the formation of dispersions, such as interfacial tension, shear rate, matrix viscosity and phase dimension. Taking all these into consideration, Willemse developed an equation relating the critical composition of the minor phase at the co-continuous region to these factors (Willemse. 1999):

$$\frac{1}{\varphi_d} = 1.38 + 0.0213 \left(\frac{\eta_m \dot{\gamma}}{\sigma} R_0\right)^{4.2} \tag{2.5}$$

where φ is the volume fraction of the dispersed phase, η_m is the viscosity of the matrix, $\dot{\gamma}$ is the shear rate, σ is the interfacial tension and R_0 is the thread radius. This relation gives the lower and upper limit, respectively, of the range of co-continuity region in volume fraction. However, this equation is also limited as the thread radius needs to be examined first.

2.4.2.3 Influence of Interfacial Tension on the Morphology

The formation of a continuous phase during polymer blending, and also its stability,

strongly depends on the interfacial tension between two polymer liquid phases. The size of the dispersed phase usually decreases as the interfacial tension diminishes. A binary polymer blend system with a low interfacial tension tends to form large co-continuous region and improve system stability (Verhoogt et al. 1994; Willense et al. 1999).

Most polymer blend systems are unstable. Addition of a compatibilizer can be an efficient way to stabilize the co-continuous morphology by reducing the interfacial tension and minimizing the interfacial energy. The compatibilizer contributes to improve the interfacial adhesion, strengthen the interface and consequently, achieve a smaller minor phase size and finer morphology (Matos and Favis 1995; Sakellariou et al. 1993; Willis and Favis, 1988).

A block or graft copolymer, usually derived from the two homopolymers in the binary system, is among the most frequently used compatibilizers. It was shown that the addition of a diblock copolymer in a binary blend system can improve the stability of a molten polymer thread as the interfacial tension in that system was reduced by a factor of 4 (Elemans et al. 1990).

Different block segments in the copolymer exhibit a strong affinity to one of the polymer phase. The compatibilizer usually stays at the interface, with its molecular chains penetrating into both polymer phases, reduces interfacial tension and prevents coalescence by steric stabilization of the microstructures (Elemans et al. 1990, Mekhilef et al. 1997).

Especially for the incompatible polymer blends, a small amount of diblock copolymer can contribute to stabilizing the interface and hindering coalescence, which leads to a morphology with small phase size and a narrow phase size distribution (Bourry and Favis, 1998; Li et al. 2002). Wills and Favis noticed that there appears to be a critical value of the compatibilizer percentage in the system after which very little change of phase size is observed (Willis and Favis, 1988). This critical value depends on the interfacial area.

2.4.2.4 Influence of Processing Conditions on the Morphology

Processing conditions, including processing temperature, processing time and annealing time after polymer blending, affect all aspects of the morphology and hence the blend properties.

Processing temperature must be high enough to melt both polymers and achieve a certain liquidity for the blending process. However, when blending with a polymer with low thermostability, high temperature can be an issue as it may cause thermo-introduced degradation. Also a polymer blend system with high system temperature during processing will take a longer time to freeze-in its morphology, which results in a growing and larger phase size. Considering these points, the processing temperature is kept as low as possible as long as the blend system is still processible in most cases.

A molten blend system achieves the final morphology only if the system reaches an equilibrium state under the processing temperature and the shear rate. Normally this

is monitored via the temperature and the torque value during. During blending, the torque value decreases gradually as the polymer blend achieves better mixing and a finer distribution. When the system approaches its final morphology, it becomes stable as well as the system temperature.

From a thermodynamic point of view, the co-continuous morphology is a thermodynamically non-equilibrium structure. Removing the heating and shearing during the blending, the system will gradually return to a conventional morphology, where droplets of one phase are dispersed in a matrix of the other phase, which lower the interfacial area and thus free energy. This phenomenon is considered as static annealing. However, due to the high viscosity of polymers, which increases as the system temperature decreases, it takes time for the system to change its morphology, hence it is possible to freeze-in this morphology right after its formation by decreasing the system temperature. It makes static annealing an important factor affecting the formation of final morphology after polymer blending. Yang and Han report the influence of annealing time on phase size and its distribution in polymer blends (Yang and Han, 1996). The average domain size increases and its distribution broadens as annealing time increases. Due to higher liquidity of the polymer at higher temperature, the system changes its morphology via phase size growth at a much faster rate if the system temperature is kept high after the blending. In other words, keeping the system at high temperature for long annealing times will lead to a higher probability of phase motion and coalescence, and hence greater phase size and

wider phase size distribution. Sarazin et al. studied the temperature-introduced coalescence effect on poly(epsilon-caprolactone)/polystyrene (PCL/PS) polymer blends and showed the same trend (Figure 2.12) and the effect of annealing time (Figure 2.13) (Sarazin and Favis, 2005, Sarazin et al. 2004).

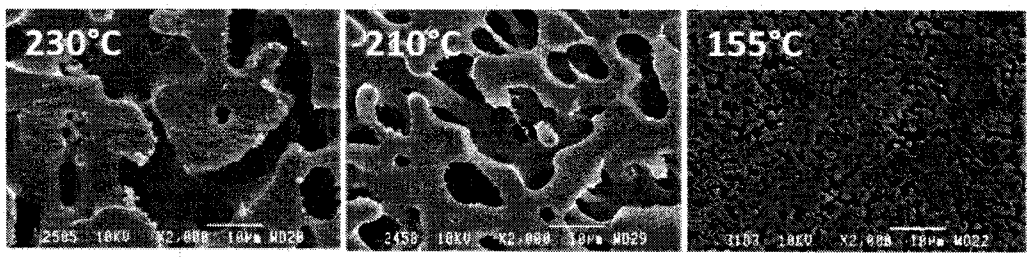

Figure 2.12 Effect of annealing temperature on binary blends morphology (show the pore-size and distribution) (taken from Sarazin and Favis, 2005)

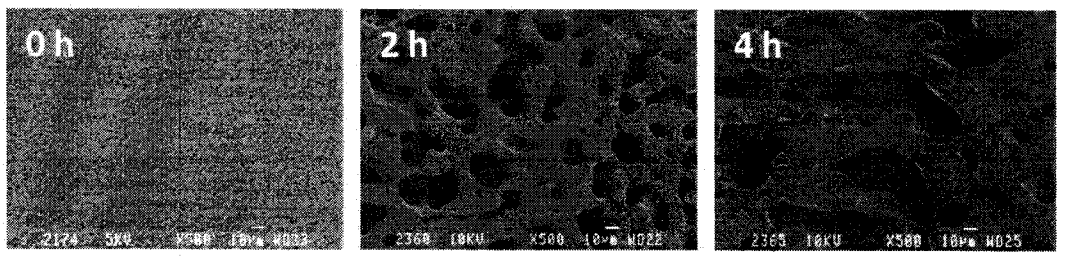

Figure 2.13 Effect of annealing time on binary blends morphology (show the pore-size and distribution) (taken from Sarazin et al, 2004)

In some extreme examples, for example, in the polymer blends with a co-continuous morphology at asymmetric compositions, it is possible to transform the structure into a droplet/matrix morphology. This also depends on the composition range of the dual phase continuity region in the phase diagram (Figure 2.11a), for a specific polymer blends system. The system with a narrower co-continuous region tends to

disintegrate and change its morphology more readily and more easily.

Previously in our group, studies have shown that we can control the morphology in polymer blends by adjusting all these factors.

In this study, polymer blending and morphology control was applied as a route to prepare a porous polymer material. The interconnected porous material was obtained from co-continuous polymer blends by selectively removing one phase from the blends. The pore size of the porous material corresponds to the phase size of the extracted phase in the polymer blends and so it can be controlled in the same manner as phase size. Thus, porous materials with controllable pore-size, void volume and surface area can be prepared, which have their potential applications in many fields such as drug delivery and tissue engineering (Favis et al. 2004).

2.5 Surface Modification of Polymer

2.5.1 Introduction

As discussed in previous sections, polymer materials, especially biopolymers, have been widely used to prepare substrates or scaffolds used in the biomedical field.

PLA, for example, possesses biocompatibility and biodegradability suitable for biomedical applications. Its degradation products are non-toxic and less immunogenic. It degrades to natural metabolites and in the field of tissue engineering, its degradation rate is comparable with the healing time of the damaged human tissues. PLA can be tailored to particular applications by manipulation of shape, porosity, degradation time, etc.

However, the protein and cell attachment mostly depends on the surface properties. Although PLA is widely used in biomedical application, the lack of tissue compatibility and resistance to biological environment are the problems that still remain, which lead to insufficiency of the scaffolds in constructing a friendly interface with proteins and living cells. Generally, this hydrophobic polymer is unfavorable for protein and cell attachment unless modified to a hydrophilic surface with higher surface energy and a corresponding lower water contact angle. The surface of PLA lacks of functional groups to support covalent attachment, which makes the surface modification complicated.

Therefore, in certain cases that require better interaction of the material with proteins

or cells, surface modification of PLA is necessary. The goal is to modify the surface properties including the hydrophobility/hydrophilicity, surface energy, surface charge and surface roughness, in order to improve the protein/cell affinity of the polymer scaffold. Extensive work to develop practical and economical methods for surface modification of PLA towards improving hydrophilicity, has been carried out and many different biologically functional molecules have been chemically or physically immobilized on polymeric supports, including protein immobilization via graft polymerization (Ma et al. 2002[a]; Ma et al. 2003[b]; Yang et al. 2003), ozone oxidization (Suh et al. 2001), carbon negative-ion implantation (Tsuji et al. 2002; Tsuji et al. 2005), physical entrapment (Cai et al. 2002; Quirk et al. 2001; Zhu et al. 2003.), plasma modification (Hirostru et al. 2002; Inagaki et al. 2002, Inagaki et al. 2003; Tang et al. 2002) and coating of polyelectrolytes and/or biomolecules by Layer-by-layer technique (Alem et al. 2007; Chen and McCarthy, 1997; Decher, 1997; Hsieh et al. 1997; Lin et al. 2006; Zhu et al. 2003), etc. Among all these, layer-by-layer surface deposition is proved to be able to effectively modify surface properties of polymer materials, especially polymer materials with complicated internal structures.

2.5.2 Layer-by-Layer (LbL) Electrostatic Self-Assembly (ESA)

In this work the surface modification approach will use the LbL technique discussed below. The technique of LbL assembly discovered by Decher and co-workers

(Decher et al, 1992, Decher, 1997), has been employed widely, such as in biosensors, separation or dialysis membranes, nonlinear optical devices, surface modification, etc., due to its simplicity and versatility.

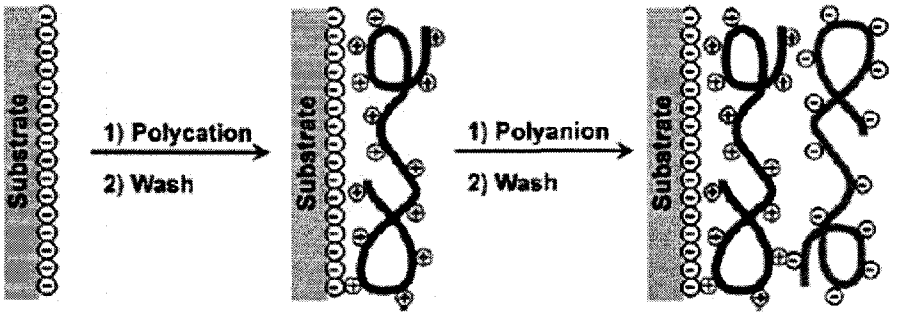

Figure 2.14 Schematic presentation of LbL surface deposition of polyelectrolytes onto a film substrate (taken from Decher, 1997)

Essentially, as shown in Figure 2.14, a polyelectrolyte, for example, is deposited from an aqueous solution onto a surface of opposite charge. After rinsing to remove the loosely adsorbed polyelectrolyte on the surface, the deposited polyelectrolyte leads to a reversal of the net surface charge, due to excess charged groups of polymer chain on the surface, allowing the subsequent deposition of a second, oppositely charged polyelectrolyte. It presents a new alternative to produce biomaterial surface coating. The process has many important advantages over other techniques for preparing ordered multilayer thin films; for example, the assembly is based on spontaneous adsorption and stoichiometric control is not necessary to maintain surface functionality, the assembled molecular films exhibit a much larger thermal and mechanical stability than that of its component, and can be prepared up to

hundreds of layers, and so on (Chen and McCarthy, 1997). Multiple repetitions of this process lead to the build-up of a strong, coherent surface coating, generally with a thickness ranging from tens to hundreds of nanometers. Most of all, the procedure can be adapted to almost any type of surface as long as surface charges are present, it is not restricted to substratum and can be used for coating arbitrarily shaped objects, which is most important for surface modification of scaffolds in tissue engineering. This technique is more practical and important for scaffolds with irregular shape and complex inner surface, while the traditional methods are generally unavailable in these cases. This technique is not limited to polyelectrolytes, other charged species including polypeptides, proteins and DNA, have also been used to prepare multilayers (Lvov, 1994; Lvov, 1995; Müller, 2001). Many of them are extracellular matrix (ECM) or extracellular matrix-like molecules. Charged macromolecules such as negatively charged poly(styrene sulfonate) (PSS), poly(acrylic acid) (PAA), heparin, glycosaminoglycan (GAG), bovine serum albumin (BSA), gelatin, chondroitin sulfate (CS), alginate sodium, hemoglobin as well as positively charged poly(diallyldimethylammonium choloride) (PDADMAC), poly(ethyleneimide) (PEI), poly(allylamine hydrochloride) (PAH), poly(L-lysine) and chitosan, are widely used to modify the polyester surface.

To effectively modify PLA surface, generally, before depositing the first layer, some treatment on the PLLA surface to improve its hydrophilicity is necessary. Aminolysis, a technique widely used in the synthetic textile industry, has recently been

recognized as a highly versatile method to impart functionality to the surface of ester-based polymers. Using multifunctional amine, or branched polyethylenimine (PEI), for example, one can add a significant density of primary amine groups to the surface in the form of new polymer end groups. These impart a positive charge to the surface, not only crucial to the layer-by-layer technique, but also provide functionality for the covalently attachment of these layers to give added strength to the multilayer-substrate bond.

Zhu et al. introduced a novel technique to introduce free amino groups onto polyester scaffolds via aminolyzing the ester groups with diamine to improve the surface hydrophilicity, also it can provide the possibility to modify the polyester surface via a simple way such as layer-by-layer (LbL) electrostatic self-assembly (ESA) of charged species as aminolyzed polyesters can be used as polycationic substrata.

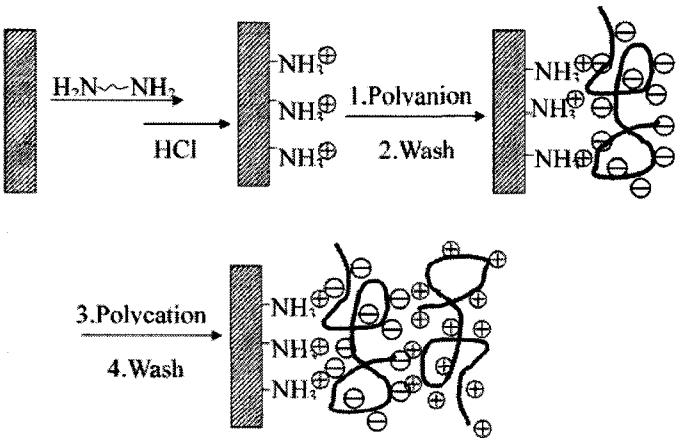

Figure 2.15 Schematic representation of aminolysis and layer-by-layer self-assembly process with oppositely charged polyelectrolytes on an aminolyzed PLLA membrane surface (taken from Zhu et al. 2003).

They reported the construction of assembly films with poly(sodium 4-styrenesulfonate) (PSS) and chitosan on the aminolyzed PLLA membrane surface via LbL deposition. By measuring the hydrophilicity of the modified PLLA surface with different numbers of deposited layers via water contact angle measurement, we can follow the LbL deposition process, as the surface wettability is primarily controlled by the polymer's outermost surface layer if the layer is uniform (Zhu et al. 2003).

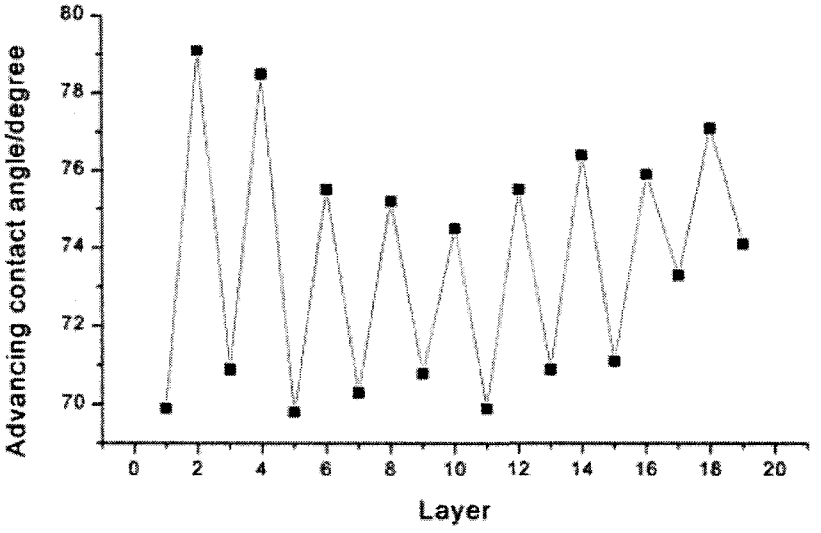

Figure 2.16 Advancing contact angle as a function of the layer number of PSS and chitosan. Odd numbers represent films with PSS as the outermost layer, whereas even number films have chitosan as the outermost layer (taken from Zhu et al. 2003).

The surface morphology of biomaterials also has a big influence on protein and cell attachment and function in addition to the surface chemistry. Therefore it is important to understand the influence of the chemical treatment on polymer morphology. So atomic force microscopy (AFM) measurements were applied and

displayed that the PLLA membrane surface became rougher and had some pores with a size of several tens to hundreds of nanometers after it was aminolyzed with 1,6-hexanediamine (Figure 2.17b). Figure 2.17c showed that one bilayer of PSS/chitosan (chitosan as the outermost layer) has little influence on the surface morphology of PLLA. After four bilayers are deposited, the surface became a little bit smoother (Figure 2.17d). This result can be explained since the deposition of polyelectrolyte layers has the ability to smooth-out a rough surface. Moreover, the pores on the surface became smaller as well. It is worth noting that this smoothing effect occurred in a scale of micrometers.

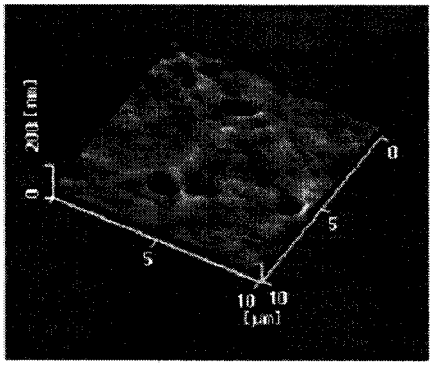

(a)

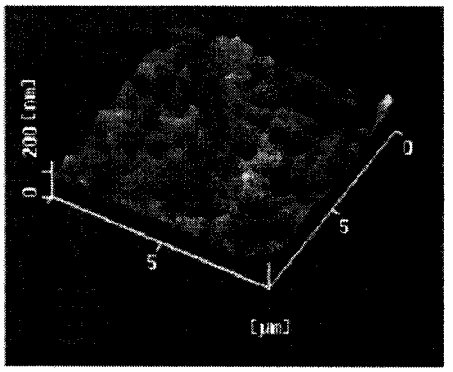

(b)

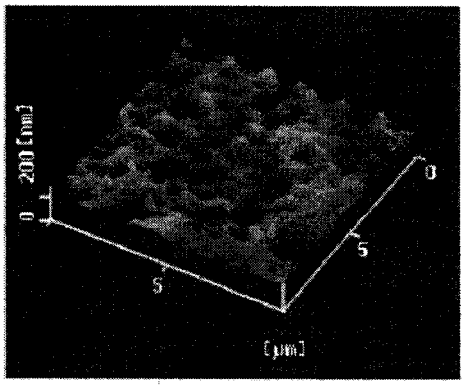

(c)

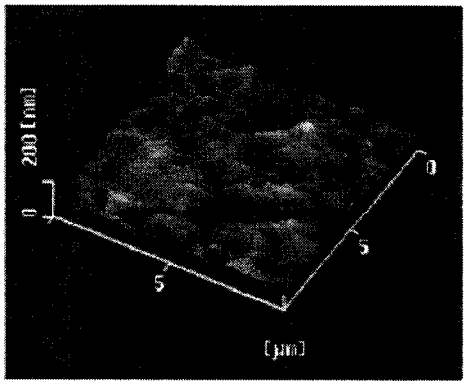

(d)

Figure 2.17. SFM images (tapping mode) of the PLLA surface: (a) control; (b) aminolyzed with 1,6-hexanediamine; (c) deposited by one bilayer of PSS/chitosan with chitosan as the outermost layer; (d) deposited by four bilayers of PSS/chitosan with chitosan as the outermost layer (taken from Zhu et al. 2003).

Lin et al. modified poly(L-lactide) (PLLA) surface via aminolysis by poly(allylamine hydrochloride) (PAH) at high pH and subsequent electrostatic self-assembly of poly(sodium stryrenesulfonate) (PSS) and PAH (Lin et al. 2006). The process was monitored by X-ray photoelectron spectroscopy (XPS) and contact angle measurement. These modified PLLAs were then used as charged substrates for further incorporation of gelatin to improve their cytocompatibility. The gelatin adsorption at pH=3.4 resulted in higher surface coverage by gelatin than pH=7.4, reported by Zhu et al. (Zhu et al. 2003).

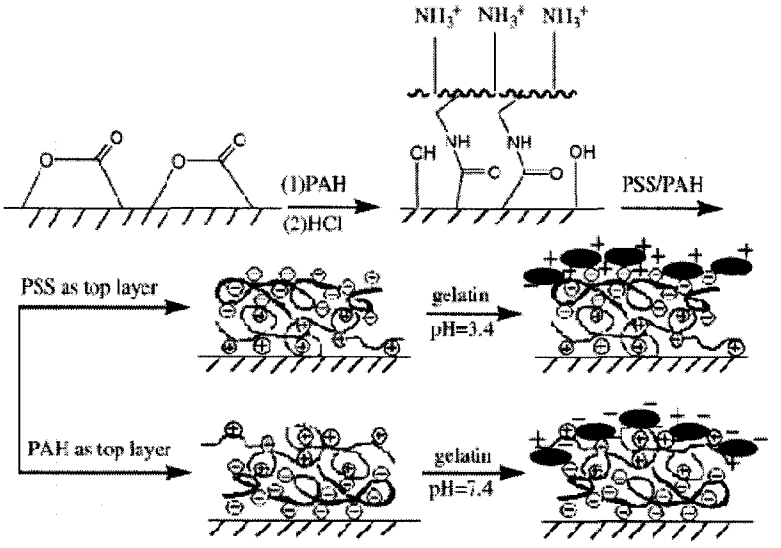

Figure 2.18 Schematic illustration of the modification of the PLLA substrates (taken

from Lin et al. 2006).

PAH has a reported pKa of ~10.6 (Chen and McCarthy, 1997) and its degree of protonation is pH dependent. At high pH PAH is able to react with PLLA by amidation as a free base to form a covalently attached PAH layer. At lower pH there was lower PAH adsorption, and at pH above the pKa of PAH, amidation was extensive, as PAH becomes increasingly deprotonated and both charge-charge repulsion and polyelectrolyte solubility are diminished.

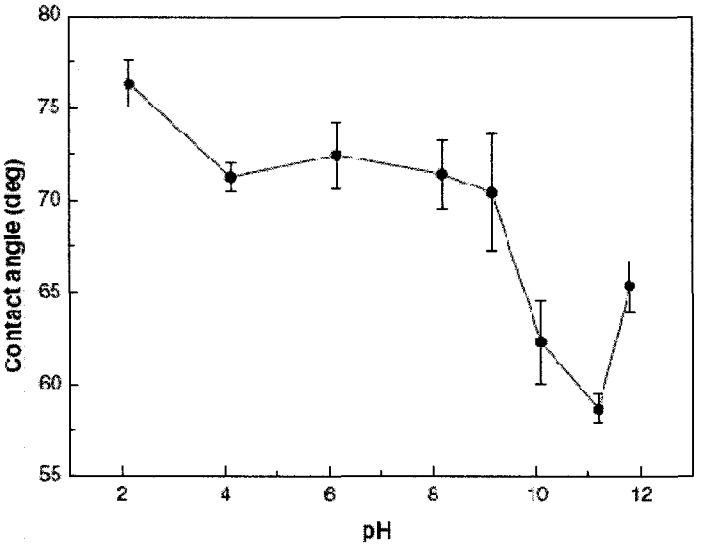

Figure 2.19 Water contact angles of the PLLA surfaces treated by PAH solution at different pH values (taken from Lin et al. 2006).

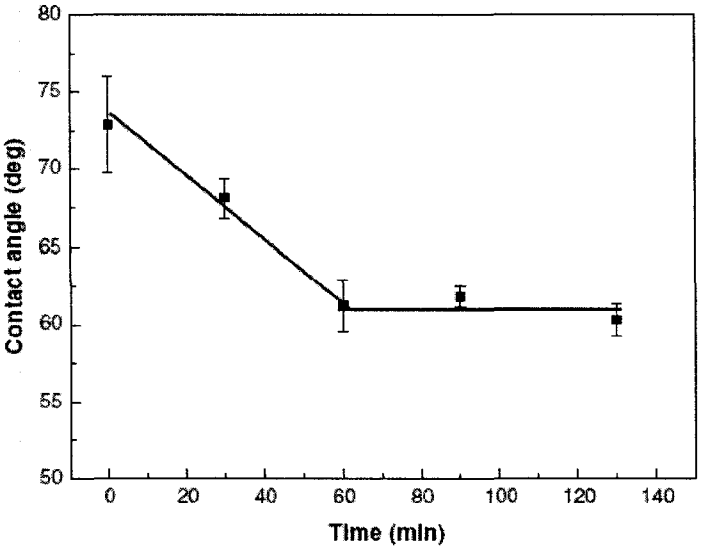

Figure 2.20 Water contact angles as a function of treatment time of the PLLA surfaces treated with PAH solution at pH=11.2 (taken from Lin et al. 2006).

The water contact angle data show that the adsorption of PSS and PAH improves the hydrophilicity of the PLLA surface, with PSS top layers being more hydrophilic than PAH top layers (lower contact angle indicates higher hydrophilicity).

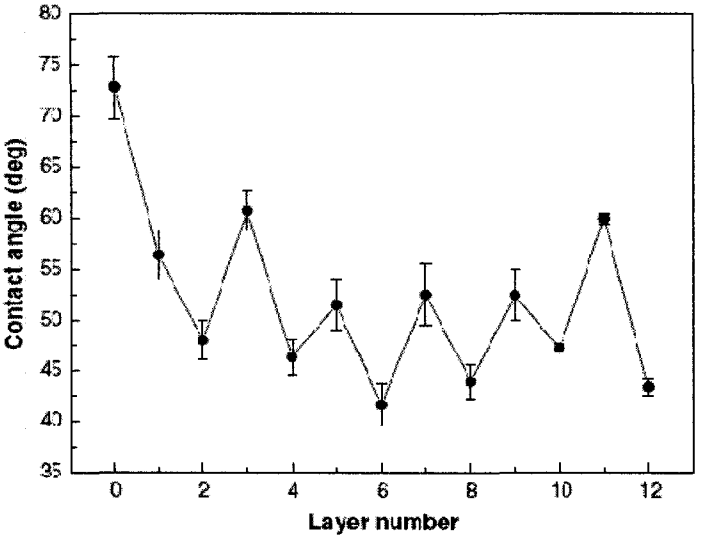

Figure 2.21 Contact angles of the PAH/PSS multilayer assembly: layers of odd

numbers have PAH as the outermost layer; layers of even numbers have PSS as the outermost layer (layer zero is the virgin PLLA) (taken from Lin et al. 2006).

The solution pH is critical in the application of gelatin as a modifier via electrostatic assembly to improve the cell compatibility of synthetic polymers. Isoelectronic polint (IEP) of the gelatin is 5.0. At pH=7.4, which is above the IEP, the gelatin molecules carry a net negative charge due to the dissociation of the carboxyl groups. This pH is however much lower than the pKa of PAH. So the PLLA/PAH surface carries a positive charge, which provides the electrostatic driving force for the adsorption of the negatively charged gelatin molecules. On the other hand, at pH=3.4, which is below the IEP of the gelatin, the positively charged gelatin is able to deposit onto the negatively charged PLLA/PAH surfaces.

Compared to the results reported for PLLA modified by PEI/gelatin assembly (Zhu et al. 2003), where eight cycles of PEI/gelatin assembly at pH=7.4 and crosslinking with glutaradehyde afterwards were involved, Lin et al. applied only one gelatin deposition at pH=3.4 after the surface was charged. This was stable enough without crosslinking treatment, and the improvement on the chondrocyte compatibility for PLLA was more prominent, and both cell attachment and viability numbers were slightly higher as well. However, probably due to the charge repulsion between the positive charge carried by the ammonium groups on the gelatin molecules and on the substrate, the amount of gelatin adsorbed on the PLLA/PAH substrate is significantly lower than that on PLLA/PSS at lower pH, and the improvement is not as dramatic.

Most of these studies are for membranes with a flat surface. Different structures of porous scaffold and flat film would cause different surface properties after modification. It is reported by Alem et al. that the LbL assembly with the nanopores has a very different picture of layer growth, the increments of thickness per cycle of deposition being much larger than on flat surfaces by factors as large as 100 for some cases (Alem et al. 2007). No significant dependence of this increment was found on the molar mass of the polyelectrolytes and on the ionic strength of the solutions, indicating that the size of the chains in the starting solutions is of little importance for this process. In contrast, the thickness of the LbL assemblies depends strongly on the pore diameter, being proportional to pore diameter at low diameter, then progressively deviating from this relationship for diameters above 250 nm. These observations strongly suggest that polyelectrolyte complexation occurs within a dense gel filling the whole nanopore, resulting from the entanglement of chains in the confined space of the pore. Upon drying, the gel collapses in a tube with wall thickness directly proportional to its diameter. Deviations from linearity result from slightly different degrees of swelling of the multilayers.

In this paper (Alem et al. 2007) authors studied the layer-by-layer (LbL) deposition of a pair of strong polyelectrolytes within the nanopores of track-etched membranes, for pore diameters ranging from ~50 to 850 nm. The end-to-end distance of the polyelectrolyte chains in solution was varied from 10 to 50 nm by selecting polyelectrolytes of low and high molar mass and by adjusting the ionic strength.

When the LbL assembly is performed within nanopores, a very different picture of growth emerges, with increments of thickness per cycle of deposition being much larger than on flat surfaces (by factors as large as 100 in some cases), and no significant dependence on molar mass or ionic strength. By using polyelectrolytes of lower molar mass, pore diameters as small as 50 nm could be filled.

To address the concern of different protein adsorption onto auto-assembled polyelectrolyte films, Ladam et al. found that the proteins strongly interact with the polyelectrolyte film, irrespective of the charge states of both the outermost layer and the protein (Ladam et al. 2000). When charges of the outermost layer and protein are similar, one usually observes the formation of protein monolayers, which can become dense. If the protein and outermost layer become oppositely charged, the adsorbed amounts are usually larger and the formation of the thick protein layers extending up to several times the largest dimension of the protein. They gave two models to explain this phenomenon, as shown in Fig. 2.22:

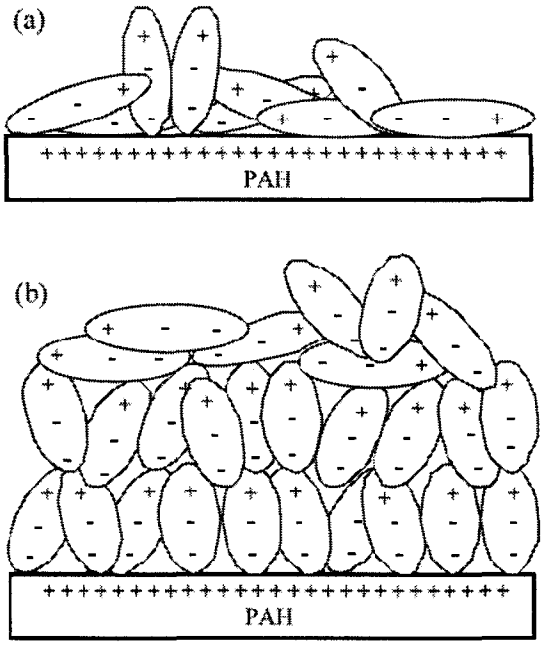

Figure 2.22 Schematic representation of the first proposed buildup process of human serum albumin (HAS) layers on films terminating with poly(allylamine hydrochloride) (PAH). (a) For low HSA concentrations: no structuration occurs; (b) for high HSA concentration: the HSA molecules immediately mainly adsorb in 'end-on' configurations on the polyelectrolyte film (taken from Ladam et al. 2000).

A dense organized layer of adsorbed proteins on films terminating with PAH should lead to a net positive surface charge that attracts new HSA molecules. This buildup process can thus repeat itself and give rise to a thick protein layer. As the layer increases in thickness, the order between the adsorbed molecules decreases, leading also to a reduction of the positive surface charge so that after several protein layers the adsorption process ultimately stops, as shown in Fig. 2.23.

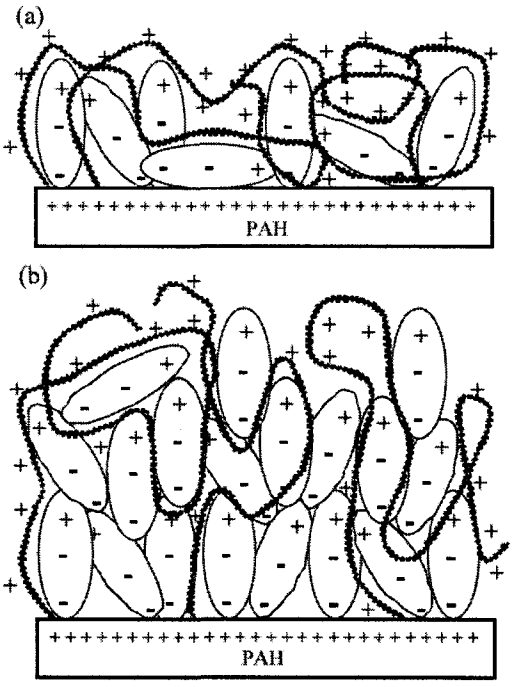

Figure 2.23 Schematic representation of the second proposed model to explain the buildup process of thick HSA films on PEM terminating with PAH. (a) For low HSA concentrations, as time evolves the PAH polylectrolytes readjust their conformations leading to a tighter interaction with the HSA molecules that prevents further protein adsorption. (b) For high HSA concentrations such a readjustment has no time to take place and polyelectrolyte loops can emerge out of the first adsorbed protein layer leading to subsequent protein adsorption (taken from Ladam et al. 2000).

Several techniques, including UV-Vis adsorption, quartz crystal microbalance (QCM), and ellipsometry can be used to characterize the buildup of the polyelectrolyte multilayers, via the mass and thickness increase upon the adsorption of each single layer (Ariga et al, 1997; Ferreira and Rubner, 1995; Harris and

Bruening, 2000). Besides, other techniques, such as atomic force microscopy (AFM), X-ray reflectometry, can be applied to obtain further information about the morphology change and polyelectrolyte multilayer structures (Arys et al, 2001; Dubas and Schlendoff, 2001; Mcaloney et al, 2001).

CHAPTER 3

EXPERIMENTAL METHODOLOGY

Figure 3.1 summarizes the total experimental procedures.

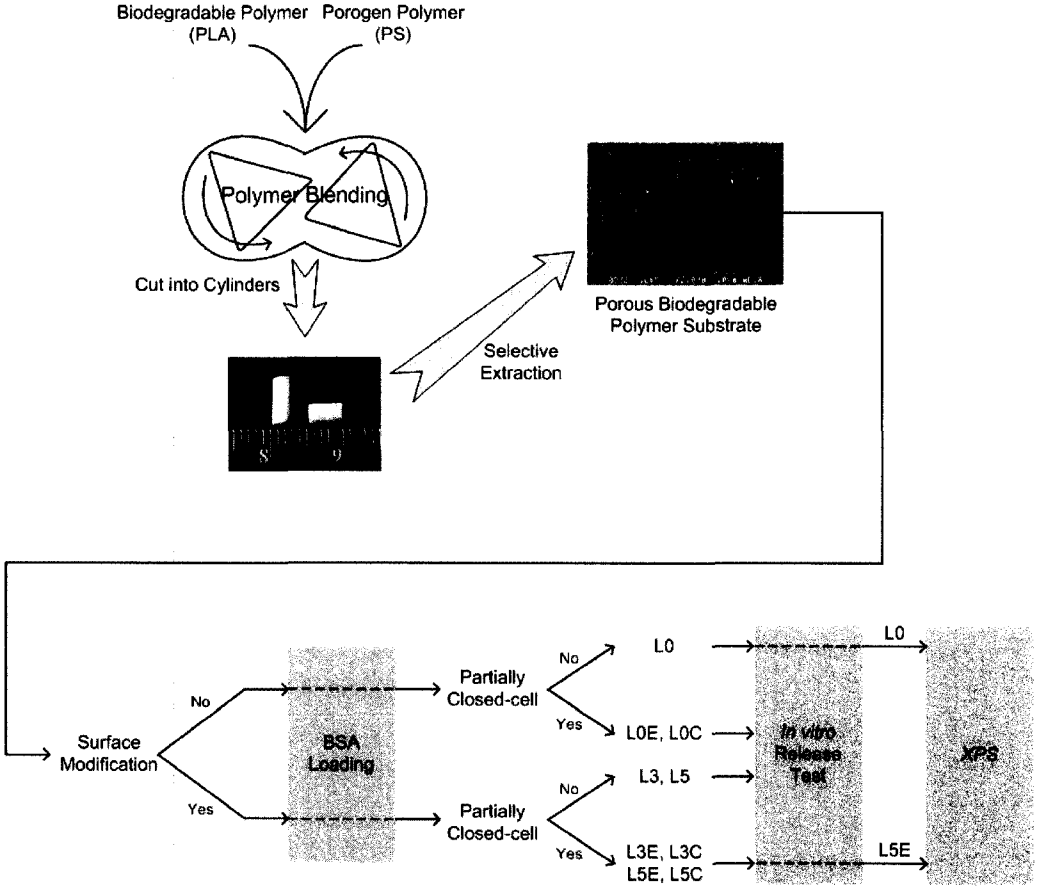

Figure 3.1 Experimental Summary

See abbreviations (page XXXII) and Appendix B

3.1 Materials

Polylactide (PLA) was obtained from NatureWorks (commercial grade: 6201D) in pellet form. Polystyrene (PS) with a molecular weight of 192,000 (commercial grade: 615APR) was purchased from Dow Chemical of Canada. Poly(diallyldimethylammonium chloride) (PADAMAC) as polycation, Mw=100,000~200,000, poly(sodium 4-styrenesulfonate) as polyanion with molecular weight of 70,000, and bovine serum albumin (BSA) solution in water (30 wt%) were purchased from Sigma-Aldrich. Properties of the polymers, polyelectrolytes and protein used in this study are listed in Table 3.1. Sodium choloride, cyclohexane and chloroform were purchased from Laoratoire MAT, Beauport (Quebec). All materials are used as received. Water used in all experiments was prepared by Milli-Q Millipore Biocel 3-stage microfiltration system which prepares filtered water with a resistivity of at least 18.2 MΩ cm.

Table 3.1 Characteristic Properties of the Materials

	Mw	Density (g/cm^3)		Glass Temp	Supplier
		20 °C	200 °C	(°C)	
PLA		1.23	1.09	55	NatureWorks
PS (615APR)	192,000	1.04	0.97	105	Dow Chemical
PDADMAC	100,000 ~200,000				Sigma-Aldrich
PSS	70,000				Sigma-Aldrich
BSA	64,000				Sigma-Aldrich

3.2 Blend Preparation

PLA/PS binary blends in 50/50 volume fraction were prepared via melt blending the two polymers in a Brabander internal mixer with roller blades. Prior to mixing, PLA and PS were dried for 48 hours in a vacuum oven at 70 °C and room temperature, respectively. In order to ensure 50/50 volume ratio in the blends, densities of PLA and PS at 200 °C were used to calculate the loading amount. The total chamber volume is 48.3 mL. The mixing chamber temperature was set as 200 °C and the blade rotation speed at 50 rpm. Polymers were mixed for 10 minutes after being fed into the chamber. During mixing, a constant flow of dry nitrogen was introduced into the chamber to protect the PLA from oxidative degradation. The PLA/PS blend was quenched for 5 minutes in ice water in order to freeze-in its morphology. Afterwards, the dried specimens were cut into cylinders with a diameter of 3.00 ± 0.10 mm and length varying from 3.50 mm to 4.50 mm, using a circular saw at high speed. Under the nitrogen blanket, the PLA and PS used here were found to be stable for over 30 min at the processing temperature.

3.3 Preparation and Characterization of Porous Device

3.3.1 Solvent Extraction and Extent of Continuity

The solvent extraction of the PS phase in the blend was performed in a Soxhlet extraction apparatus. Cyclohexane was used as the selective solvent of the PS

porogen phase in the blend. Solvent temperature inside the Soxhlet apparatus was set at 50-60 °C and the extraction lasted for one week. After extraction, the samples were dried inside a vacuum oven at 60 °C to constant weight. The extraction was carried out until the dried extracted specimens achieved constant weight.

A gravimetry measurement was applied to calculate the continuity of the extracted PS phase (Cont), which is given by:

$$Cont\ (\%) = \frac{W_i - W_d}{W_i} \times 100\% \quad (3.1)$$

where W_i and W_d are the initial weight of the specimen and the specimen weight after solvent extraction and drying, respectively.

3.3.2 Microtomy and Microscopy Surface Characterization

In order to prepare a smooth surface for microscopic measurement and surface characterization, the samples were microtomed using a Leica RM 2165 microtome, equipped with a glass knife. Because the glass transition temperature of PLA is 50-80 °C, the cutting was carried out at room temperature without further deforming the surface. The samples for Scanning Electron Microscopy (SEM) were then extracted with cyclohexane to remove the polystyrene phase then dried, coated with goad-palladium alloy, and finally observed under a Jeol JSM 840 Scanning Electron Microscopy at a voltage between 8 to 12 kV. Samples of closed-cell structures and samples for X-ray Photoelectron Spectroscopy (XPS) were cut at room temperature

using a razor blade, directly from the porous sample after solvent extraction. The SEM images were then analyzed via an x-y digitizing table to give the pore-size.

3.3.3 Pore-size and Surface Area Determination via BET

Pore-size and surface area are two essential parameters to characterize porous material. As for the three dimensional porous device we developed, the conventional image analysis technique is limited to precisely measure such porous samples as it can only derive data from two-dimensional images. Hence BET (Nitrogen adsorption/desorption) technique was applied to solve the problem.

Dynamic BET measurements were carried out by N_2 physisorption using a Quantachrome Autosorb-1 (Boyntom Beach, FL, USA) apparatus at 77.35 K using liquid nitrogen bath, in order to determine the number average diameter d_n, the volume average diameter d_v, and the surface area S. This technique is based on the gas adsorption and desorption on the surface. The gas adsorbed will form a monolayer on the surface. The amount of gas to form this monolayer can be calculated giving the volume of nitrogen used. Plus the physicochemical properties of nitrogen, the area covered by single nitrogen molecule is known. The sample cell with controlled continuous nitrogen/helium mix gas flow is placed, kept and then removed from a liquid nitrogen bath. During this process, nitrogen gas adsorption and then desorption on the surface took place. The composition change in the mix flow due to the nitrogen adsorption and desorption is recorded and analyzed by a

thermal conductivity detector, which finally calculates the adsorbed nitrogen molecule number. The surface area of the sample can be derived from this number, with the known data of area covered by single nitrogen molecule. Due to the accessibility of gas to the interior surface, BET technique is very useful for measurements of three dimensional porous samples.

The BET technique derives its name from the BET equation developed by Brunauer, Emmett, and Teller (Braunauer, 1938):

$$\frac{p}{v(p_0-p)} = \frac{1}{v_m c} + \frac{(c-1)p}{v_m b p_0} \tag{3.2}$$

The experimental pressure, p, at which a volume of vapor adsorbent, v is adsorbed to a surface, can be used to calculate the saturated volume of vapor adsorbent, v_m, when the saturated vapor pressure is known, p_0. In this equation, c is a constant proportional to the energy of adsorption of the gas. This equation is used to estimate the volume of gas required to form an adsorbed monolayer and it gives the best fit of experimental data. Then the surface area of the sample can be calculated by determining the total number of gas molecules adsorbed from the volume of gas adsorbed. Giving the number of molecules, the area occupied can be calculated by multiplying the number of molecules by the space occupied by each molecule.

Noticing that if c » 1 in Equation 3.2, the equation can be simplified into:

$$v_m = v(1 - {}^{p}/_{p_0}) \tag{3.3}$$

Hence even a single point method that measure the volume of gas and the corresponding experimental pressure can give a value of estimated v_m. Then the

surface area of the sample, S, can be calculated using the following equation:

$$S = aN\frac{v_m}{V_{nitrogen}} \tag{3.4}$$

where a, N, and $V_{nitrogen}$ are the area occupied by a single adsorbed nitrogen molecule (16.2×10^{-20} m^2), Avogadro's number and the molar volume of nitrogen, respectively. The experimental accuracy can be improved by conducting multi-point measurements.

Assuming the interconnected pores inside specimen as interconnected cylinders and knowing the extent of continuity via gravimetry measurement during the solvent extraction step, and the sample void volume (50% of the sample), the pore-size (diameter d) can be given by

$$d = 4V/S \tag{3.5}$$

in which V is the total volume of pores and S is the interior surface area. The total pore volume was determined from the adsoption branch of the N_2 isotherm at $P/P_0 =$ 0.95. The experimental error is ± 4%. This method was applied previously by Li and Favis as a characterization method of highly continuous phases (Li and Favis, 2001). The detailed explanation for the experimental and theoretical procedure is reported elsewhere (Li, 2001).

3.4 High Pressure-Vacuum Loading Apparatus and Loading Efficacy Calculation

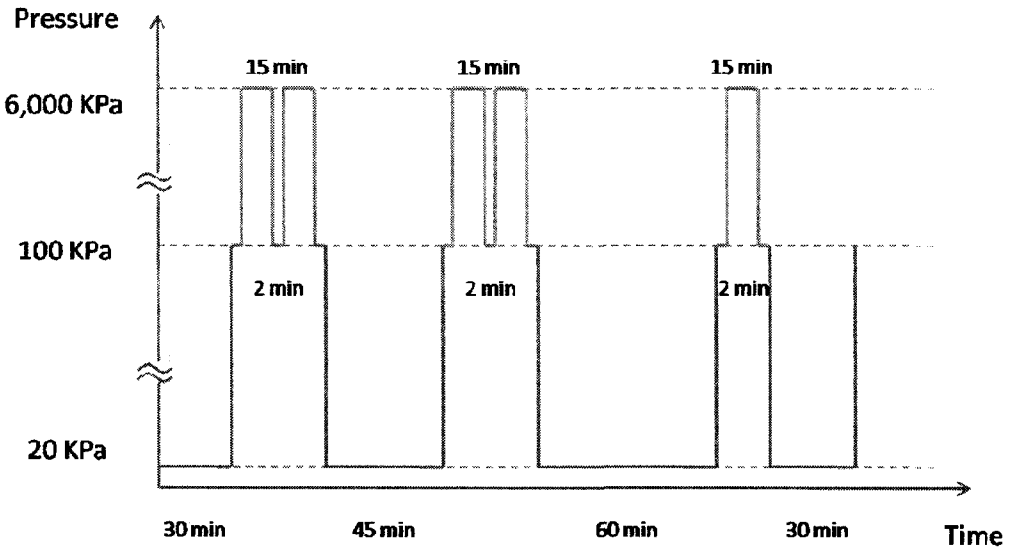

Figure 3.2 Schematic presentation of high-pressure-vacuum loading protocol

In order to force both polyelectrolyte and BSA solutions to penetrate into the porous structures, an in-house high pressure loading device was used, as shown in Figure 3.2. To ensure the solution accessibility to the micro-pores, we followed a vacuum-high pressure cycle loading procedure firstly applied by Roy et al. (Roy et al. 2006). Dry test tubes are firstly filled with loading solution (BSA solution or polyelectrolyte solution as needed). Dried porous sample is put into a home-made sample holder after recording its weight. Then the sample holder with sample in it is immersed into the solution. Because the porous sample containing half of the volume of air, it will float on the solution without holding, hence cannot reach desirable loading efficacy. Thus the sample holder is used to keep the sample position inside the test tube to ensure the solution surrounding. The set-up for this sample holder is shown in Figure 3.3. Then the test tube is placed into the high-pressure loading device. The procedure

follows a vacuum-pressure cycle as follows for each layer: V(30 min) + P(15 min) + P(15 min) + V (45 min) + P(15 min) + P(15 min) + V(60 min) + P(15 min) + V(30 Min), where V and P stand for vacuum and high-pressure, respectively. The time in parenthesis indicates how long a high-pressure step or vacuum step should be applied. In between each step, the solution was maintained at atmospheric pressure for 2 minutes. Finishing the loading cycle, the loaded sample is taken out from the sample holder and then washed with Milli-Q water to remove any unattached macromolecules on outer surfaces. Especially for the samples loaded with polyelectrolytes, samples were then further kept in Milli-Q water under constant shaking for 4 hours to deplete the unattached polyelectrolytes on the both outer and inner surface in the pores. Water was refreshed each hour. After washing, the samples were put in a vacuum oven at 40 °C overnight to reach constant weight. The mass change is recorded afterwards, to give the BSA or polyelectrolyte loaded.

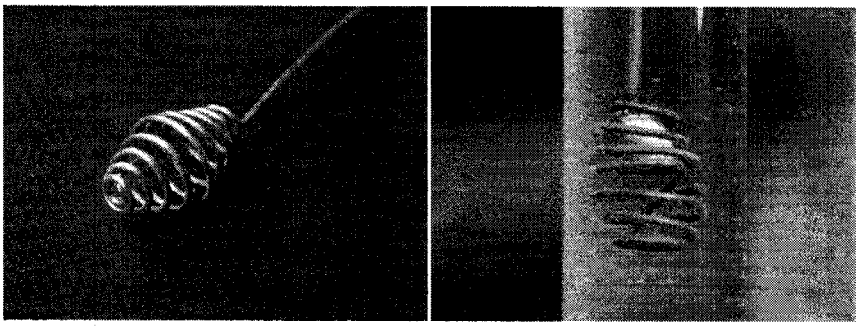

Figure 3.3 Porous sample inside test tube, with sample holder keeping its position

The BSA loading efficacy was calculated for every sample after BSA loading:

$$Loading\ Efficacy = \frac{M_l - M_i}{M_i} \times 100\% \qquad (3.6)$$

where M_i and M_l stand for the sample mass before and after the BSA loading, respectively. The BSA solution accessibility into the micro-pores was calculated also:

$$Solution\ Accessibility = \frac{V_e}{V_v} \times 100\% \quad (3.7)$$

where V_e is the volume of BSA solution penetrated into the porous device calculated from the amount of BSA loaded. V_v is the void volume of the porous sample, calculated from the recorded data for each blends. Calculations of V_e and V_v are listed below:

$$M_{BSA\ loaded} = M_{sample\ mass\ after\ BSA\ loading} - M_{sample\ mass\ before\ BSA\ loading} \quad (3.8)$$

$$V_e = M_{BSA\ loaded}/Conc.of\ BSA\ solution \quad (3.9)$$

$$V_v = V_{PS\ phase} = V_{PLA\ phase} = \frac{M_{sample\ mass\ before\ loading}}{\rho_{PLA\ at\ 200°C}} \quad (3.10)$$

where density of PLA at 200°C is 1.09 g/mL.

In this process, the pressure used was 6,000 KPa and the vacuum 20 KPa, as a previous study showed that this pressure gives an optimum condition for pressure-vacuum protocol to load water into the porous PLA, and highest solution accessibility to the pores. Higher pressures do not result in any greater accessibility to the porous device (Salehi et al, 2008).

3.5 Modification of the Porous Devices

Two strategies, Layer-by-layer (LbL) surface deposition and partially closed-cell, are applied to modify the porous PLA device.

3.5.1 Layer-by-Layer Surface Deposition of Polyelectrolytes into Porous PLA

Previously our group successfully applied Layer-by-layer (LbL) surface deposition of polyelectrolytes onto porous template in order to fabricate ultraporous material (Roy et al. 2006). Salehi et al. showed the potential of this technique in surface modification in aim to control drug release (Salehi et al. 2008). As a variation of the approach described by Caruso et al. (Caruso et al. 1996), PDADMAC and PSS were used as polycation and polyanion for the LbL system. Both polyelectrolytes were in aqueous solution with concentration of 10 mg/mL and 1 M NaCl in order to keep the polyelectrolyte conformation in solution. The preparation of polyelectrolyte solution is explained in the next section. One layer of polyelectrolyte was deposited onto the sample surface following the high-pressure-vacuum loading protocol described in previous section. Repeated loading of polyanion followed by polycation into the porous substrate creates polyelectrolyte film on the sample surface. PDADMAC was chosen as first layer for deposition as it has higher affinity and better stability on PLA surface compared to PSS. Samples newly loaded with polyelectrolyte were rinsed by deionized water and then washed for 4 h under constant shaking in order to remove unbounded polyelectrolyte on sample surface. Water was refreshed for each hour. Afterwards the samples were dried in a vacuum oven at 37 °C for overnight. Depending on needs, 3 or 5 layers of polyelectrolytes were deposited, with PDADMAC as the outermost layer to maintain positive charge on the surface.

3.5.1.1 Preparation of Polyelectrolyte Solution

In order to prepare standard solution from a PDADMAC solution of 20 wt%, we used the following equation to calculate PDADMAC concentration:

$$20\ \text{wt\%} = \frac{20\ \text{g PDADMAC}}{100\ \text{g Water}} \times \frac{1000\ \text{mg}}{\text{mL}} = \frac{200\ \text{mg PDADMAC}}{\text{mL}} \quad (3.11)$$

In order to prepare 25 mL PDADMAC solution with concentration of 10 mg/mL, 1.25 mL of PDADMAC solution of 200 mg/mL should be added to 23.75 mL of deionized water with 1 M NaCl. The calculation of PDADMAC (30 mg/mL) used is shown as following:

$$V_{\text{PD 200mg/mL}} = \frac{\text{Conc.}_{\text{standard}} \times V_{\text{standard}}}{\text{Conc.}_{\text{PD 200mg/mL}}} = 25\ \text{mL} \times \frac{10\ \text{mg}}{\text{mL}} \div \frac{200\ \text{mg}}{\text{mL}} = 1.25\ \text{mL} \quad (3.12)$$

The same calculations are applied to prepare standard solution from a PSS solution of 30 wt%:

$$30\ \text{wt\%} = \frac{30\ \text{g PSS}}{100\ \text{g Water}} \times \frac{1000\ \text{mg}}{\text{mL}} = \frac{300\ \text{mg PSS}}{\text{mL}} \quad (3.13)$$

In order to prepare 25 mL PSS solution with concentration of 10 mg/mL, 0.67 mL of PSS solution of 300 mg/mL should be added to 24.33 mL of deionized water with 1 M NaCl. The calculation of PSS (30 mg/mL) used is shown as following:

$$V_{\text{PSS 300mg/mL}} = \frac{\text{Conc.}_{\text{standard}} \times V_{\text{standard}}}{\text{Conc.}_{\text{PSS 300mg/mL}}} = 25\ \text{mL} \times \frac{10\ \text{mg}}{\text{mL}} \div \frac{300\ \text{mg}}{\text{mL}} = 0.67\ \text{mL} \quad (3.14)$$

3.5.2 Partially Closed-Cell Morphology

In order to develop porous carriers with better control in protein release, a partially closed-cell strategy was applied to block the tunnels connecting to sample surface. The protocol defined in section 3.3 allows for the preparation of porous materials

with a symmetric, open-cell porosity, defined as a state in which porosity is maintained throughout the material, from center to surface. Closed-cell morphology, including a porous core and a solid skin at the surface, can be used to limit the external open surface area available for both medium penetration and drug release. This kind of morphology, was created by immersing the porous PLA sample into chloroform, a solvent for polylactide. This results in an external skin on the sample surface and thus seals the outer surface. The skin thickness can be controlled via the immersion time. Increasing this immersion time will lead to a thicker skin, but also decreases the sample dimensions and causes loss of BSA. In this study, all samples were immersed in chloroform for 5 s and the skin thickness was observed by SEM. After drying the sample for 24h, two strategies were applied to create a partial opening on sample. In one case, closed cell cylindrical samples were cut at one end with a razor blade resulting in a sample with only one base of the cylinder being open. In another case, cylindrical samples with a closed-cell morphology were placed in the sample holder in the microtome, at 45° to their axial direction, and then cut 120 ± 20 μm from the edge. This results in a much more closed cell sample where only one corner of the cylindrical device is open. All the sample dimension changes were recorded in order to recalculate the BSA remaining inside the sample. The open surface areas of these two strategies were measured via an x-y digitizing table.

3.6 In Vitro BSA Release Test

In order to analyze the controlled release of BSA from porous PLA substrates, cylindrical BSA carrier was weighted and then immersed into 3 mL of Milli-Q deionized water in a spectrophotometry cell properly covered and sealed. The cell was incubated at 37 ± 0.3 °C with constant vertical shaking at 5 rpm, in order to give a homogeneous dispersion of the released BSA inside the UV cell. At predetermined time intervals, the concentration of BSA released from the carrier and dispersed into the medium was monitored using a UV-Vis spectrophotometer (Beckman Coulter DU 640) at a wavelength of 280 nm. The BSA concentration in medium was calculated from the reading of spectrophotometer using a calibration curve obtained from a series of standard BSA solution, made in prior of the release test. The preparation of standard BSA solution is described in the following section. The estimated error in this release study is ± 5%. The supernatant was also collected after the release test and used to determine the pH value in the incubation medium. Samples after release test were dried and weighted as an indirect method to measure the total amount of BSA released, assuming the mass change is all due to BSA release.

Water evaporation from the UV cell cause problems concerning the calculation of BSA released from the medium volume. In order to minimize its influence, firstly we used a plastic head with seal of Teflon tape to cover the cell. Besides, in order to precisely calculate the BSA release in the medium, the weight of the cover (plus Teflon seal), the UV cell, the sample and the water loaded were weighted separately.

During the release test, the total system weight (cover + cell + sample + water left) was recorded right after each test at the same time interval. The system mass change can give us an idea about the water evaporated and hence the water remaining in the cell.

3.6.1 Preparation of Standard BSA Solutions

In this study, we adopted UV spectrophotometer in the *in vitro* BSA release test in order to measure the BSA concentration in the release medium during the test.

In the UV spectrophotometer, a monochromatic incident light is created by the light source and then passed through the slits and dispersion device, as shown in Figure 3.4. The light passes through the sample solution, which is in a UV cell made of quartz. The transmitted light was detected by a light sensor and recorded by the computer. It can collect the transmittance data at a single wavelength, or within a wavelength window.

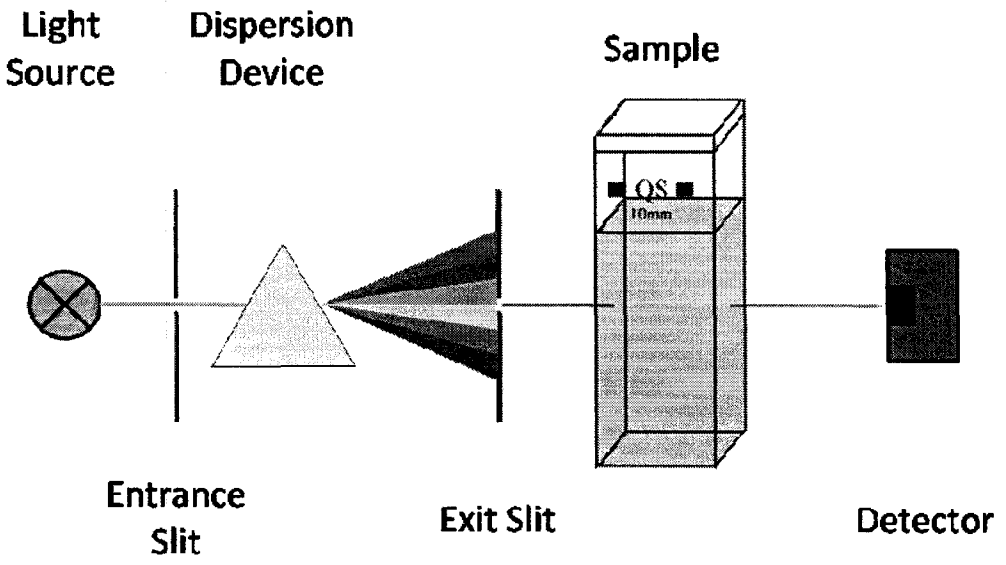

Figure 3.4 Schematic view of a spectrophotometer

Beer-Lambert law gives the relationship between the sample absorbance and sample concentration:

(3.15)

where A, P_0, P, k, b, c are absorbance, intensity of the incident light, intensity of the transmitted light, molar absorptivity of the absorber, path length and sample concentration, respectively. It shows that the solution concentration is proportional to its absorbance. In this study, the absorbance of BSA in water was taken at a wavelength of 280 nm, where the ultraviolet absorbance peak appears.

In order to establish a relationship between the BSA concentration and the reading from UV-Vis spectroscopy, we prepared standard solutions with various concentrations from BSA solution of 30 wt%. We used following equations to calculate BSA concentration:

$$C = 30\ wt\% = \frac{30\ g\ BSA}{100\ g\ Water} \times \frac{1000\ mg}{mL} = \frac{300\ mg\ BSA}{mL} \quad (3.16)$$

using the following equations we calculated the volume needed (V_{BSA}) from original BSA solution of 30 wt% to prepare standard solution with set concentration of C_s. The data are listed in Table 3.2.

$$CV_{BSA} = C_s V_s \quad (3.17)$$

$$V_{water} = V_s - V_{BSA} \quad (3.18)$$

in which V_s is the volume of standard solution to be prepared and V_{Water} is the water to be added.

Table 3.2 Preparation of BSA solutions of standard concentrations

C_s (mg/mL)	V_s (mL)	C (mg/mL)	V_{BSA} (μL)	V_{Water} (mL)
0.12	25	300	10	24.99
0.36	25	300	30	24.97
0.60	25	300	50	24.95
1.20	25	300	100	24.90
1.8	25	300	150	24.85
2.40	25	300	200	24.80
3.00	25	300	250	24.75

Calibration Curve

Using the standard BSA solutions, the spectrophotometer can provide a calibration diagram with an equation of reading (x) and BSA concentration in solution (y). This equation was used to determine the BSA concentration in the UV cell at different

times in the following release test. A new set of standards were prepared to establish a new calibration curve before each *in vitro* BSA release test, in order to minimize experiment error and obtain accurate data. One example of calibration curve of UV spectrophotometer readings and BSA concentrations is shown below:

Table 3.3 UV spectrophotometer readings for standard BSA solutions

BSA Concentration (mg/mL)	UV Reading
0.00	0.0002
0.12	0.0870
0.36	0.2685
0.60	0.4399
1.20	0.8964
1.80	1.3373
2.40	1.8026
3.00	2.2371

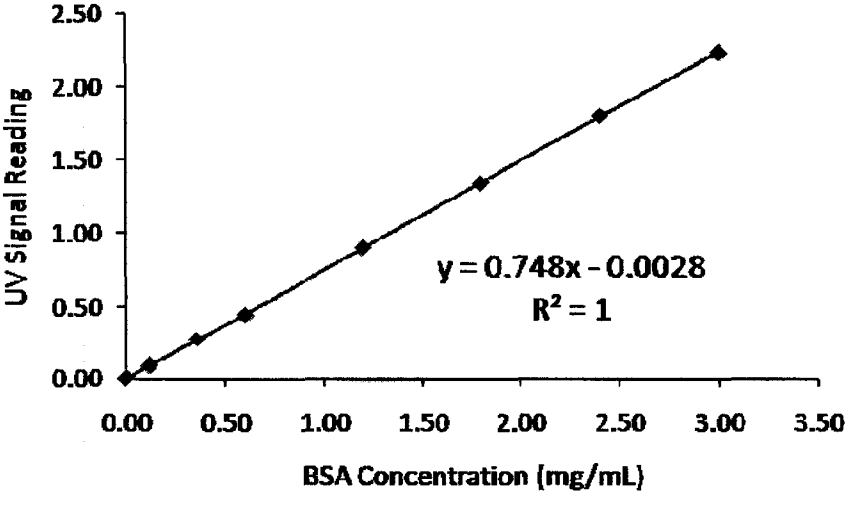

Figure 3.5 Calibration curve of BSA concentration in water, measured via UV at 280

nm

Calibration equation is:

$$\text{UV Readling} = 0.748 \times \text{Conc.} - 0.0028 \ (R^2 = 1) \qquad (3.19)$$

3.7 Protein Distribution Study

In order to have an idea of the protein distribution within the porous PLA substrate at different release stages, X-ray photoelectron spectroscopy (XPS) was applied to analyze the nitrogen atom distribution in the porous sample. The experiment was performed on an ESCALAB MKII instrument (VA Scientific Limited, UK), which gave atom composition at the sample surface. An Mg Kα X-ray source (hυ = 1253.6) with an analyzer pass energy of 100 eV was operated at 20 mA and 15 kV. All the measurements presented here were performed inside an ultra-high-vacuum (UHV) chamber with a base pressure of less than 10^{-9} Torr. In all cases, the binding energy of the C 1s core levels (286.5 eV) was used as an internal standard to distinguish between band-bending and chemical shifting. Porous samples without surface modification by LbL, directly loaded with BSA and samples modified with 5 layers of polyelectrolytes and closed-cell with one-end open at 0%, 25% and 50% BSA cumulative release percentage were chosen and studied the protein distribution within the porous PLA substrate. Samples for XPS analysis were all sectioned from the middle as well as 1 mm above and below the midline. This results in three

internal surfaces from three levels of each sample. The XPS, equipped with a filter of 1 mm in diameter, was performed at four points across the diameter of these internal surfaces of sectioned porous substrates. The arrangement of test spots is shown in Figure 3.6. Each point was scanned 64 times in order to limit the background noise. After that the data was analyzed by VA Avantage software which gave the nitrogen composition, and hence the relative BSA concentration at each point. In order to avoid contamination, the blade used to section the samples was rinsed by ethanol and dried prior to cutting. To notice that, the nitrogen atoms in protein and polyelectrolyte (PDADMAC) both contribute to the nitrogen composition for samples modified with LbL surface modification. Only one sample in each case were analyzed.

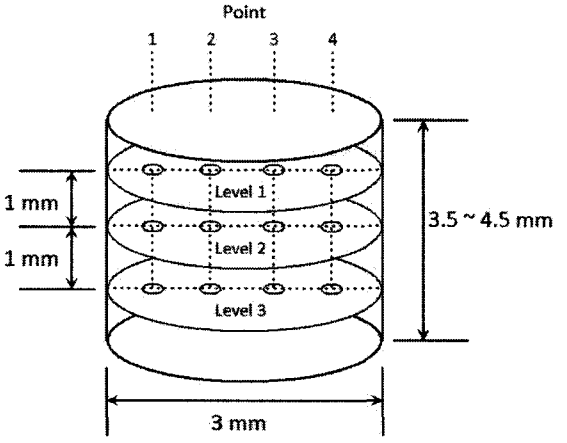

Figure 3.6 Arrangement of spots for XPS test, showing also the sample dimension

CHAPTER 4

CONTROLLING BURST AND FINAL DRUG RELEASE TIMES FROM POROUS POLYLACTIDE DEVICES DERIVED FROM CO-CONTINUOUS POLYMER BLENDS

4.1 Article Presentation

Controlled drug release systems are already extensively used in various applications. Such delivery systems offer numerous advantages as compared to conventional dosage forms. An ideal controlled drug release system operates as a steady state system where the rate of drug release matches the rate of drug elimination again keeping the drug dosage within the therapeutic window for the vast majority of the treatment. In order to favor innoxious products by biodegradation, drug delivery applications using biodegradable polymeric scaffolds are becoming an important means of delivering therapeutic agents. Biodegradable or bioerodible polymer matrices in drug delivery application have been intensively investigated for the last three decades. Due to their remarkable biodegradablility and biocompatiblility through natural pathways which allow them to degrade into naturally occurring substances, polylactide (PLA), poly(glycolic acid) (PGA), polycaprolactone (PCL) and especially the copolymer of lactide and glycolide such as poly(lactide-co-

glycolide), are the primary polymeric candidates investigated and used. In order to solve these problems a number of approaches have been investigated.

The objective of this artile is introduce both an LbL surface modification protocol and a partially closed-cell strategy as routes to control the initial burst release and the final drug release times from porous PLA devices derived from co-continuous polymer blends. Samples with various numbers of polyelectrolytes layers and different open surface area were prepared and *in vitro* drug release tests were carried out using these samples. The results show the effectiveness of these two strategies. The BSA concentration in the device was also examined in order to elucidate the mechanism of release.

Controlling Burst and Final Drug Release Times from Porous Polylactide Devices Derived from Co-Continuous Polymer Blends

Zhenyu Xiang, Pierre Sarazin and Basil D. Favis[1]

CREPEC, Department of Chemical Engineering, École Polytechnique de Montréal,

P.O. Box 6079 Station Centre-ville, Montréal, (QC) Canada H3C 3A7

[1] To whom correspondence should be addressed. Tel: +1-514-340-4711 ext. 4527;

Fax: +1-514-340-4159. *E-mail address*: basil.favis@polymtl.ca

4.2 Controlling Burst and Final Drug Release Times from Porous Devices Derived from Co-continuous Polymer Blends

4.2.1 Abstract

This work has demonstrated that it is possible to exercise a wide range of control over both the initial burst release and the final drug release times from porous PLA devices derived from co-continuous polymer blends. Two strategies were used, a layer-by-layer polyelectrolyte surface deposition approach on the porous PLA surface and the application of a partially closed-cell protocol. A PLA porous substrate with a pore-size of 1.5 μm, derived from a PLA/PS blend via selective solvent extraction of the PS phase, was used as the drug delivery device. The surface area and pore dimensions were examined via BET nitrogen adsorption and image analysis. Porous PLA substrates with 0, 3 and 5 layers of polyelectrolyte and with open areas of 100%, 12 % and 2% were studied both separately and in combination. In vitro release tests were performed to study the release profile of BSA from the devices via UV spectrophotometry. It is shown that, while both are important, surface modification is more dominant in controlling the release rate than the partially closed cell approach. When a 5 polyelectrolyte layer surface modification of the PLA and a partially closed cell approach (2 % open area) are combined, in the L5C sample, the synergy is dramatic with a 5 times reduction in the first two hour

burst release amount and a total release time which is extended by 123 times as compared to the 100% open cell, surface unmodified, reference sample. The L5C sample ultimately releases 89% of the total BSA loaded demonstrating the high level of interconnectivity of the micro channels in the porous PLA. The mechanism of release in this system is clearly diffusion controlled with well defined concentration gradients, as measured by XPS, observed in the direction of release for both the 100% open cell system (L0) and the surface modified, partially closed sample with one end open (L5E). These effects point towards a diffusion mechanism combined with a sorption/desorption interaction of the BSA with the modified PLA surface.

4.2.2 Introduction

The main objective of drug delivery systems is to achieve an effective therapeutic administration via a sustained drug release over an extended period of time. Controlled drug release systems are already extensively used in various applications, such as: surgical implants, sutures and wound dressings with pharmaceutical agents (Balakrishnan et al. 2006; Gursel et al. 2001; Moioli et al. 2007). Such delivery systems offer numerous advantages as compared to conventional dosage forms such as endermic injection. Conventional oral drug administration normally works in an uncontrolled manner which results in fluctuations in the local drug concentration in plasma. This typically results in a short time period at the effective therapeutic level and hence requires multiple drug administrations. This can lead to other problems

such as degradation of the drug in the gastro-intestinal tract. An ideal, controlled drug release system should protect the drug agents from the hostile immunological system of the body, minimize burst release and have significant control over the time period of release of an optimal drug concentration. The improved effect of the drug on therapeutic activity reduces side effects such as toxicity and also the number of drug administrations required to keep the drug concentration within a certain effective window. Controlled release over an extended period is highly beneficial for drugs that are rapidly metabolized from the body after administration. An ideal controlled drug release system operates as a steady state system where the rate of drug release matches the rate of drug elimination again keeping the drug dosage within the therapeutic window for the vast majority of the treatment.

Controlled drug release systems often use macromolecules of synthetic and biological origin as carriers for the drugs. In order to favor innoxious products by biodegradation, drug delivery applications using biodegradable polymeric scaffolds are becoming an important means of delivering therapeutic agents. Biodegradable or bioerodible polymer matrices in drug delivery application have been intensively investigated for the last three decades (Huang et al. 2004; Jain, 2000; Jiang and Schwendeman, 2000; Keyes-Baig, 2004; Kim et al. 2003; Liu et al. 2003; Miao et al. 2005; Park et al. 2005; Wang et al. 2002). Among the various materials employed in controlled drug delivery systems, the thermoplastic aliphatic polyesters such as polylactide (PLA), poly(glycolic acid) (PGA), polycaprolactone (PCL) and

especially the copolymer of lactide and glycolide such as poly(lactide-co-glycolide), are the primary polymeric candidates investigated and used. This is in large part due to their remarkable biodegradablility and biocompatiblility through natural pathways which allow them to degrade into naturally occurring substances (Jain, 2000; Jiang and Schwendeman, 2000; Kim et al. 2003; Miao et al. 2006). For example, polylactide undergoes hydrolytic scission to its monomeric form, lactic acid, which can be eliminated from the human body by incorporation into the tricarboxylic acid cycle. Due to these advantages, these biodegradable polymers are approved for use in human clinical applications including drug delivery use. For most drug delivery systems, two mechanisms are predominant in the release of drugs: a diffusion controlled mechanism and a degradation controlled mechanism (Wang et al. 2004). Drug release from hydrolytically liable polymers like PLA can proceed by both mechanisms, depending on the polymer degradation rate. However, variations in polymer degradation rates can lead to irreproducible drug release and hence compromise the toxicity profile of the drug therapy. The onset of polymer degradation could also cause structural deterioration in the case of implanted devices. As a result, the risk of dose dumping is increased if the partially degraded system collapses or, retrieval of the device is required when unexpected reactions occur during treatment. Furthermore, the low degree of functionality and low hydrophilicity of these biodegradable polymer materials lead to issues such as high initial burst release, and relatively low efficiency of drug loading or encapsulation

due to weak interactions between the drug and the polymeric delivery system.

In order to solve these problems a number of approaches have been investigated including the synthesis of novel polymers with a higher affinity to drug proteins, or the application of various surface modification methods to change the surface properties of these hydrophobic polymers (Barry et al. 2005; Heuberger, 2005; Quirk et al. 2001; Tang et al. 2006; Yoon et al. 2004; Zacharia et al. 2007; Zhu et al, 2003). In the past two decades, the layer-by-layer (LbL) self-assembly technique has emerged as a versatile and convenient method to build up thin multilayers with hyphdrophilic segments or polyelectrolyte functional groups with a precise control of layer thickness and composition (Heuberger, 2005; Tang et al. 2006; Zacharia et al. 2007; Zhu et al, 2003). This technique has two potential applications in controlled drug delivery. One is to construct a multilayer matrix film and then incorporate drug molecules into the matrix, however in this method, the relatively low loading capacity of the matrix film is an important issue (Tang et al. 2006). The other possibility is to modify the polymeric delivery device substrate surface, increase its hydrophilicity, improve the drug adsorption and also the release profile.

Another approach to reduce burst release and drug dosage is to use a closed-cell approach. Typically, closed–cell systems are applicable only for biodegradable polymers since the wall needs to degrade over time to allow drug release. Closed–cell structures have been examined in controlled release using terms such as multi-reservoir or double–wall drug release systems (Matsumoto et al. 2005; Rahman and

Mathiowitz, 2004). This structure offers a better control of the release kinetics as the formation of double-walled microspheres with the drug loaded in the inner core provide a lower burst effect than polymeric microspheres made from a single polymer. There are several methods to fabricate microspheres with a two-layered structure. One method is phase separation of a binary blend from polymer solution, the second method is to simply encapsulate the therapeutic agent into microspheres first and then coat the microspheres with a second polymer. Rahman et al. reported the preparation of double-walled microspheres derived from polylactic acid and polyglycolic acid using solvent evaporation method and the controlled localization of the protein within that system (Rahman and Mathiowitz, 2004). Matsumoto et al. also reported similar studies, showing that the outer non-drug holding layer serves to suppress initial burst and the loss of the drug during manufacturing while the inner drug-holding layer controls the drug release rate (Matsumoto et al. 2005). A so-called closed-cell system possesses a different structure from center to surface with normally a porous structure in the center and a non-porous structure at the surface. Thus the formation of an outer wall on the porous substrate, in order to limit the open surface area, can also contribute to achieving a sustained release profile.

Porous polymer materials have wide applications as scaffolds in biomedical engineering, including use in skin generation, bone generation and cell in-growth for example. Different applications can have different pore-size requirements (Li et al. 2006; Whang et al. 1995; Xie et al, 2006). Various fabrication techniques have been

used to produce porous polymer materials, including solvent/non-solvent sintering, supercritical fluid-gassing, particulate leaching, thermal-induced phase separation and fiber bonding (Guan et al. 2005; Mikos et al. 1994; Mo and Weber, 2004; Mooney et al. 1996; Nam and Park, 1999). The pore-size of the porous materials derived from these techniques varies from 1 μm to several hundreds of microns. Among them, porogen leaching is commonly used, as it allows for an easy control of pore structure. However, the above approaches typically suffer from a number of problems such as an incomplete continuity of the porosity through the device and very poor control of the pore size and size distribution. Many of the applications of porous polymers are in the field of tissue engineering where porous scaffolds of controlled morphology are a critical requirement. In that case, the pore size requirement is quite large generally in the 100 micron range. When the pore size is reduced to the 1 micron range, a high surface area to volume device is achieved and such systems could have potential to be used as a drug delivery device.

In this laboratory we have demonstrated in previous work that it is possible to generate highly controlled fully continuous porous polymeric materials via the control of the co-continuous morphology in polymer blends (Favis et al. 2004; Li et al. 2002; Sarazin and Favis, 2003; Yuan and Favis, 2004). In immiscible binary polymer blends, the morphology depends on the interfacial properties and relative composition of each component. When the composition of each phase reaches a certain level, the morphology reaches a so-called co-continuous region in which each

polymer phase forms a continuous structure in the bulk and mutually interpenetrate each other. The influence of processing time and processing temperature on the formation of co-continuous structures have also been considered (Favis et al. 2004). It has been shown that temperature-induced coalescence effects during melt mixing as well as static annealing times, can both strongly affect the co-continuous microstructure phase size (Sarazin and Favis, 2005). The controlled combination of interfacial tension, viscosity, temperature and phase concentration effects allow for the pore size of the co-continuous morphology to be controlled over 4 orders of magnitude from about 50 nm to 500 microns (Sarazin and Favis, 2005). Furthermore, extraction of one of the phases from such a binary co-continuous polymer blend results in a porous polymer material, with a completely interconnected porosity and a highly controlled pore-size. In other works, Xavier et al. developed a surface modification protocol for such three dimensional porous polymer devices using the layer-by-layer (LbL) surface deposition of polyelectrolyte (Roy et al, 2006; Roy et al. 2007). This technique was used to generate an ultra-porous microstructure with over 98% void volume. Pouneh et al. used this surface modification protocol to study, for the first time, the in vitro release of BSA from porous polymer substrates generated from co-continuous polymer blends (Salehi et al. 2008). In that work BSA was loaded into the surface modified porous device under pressure and the release was monitored by UV spectrophotometry. That work, however, at best, was only able to generate devices that demonstrated a total release time of 40 hours.

The objective of this study is to use both an LbL surface modification protocol and a partially closed-cell strategy to control the initial burst release and the final drug release times from porous PLA devices derived from co-continuous polymer blends. Bovine serum albumin will be used as a model drug and its release from the device will be monitored by UV spectrophotometry. The BSA concentration in the device will be examined by X-ray photoelectron spectroscopy in order to elucidate the mechanism of release.

4.2.3. Experiments

Note that all experimental procedures shown below are summarized in Figure 4.1.

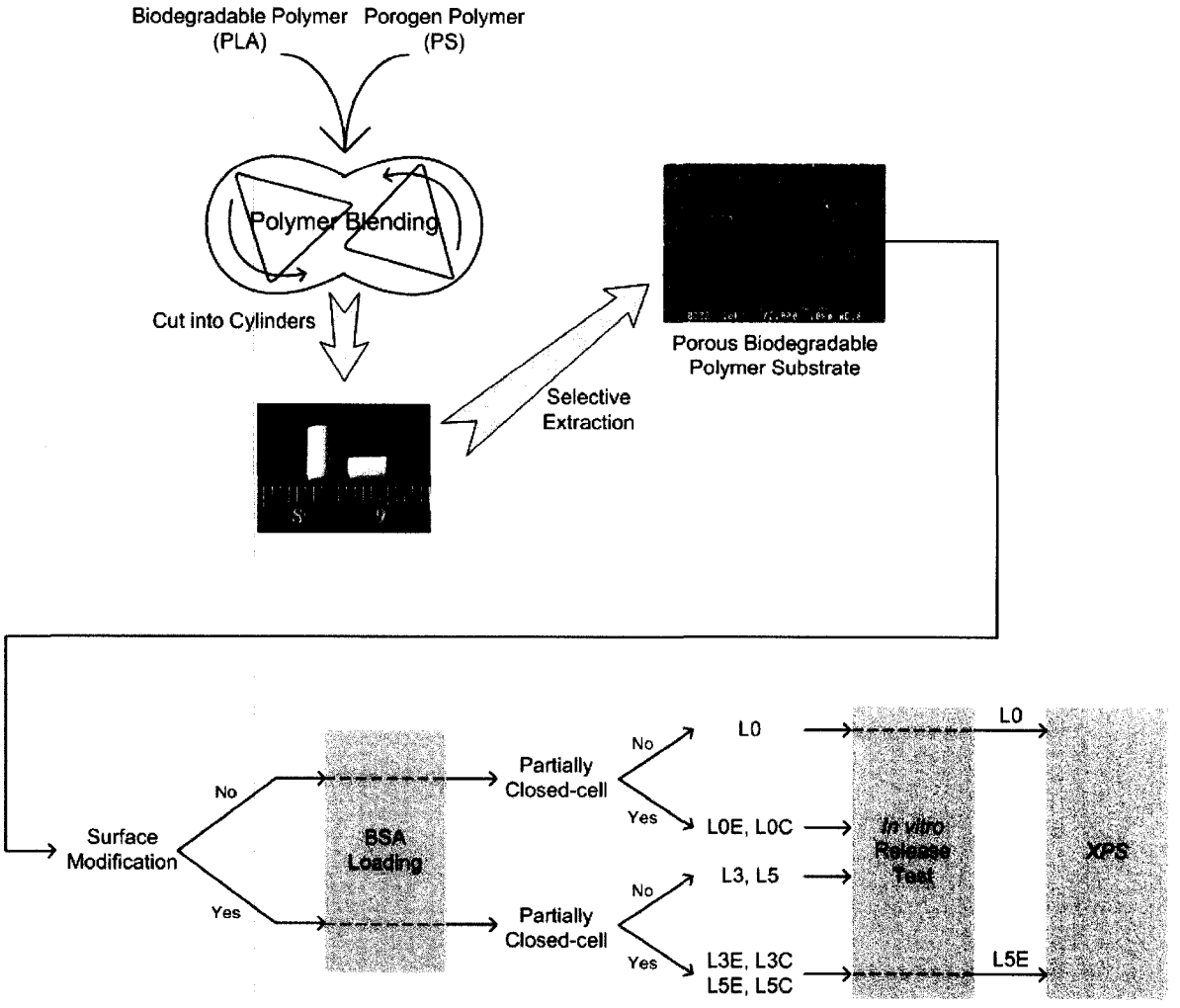

Figure 4.1 Experimental Process

4.2.3.1 Materials

Polylactide (PLA) was obtained from NatureWorks (commercial grade: 6201D) in pellet form. Polystyrene (PS) with a molecular weight of 192,000 (commercial grade: 615APR) was purchased from Dow Chemical of Canada. Poly(diallyldimethylammonium chloride) (PADAMAC) as polycation, Mw=100000~200000, poly(sodium 4-styrenesulfonate) as polyanion with molecular weight of 70000, and albumin solution in water from bovine serum (30 wt%) were purchased from Sigma-Aldrich. Sodium choloride, cyclohexane and chloroform were purchased from Laboratoire MAT, Beauport (Quebec). All materials were used as received. Water used in all experiments was prepared by Milli-Q Millipore Biocel 3-stage microfiltration system which prepares filtered water with a resistivity of at least 18.2 MΩ cm. Properties of the polymers used are listed in Table 4.1.

Table 4.1 Characteristic Properties of the Materials

	M_w	Density (g/cm^3)		T_g (°C)	Supplier
		20 °C	200 °C		
PLA		1.23	1.09	55	NatureWorks
PS(615APR)	192,000	1.04	0.97	105	Dow Chemical
PDADMAC	100,000~200,000				Sigma-Aldrich
PSS	70,000				Sigma-Aldrich
BSA	64,000				Sigma-Aldrich

4.2.3.1 Blend Preparation

PLA/PS binary blends in 50/50 volume fraction were prepared via melt blending the two polymers in a Brabander internal mixer with roller blades. Prior to mixing, PLA and PS were dried for 48 hours in a vacuum oven at 70 °C and room temperature,

respectively. The mixing chamber temperature was set at 200 °C and the blade rotation speed at 50 rpm. Polymers were mixed for 10 minutes after being fed into the chamber. During mixing, a constant flow of dry nitrogen was introduced into the chamber to protect the PLA from oxidative degradation. The PLA/PS blend was quenched for 5 minutes in ice water in order to freeze-in its morphology. Afterwards, the dried specimens were cut into cylinders with a diameter of 3.00 ± 0.10 mm and length varying from 3.50 mm to 4.50 mm, using a circular saw at high speed. Under the nitrogen blanket, the PLA and PS used here were found to be stable for over 30 min.

4.2.3.2 Solvent Extraction and Extent of Continuity

The solvent extraction of the PS phase in the blend was performed in a Soxhlet extraction apparatus. Cyclohexane was used as the selective solvent of the PS porogen phase in the blend. The solvent temperature inside the Soxhlet apparatus was set at 50-60 °C and the extraction lasted for one week. After extraction, the samples were dried inside a vacuum oven at 60 °C to constant weight. The extraction was carried out until the dried extracted specimens achieved constant weight.

A gravimetry measurement was applied to calculate the continuity of the extracted PS phase (Cont), which is given by

$$\text{Cont}(\%)=\frac{W_i - W_d}{W_i}\times 100\% \qquad (4.1)$$

where W_i and W_d are the initial weight of the specimen and the specimen weight after solvent extraction and drying, respectively.

4.2.3.3 Microtomy and Microscopy Surface Characterization

In order to prepare a smooth surface for microscopic measurement and surface characterization, the samples were microtomed at room temperature using a Leica RM 2165 microtome, equipped with a glass knife. The samples for Scanning Electron Microscopy (SEM) were then extracted with cyclohexane to remove the polystyrene phase, then dried, coated with goad-palladium alloy, and finally observed under a Jeol JSM 840 Scanning Electron Microscopy at a voltage between 8 to 12 kV. Samples of closed-cell structures and samples for X-ray Photoelectron Spectroscopy (XPS) were cut at room temperature using a razor blade, directly from the porous sample after solvent extraction.

4.2.3.4 Pore-size and Surface Area Determination via BET

BET (Nitrogen adsorption/desorption) measurements were carried out by N_2 physisorption using a Quantachrome Autosorb-1 (Boyntom Beach, FL, USA) apparatus at 77.35 K, in order to determine the number average diameter d_n, the volume average diameter d_v, and the surface area S. Assuming the interconnected pores inside specimen as interconnected cylinders and knowing the extent of continuity via gravimetry measurement during the solvent extraction step, the pore-size (diameter d) can be given by

$$d = 4V/S, \tag{4.2}$$

in which V is the total volume of pores and S is the surface area. The pore size distributions were calculated from the adsorption branch of the isotherm using the thermodynamic-based Barrett-Joyner-Halenda (BJH) method. The total pore volume was determined from the adsoption branch of the N_2 isotherm at P/P_0=0.95.The experimental error is ±4%. This method was applied previously by Li and Favis as a characterization method of highly continuous phases and the detailed explanation for the experimental and theoretical procedure is reported elsewhere (Li and Favis, 2001; Li et al. 2002).

4.2.3.5 High- Pressure Loading Apparatus

In order to force both polyelectrolyte and BSA solutions to penetrate into the porous structures, an in-house high pressure loading device was used. To ensure the solution accessibility to the micro-pores, we followed a vacuum-high pressure cycle loading procedure as follows for each polyelectrolyte layer (same protocol for BSA loading) : V(30 min) + P(15 min) + P(15 min) + V (45 min) + P(15 min) + P(15 min) + V(60 min) + P(15 min) + V(30 Min), where V and P stand for vacuum and high-pressure, respectively. In between each step, the solution was maintained at atmospheric pressure for 2 minutes. The loaded samples were washed with Milli-Q water to remove any unattached macromolecules on outer surfaces. For the samples loaded with polyelectrolytes, samples were then kept in Milli-Q water under constant shaking for 4 hours for each layer deposited, to deplete the unattached polyelectrolytes on the both outer and inner surface in the pores. Water was

refreshed each hour. After washing, the samples were put in a vacuum oven at 40 °C overnight to reach constant weight.

In this process, the pressure used was 6, 000 KPa and the vacuum 20 KPa, as a previous study showed that this pressure gives an optimum condition for pressure-vacuum protocol to load water into the porous PLA, and highest solution accessibility to the pores. Higher pressures do not result in any greater accessibility to the porous device (Salehi et al. 2008).

4.2.3.6 Layer-by-Layer Surface Deposition of Polyelectrolytes into Porous PLA

The process involves the repeated loading of polyanion solution followed by a solution of polycation into the porous substrate with a four hour vigorous water rinsing between each two polyelectrolyte deposition steps in order to remove excess, non-adsorbed polyelectrolyte. In this study, positively charged PDADMAC and negatively charged PSS were used as the polyelectrolyte pair in aqueous form. The solutions contained 10 mg/mL polyelectrolyte and 1 M NaCl which helps to maintain the polyelectrolyte in solution. At least three layers of polyelectrolytes were deposited onto the substrate inner surface to form a uniformly charged surface. PDADMAC was chosen as the first layer deposited onto the PLA surface due to its ready adsorption and better stability on PLA as compared to PSS. The vacuum-high pressure loading protocol descried earlier was followed to help the solution penetrate into the sample pores. After the final polyelectrolyte layer was deposited onto the substrate inner surface, an aqueous solution of BSA at a concentration of 150mg/mL

was loaded into the porous sample following the same vacuum-high pressure loading protocol. Following this procedure, the samples were placed in a vacuum oven at 37 °C for 12 h.

4.2.3.7 Close-cell and Partially Closed Morphology

The protocol defined earlier allows for the preparation of porous materials with a symmetric, open-cell porosity, defined as a state in which porosity is maintained throughout the material, from center to surface. In order to limit the external surface area available for release, a closed-cell morphology, including a porous core and a solid skin at the surface, was created by immersing the porous PLA sample into chloroform, a solvent for polylactide. This results in an external skin on the sample surface and thus seals the outer surface. The skin thickness can be controlled via the immersion time. Increasing this immersion time will lead to a thicker skin, and also decreases the sample dimensions available for loading. In this study, all samples were immersed in chloroform for 5 s and the skin thickness was observed by SEM. After drying the sample for 24h, two strategies were applied to create a partial opening on sample. In one case, closed cell cylindrical samples were cut at one end with a razor blade resulting in a sample with only one base of the cylinder being open and an open area of 12%. In another case, cylindrical samples with a closed-cell morphology were placed in the sample holder in the microtome, at 45° to their axial direction, and then cut 120 ± 20 μm from the edge. This results in a much more closed cell sample where only one corner of the cylindrical device is open with an open area of 2%. All the sample dimension changes were recorded in order to recalculate the BSA remaining inside the sample. The open surface areas of these two strategies were measured via an x-y digitizing table.

4.2.3.8 In Vitro BSA Release Studies

Cylindrical BSA carriers were immersed in 3 mL of Milli-Q water in a spectrophotometry cell properly covered and sealed. Incubation took place at 37 ± 0.3 °C with constant vertical shaking at 5 rpm. At predetermined time intervals, the concentration of BSA released from the carrier and dispersed into the medium was monitored using a UV-Vis spectrophotometer (Beckman Coulter DU 640) at a wavelength of 280 nm. The BSA concentration was derived from a master curve using a series of standards of different BSA concentrations. The estimated error in this release study is ±5%. All the release experiments were repeated at least four times and their results were averaged. The supernatant was also used to determine the pH value in the incubation medium at the end of each release study.

4.2.3.9 Protein Distribution Study via X-ray Photoelectron Spectroscopy (XPS)

XPS spectroscopy was used in order to determine the protein distribution within the porous PLA devices at various times of release. The experiments were performed on an ESCALAB MKII instrument (VA Scientific Limited, UK) to characterize the relative nitrogen concentration in the BSA within the porous substrate loaded with protein. An Mg Kα X-ray source (hυ = 1253.6) with an analyzer pass energy of 100 eV was operated at 20 mA and 15 kV. All the measurements presented here were performed inside an ultra-high-vacuum (UHV) chamber with a base pressure of less than 10^{-9} Torr. In all cases, the binding energy of the C 1s core levels (286.5 eV) was used as an internal standard to distinguish between band-bending and chemical

shifting. Porous samples directly loaded with BSA without surface modification by LbL, and samples modified with 5 layers of polyelectrolytes and closed-cell with one-end open were chosen for study. The protein distribution within these porous PLA substrates was studied at 0%, 25% and 50% BSA cumulative release percentage. Samples for XPS analysis were all sectioned from the middle as well as 1 mm above and below the midline. This results in three internal surfaces from three levels of each sample. The XPS, equipped with a filter of 500 μm in diameter, was performed at four points across the diameter of these internal surfaces of sectioned porous substrates. Each point was scanned 64 times in order to limit the background noise. After that, the data was analyzed by VA Avantage software which gave the nitrogen composition and hence the relative BSA concentration at each point.

4.2.4 Results and Discussion

4.2.4.1 Porous Device Morphology

The melt blending of PLA/PS 50/50 (V/V) followed by the selective extraction of the PS phase in the blend by selective solvent dissolution produces a porous PLA with an almost completely interconnected porosity of highly controlled pore size and void volume. Gravimetry measurements following the selective extraction of PS indicate that the continuity of the porous structure (extracted PS phase) for all samples is greater than 90% (data not shown here), as observed previously (Salehi et al. 2008).

The pore-size of the porous PLA substrate after selective solvent extraction was examined both qualitatively by SEM and quantitatively, by BET testing. The porous morphology of the PLA/PS, as examined by SEM, is shown in 4.4a and indicates a fine continuous porosity in PLA. Since it is very difficult to quantify a three-dimensional porosity via two-dimensional microscopic observation, BET testing, following a previously developed protocol (Li. et al. 2002), was used. The pore size diameter estimated in this way is 1.6 μm and the internal surface area of the device is 1.526 m^2/g.

4.2.4.2 BSA Loading Effects

In order to determine the influence of device dimensions on the loading of BSA, porous PLA cylinders with the same diameter but with lengths varying from 2 mm to 6 mm were prepared and loaded with 150mg/mL BSA solution in water. These samples (all with unmodified surfaces) were loaded with BSA according to the protocol outlined in the experimental and then dried. The dried samples were weighed and the mass increases due to BSA loaded into the samples were plotted against the corresponding sample length (Figure 4.2).

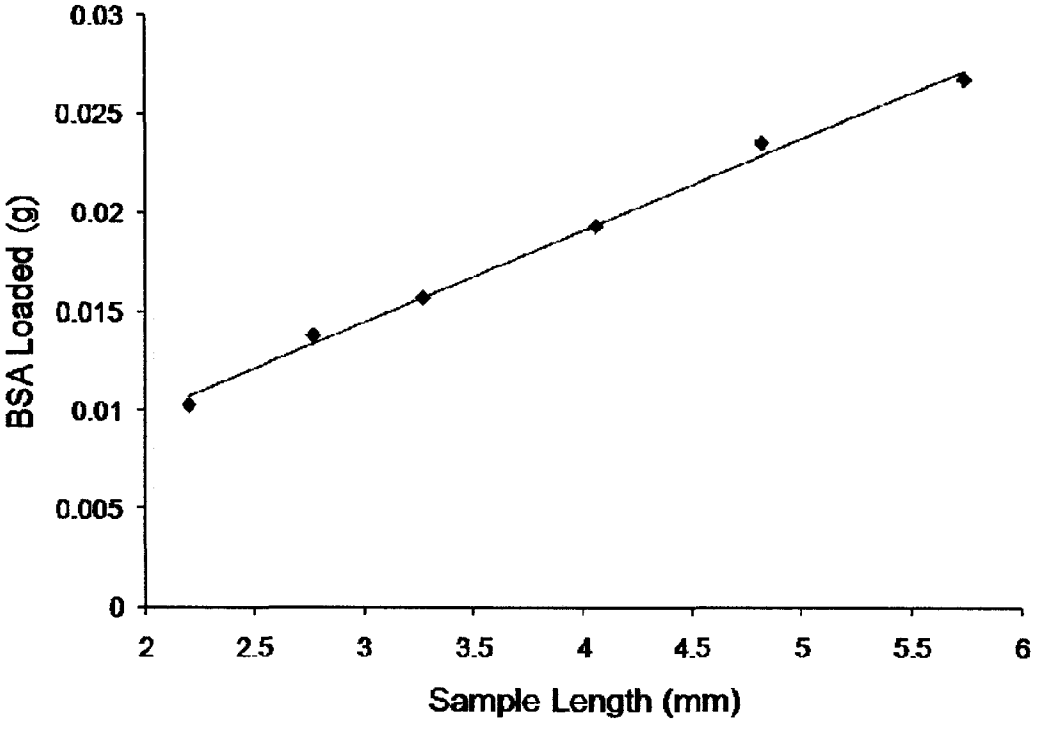

Figure 4.2 Mass of BSA Loaded into Samples with Lengths from 2 to 6 mm.

The results show a linear relationship between these two, indicating that the BSA solution was able to penetrate into the fine pores throughout the PLA substrate, irrespective of its length. The amount of BSA loaded, with respect to the initial empty weight of the device, was calculated in the following way:

$$\text{Amount Loaded (\% wt increase)} = \frac{W_b - W_i}{W_i} \times 100 \qquad (4.3)$$

in which W_i and W_b are the sample weight before and after BSA loading, respectively. For all the samples in this study, the amount loaded is 14.5 ± 1.2 %.

For the samples deposited with polyelectrolyte prior to BSA loading, the loading efficacy did not exhibit any detectable differences. This is due to the fact that the polyelectrolyte adsorbed onto the PLA occupies a minimal volume in the interconnected tortuous channels throughout the sample. Note that in a previous study it was found that the polyelectrolyte layer thickness as measured by ellipsometry on a flat model surface, was only 1.75 nm (Salehi et al. 2008). However, Alam et al. (Alem et al. 2007) reported that the thickness of polyelectrolyte layers deposited onto the internal surface of a porous system could, in some cases, be as high as 100 times greater as compared to flat surfaces due to confinement effects on polyelectrolyte multilayer growth inside small pores. It should be noted that in their case the pore sizes examined were in nanometer-scale, which is significantly smaller than this work.

4.2.4.3 Surface Modification via Layer-by-layer Technique

We used the sequential deposition of oppositely charged polyelectrolytes onto the surface, using an LbL deposition technique, to modifiy the hydrophobic PLA surface properties. Since BSA possesses an overall negative charge, LbL deposition allows for an excellent opportunity to prepare a highly uniform positively charged surface prior to BSA loading. The overall objective is to significantly reduce release times through these surface interactions. In this study, positively charged PDADMAC and negatively charged PSS were used as the polyelectrolyte pair. Either three or five layers of polyelectrolyte, in total, were deposited onto the substrate inner surface. PDADMAC was chosen as the first layer since it has been shown in previous work from our laboratory that it has a much higher affinity for the PLA surface than PSS (Salehi et al. 2008). Layers of alternate charge were deposited in turn, but in all cases the PDADMAC layer was deposited last in order to ensure that the porous surface displayed a uniform positive charge.

In this study, the LbL surface deposition was applied to porous PLA substrate with averaged pore-size of 1.56 μm. As discussed before, the loading experiment revealed a high level of interconnectivity within the polymer device and aqueous solution was highly accessible to most of the available porous volume. The BSA solution in water, which has a higher viscosity (0.0189 Pa•s at 25 °C) than that of the polyelectrolyte solution in water, can penetrate into the fine pores throughout the PLA substrate with the aid of the vacuum-pressure loading apparatus. Hence the fine

pores are also highly accessible to the two polyelectrolyte aqueous solutions used. After a 4-hour loading process and following a 4-hour washing step for each deposited layer, the porous substrates were dried and weighed.

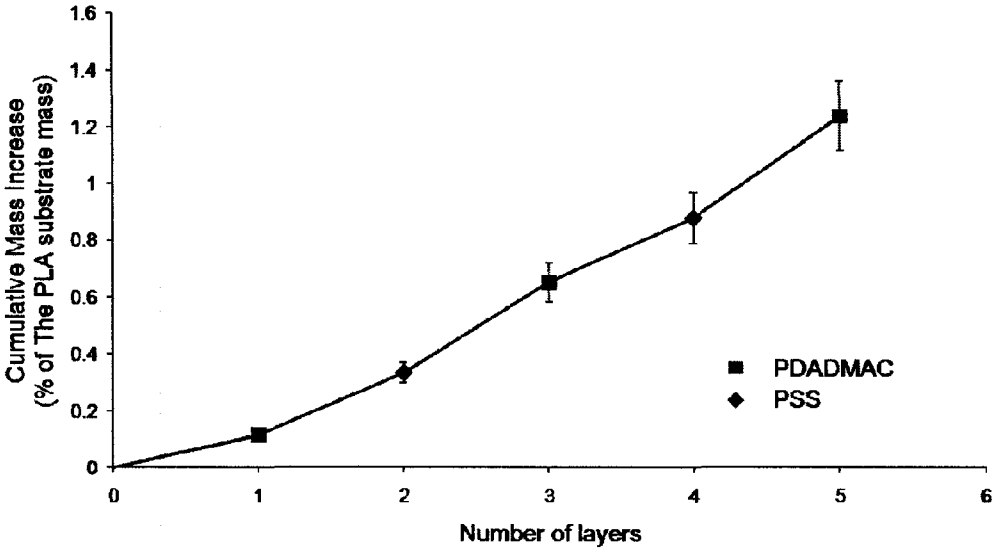

Figure 4.3 Deposited Polyelectrolyte Mass as a Function of the Number of Layers Deposited by the LbL Approach. Mass increase was compared to blank PLA substrate in percentage. ■ and ♦ stand for PDADMAC and PSS, respectively.

Figure 4.3 provides strong evidence for the alternating polyelectrolyte PDADMAC/PSS assembly up to 5 layers obtained by gravimetric measurements. In this mass increase curve, the different slopes between the first PDADMAC layer deposition onto PLA and the following PDADMAC deposition onto the previously deposited PSS layer, indicate the different strengths of the electrostatic interaction between PDADMAC/PLA and PDADMAC/PSS pairs. The step-like slope for PDADMAC and PSS is due to their different densities. As can be seen from the

figure, the amount deposited in a particular step is highly uniform, indicating excellent repeatability and the formation of highly uniform surface layers. Experimental results shown here are in good agreement with data reported by Roy et al. (Roy et al. 2006).

4.2.4.4 Partially Closed-Cell Strategy

Using the protocol outlined in the Experimental, a completely open-cell cylindrical PLA sample is obtained. This sample possesses a continuous multi-channel porosity throughout, from the core of the device right up to the surface. On the other hand, by definition, closed–cell systems possess a continuous porous structure only in the core with a non-porous structure at the surface. Closed–cell structures are potentially interesting since they are an approach which can be used to prolong delivery times and also mediate the burst release effect (Salehi et al. 2008). The partially-closed cell approach described below is quite different from the previous studies described in the Introduction.

In the current case a partially closed cell device would be expected to increase tortuosity inside the sample and significantly increase the drug release pathway within the device. In order to limit the open surface area of the porous devices used in this study, we applied a simple closed-cell strategy briefly introduced in previous work from this laboratory (Salehi et al. 2008). In In that study, we showed that the whole sample could be completely sealed and that BSA release was totally eliminated over a 20 day period. In this work we used chloroform, a solvent for

polylactide, and hence form an external skin on the entire sample surface. By immersing the porous PLA substrates into chloroform for 5 seconds, it was found that the skin thickness can be controlled to 70 ±20 μm, with a decreased average substrate diameter of 2.90 mm (as compared to 3.00 mm). As shown in the cross-section views in Figure 4.4b and 4.4c, the skin thickness is very uniform over the entire sample. Increasing the immersion time results in a thicker skin, and also a smaller sample dimension.

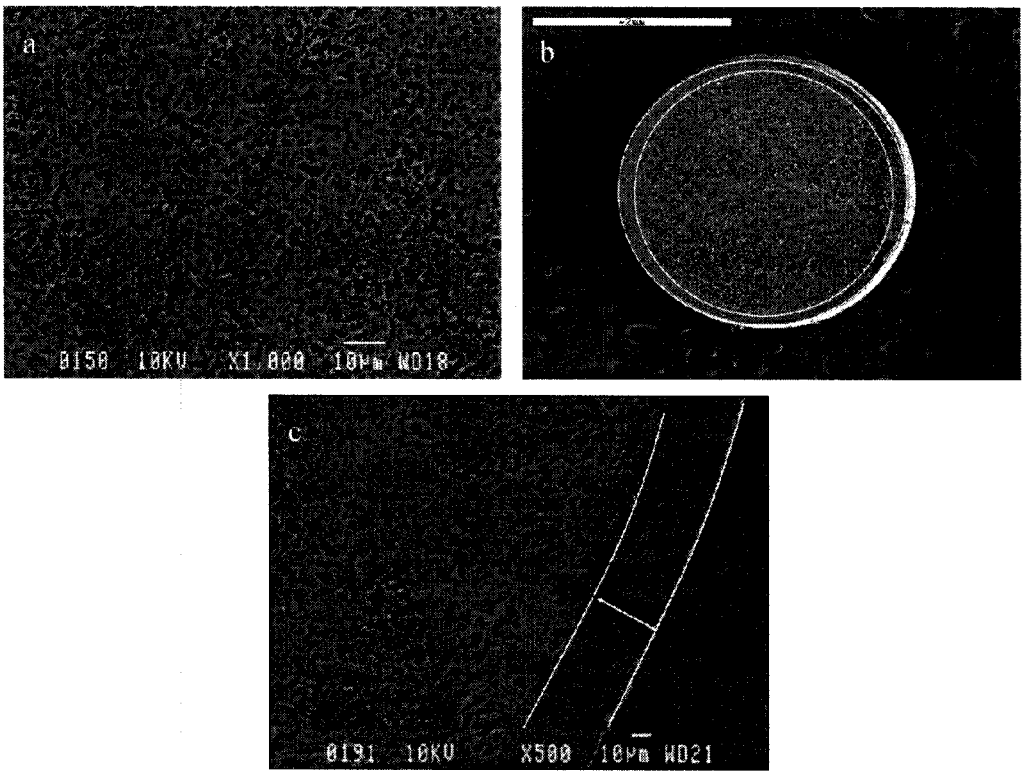

Figure 4.4 SEM Images showing the Porous PLA Devices

a) Porous PLA (after PS extracted), the white bar stands for 10 μm;

b) Porous PLA in closed-cell form (one end open), showing the cross-section view from top, the white bar stands for 2 mm;

c) Porous PLA in closed-cell form, showing the skin thickness, the white bar stands for 10 μm.

Two strategies were applied with respect to the preparation of partially closed samples. In one case, cylindrical samples, already loaded with BSA and with a completely closed-cell structure were cut at one base using a razor blade to result in a one-end opening, as shown in Figure 4.4b and 4.4c. In this case, while one end is fully open, the other base and side surfaces of the cylindrical sample are still sealed by a skin with a thickness of 70 μm. In another case, in order to reduce the open area even further, fully closed cylindrical samples were cut only at the edge of one base. In this case, samples with a closed-cell morphology were cut 120 ± 20 μm from the edge using microtomy at 45° to the axial direction, creating a corner opening as shown in Figure 4.5a (top view) and 4.5b (side section view). Thus, only a very small opening is created at one corner of one end of the substrate. The open surface areas of the different samples were measured via semiautomatic image analysis (Salehi et al. 2008). The open surface area of the standard fully 100% open-cell porous PLA sample (4.0 mm in length and 3.0 mm in diameter) is 25.92 mm^2. The sample with one base open (3.8 mm in length and 2.9 mm in diameter) was 3.15 ± 0.022 mm^2 resulting in a 12% open area. The open-corner samples had an open area of 0.54 ± 0.095 mm^2 resulting in a 2% open area. All the sample dimension changes during the closed-cell and re-opening procedures were recorded in order to recalculate the quantity of BSA remaining inside the sample.

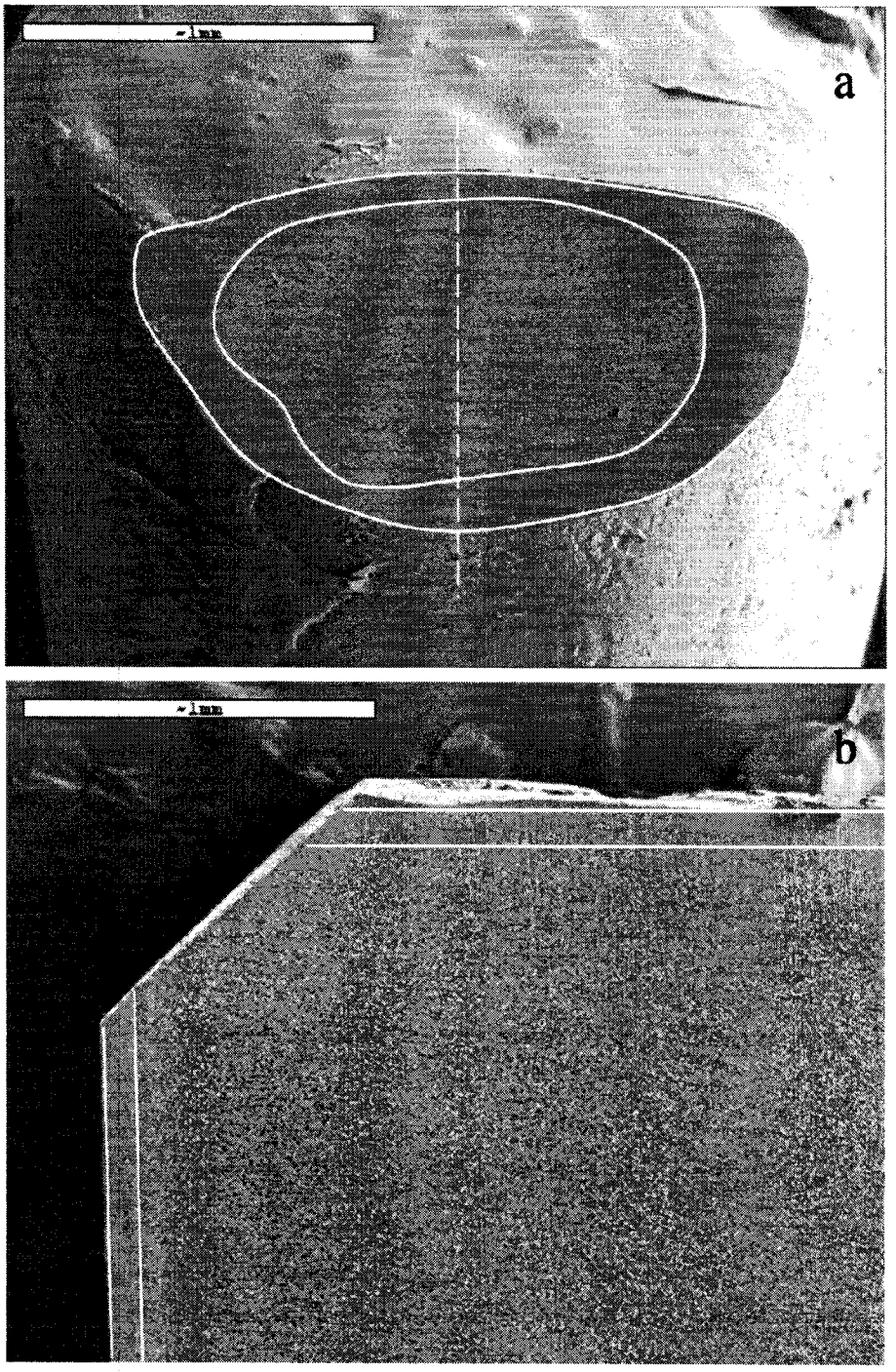

Figure 4.5 SEM Images showing Porous PLA in Closed-cell Form

a) Top view of the opened area, the white bar stands for 1 mm;

b) Sectioned side view of the opened area, following the dashed line in a), the white bar stands for 1 mm.

4.2.4.5 In-Vitro Release of BSA from Partially Closed Cell Porous Devices

Bovine Serum Albumin (BSA), which is well characterized and intensively studied in other groups, is widely used as a model bioactive compound. In our study 150mg/mL BSA solution in water was loaded into the porous PLA substrate and dried. Previous studies (Salehi et al. 2008) had shown that a change in the testing medium from phosphate buffer solution (PBS, pH = 7.4) to Milli-Q water did not exhibit a significant effect on the final release profiles (Salehi et al. 2008), thus Milli-Q water was used as the in vitro release medium. In this study the pH value of the release medium was measured at the end of all in-vitro release tests and recorded as 7.0 ± 0.25 in all cases, indicating no significant change in the pH value of the medium during the release test. Although the byproducts from PLA degradation are acidic in general, this process is very slow and takes longer than months to have an appreciable degradation which is much longer than the release time period in the present case. Furthermore, BSA maintains its normal conformation at a pH value between 4.3 and 8 (Foster, 1977), where the medium pH value in this study lies.

Table 4.2 lists all the characteristics of the BSA release profile from various samples.

Table 4.2 BSA Release from PLA Substrates

[1] Best fit linear regression between zero time point and all data collected to 2 hours

[2] Total amount released by the end of the experiment

L0, L3 and L5 stand for 0, 3 and 5 layers of polyelectrolyte surface deposition, respectively. E and C stand for samples with one-end open and samples with one corner open, respectively

Porous Polymers	Burst Release Rate [1] (Release%/hour)	BSA Release Amount after 2 hours (%)	Final Release Percentage [2]
L0	50.1	91.1	97.8
L0E	48.0	62.6	96.0
L0C	37.4	49.9	95.0
L3	32.7	42.9	90.1
L3E	24.6	39.9	90.6
L3C	17.3	24.1	93.9
L5	25.4	24.7	93.5
L5E	15.7	22.5	86.4
L5C	12.7	18.5	89.2

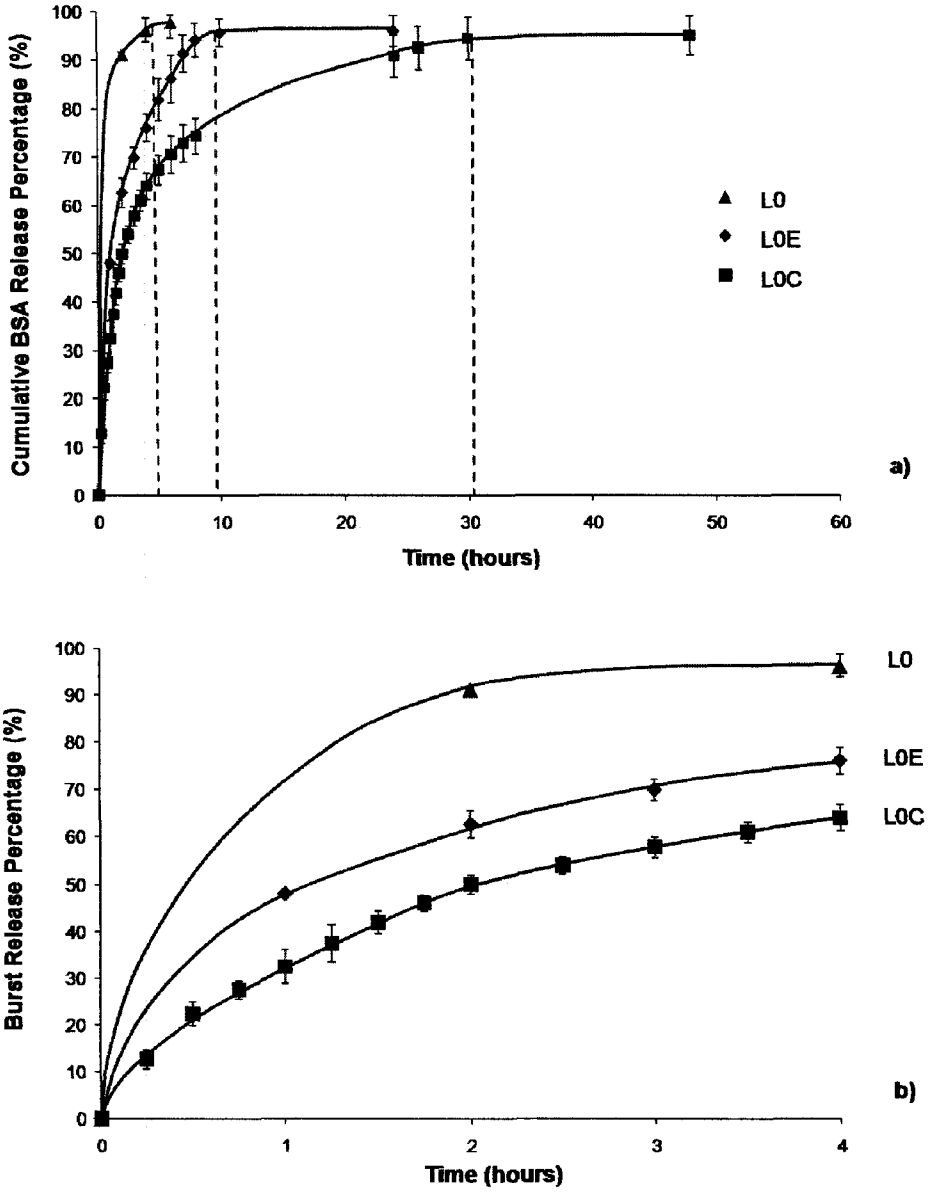

Figure 4.6 Effect of a Partially Closed-cell Structure on the Drug Release for Unmodified Porous PLA Samples

L0: unmodified Porous PLA with open surface area of 25.918 mm^2; L0E: Close-cell structure with one end open, open surface area 3.15 ± 0.022 mm^2; L0C: Close-cell structure with one corner open, open surface area 0.54 ± 0.095 mm^2.

a) Cumulative BSA release percentage against release time.

b) Burst release within first 4 hours of the release test.

Figure 4.6a shows the effect of a partially closed-cell strategy on the complete release profile while Figure 4.6b shows the details of those same experiments for burst release within the first 4 hours of the test. In Figure 4.7a, the cumulative BSA release percentage for each sample at 2 h and 4 h were plotted against the open surface area, showing the clear relationship between these two. In Figure 7b the total release time was also plotted against the open surface area. The results indicate that for the 100% open-cell PLA device (L0) without any surface modification, there is a very strong burst effect with over 90% of BSA releasing in the first hour (Fig.4.6a). The cumulative release percentage reaches close to 100% release within 3.5 h. In the case of the partially closed-cell PLA devices with one end open (sample L0E) and one corner open (sample L0C), Figure 4.6b shows that there is a significantly lower burst with a 30% and 41% reduction in burst at 2 hours respectively. Figure 4.6a shows that the total release time was extended by approximately 3 times for the open end, L0E sample, and 9 times for the open corner, L0C one, respectively. These results clearly indicate the successful application of a closed-cell strategy in controlling and attenuating release phenomena in these systems. It also clearly indicates that the partially closed samples are still able to fully discharge all the BSA (close to 100% release) indicating the high degree of interconnectivity of the channels in the device. Evidently, the two partially closed samples significantly

increase tortuosity effects through the device by restricting the route through which BSA can diffuse out of the sample. This significantly increases the release pathway of the BSA in the device. Figure 4.6b shows that the open surface area and the total release time are related through a power law relationship. As the open surface area decreases, the total release time increases by a power of -0.50.

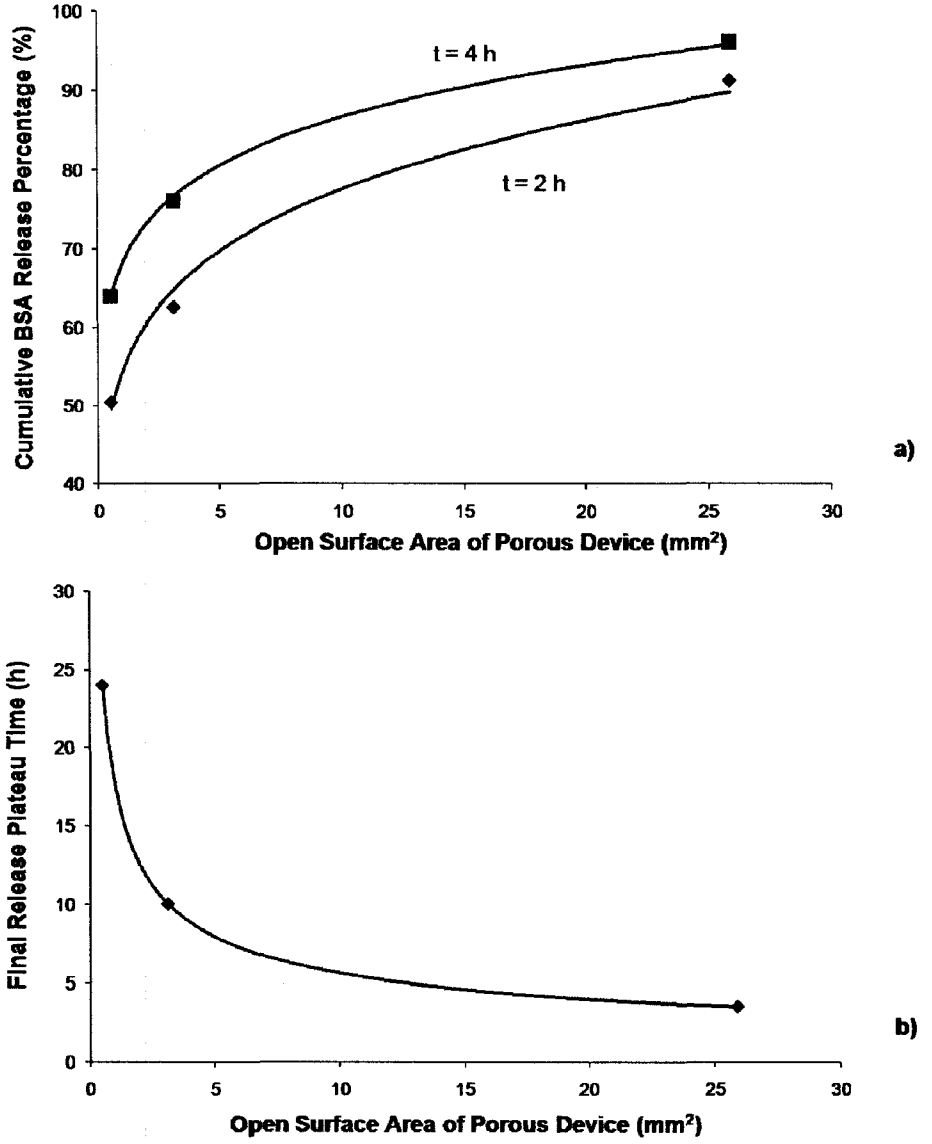

Figure 4.7 Relationship between Open Surface Area and Release Profiles Characteristics

a) Cumulative BSA release percentage against opened surface area at time 2 hours and 4 hours of the release test.

b) Total release time against opened surface area.

4.2.4.6 Combined Effect of PLA Surface Modification and a Partially-Closed Structure on Release

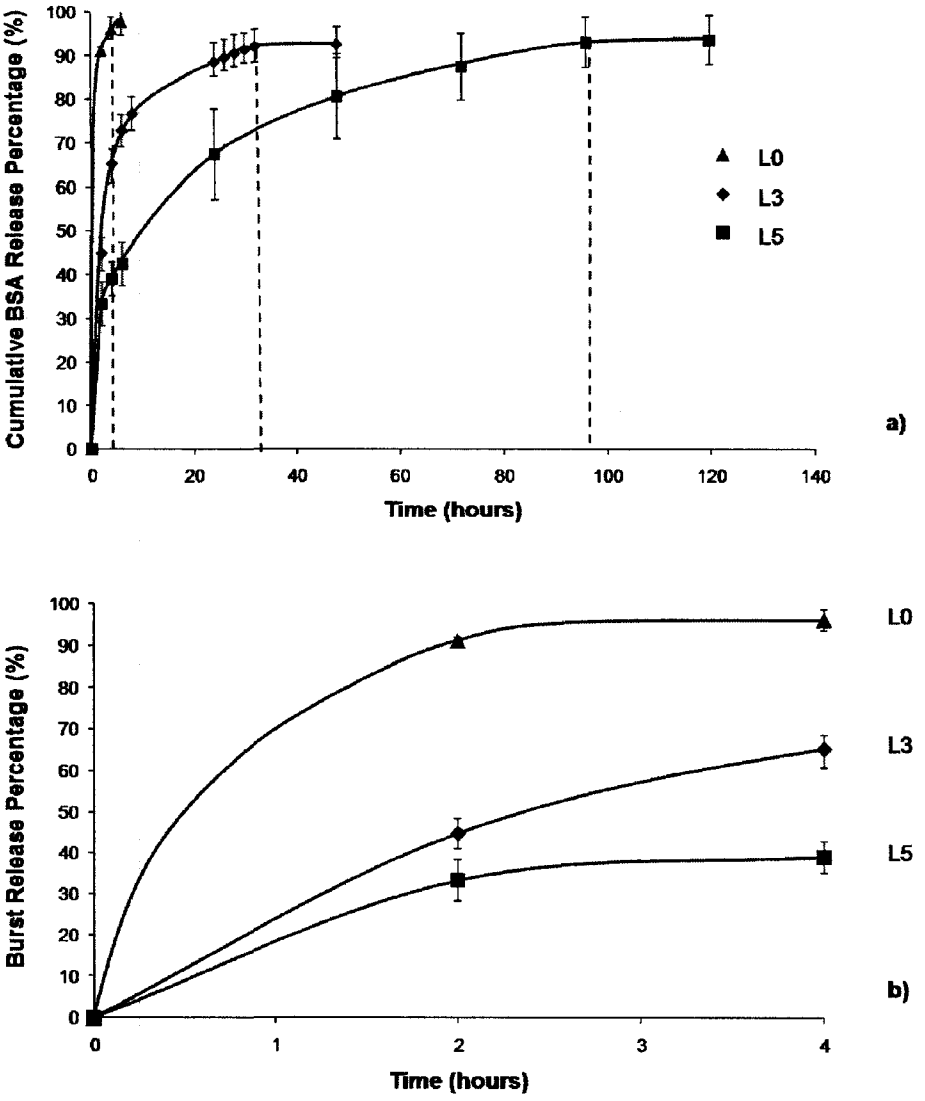

Figure 4.8 Effect of Number of Polyelectrolyte Layers on the Drug Release

L0, L3 and L5 stands for 0, 3 and 5 layers of polyelectrolyte surface deposition, respectively.

In Figure 4.8a, as a baseline reference we show the BSA release profile from the 100% open-cell porous PLA deposited with 0, 3 and 5 layers of polyelectrolyte (samples L0, L3 and L5 respectively). As discussed above the porous PLA without polyelectrolyte surface deposition (PLA/BSA) demonstrates a strong burst effect with complete BSA release within 3.5 h. In the case of 100% open-cell porous PLA loaded with 3 layers of polyelectrolyte (PLA/PDADMAC/PSS/PDADMAC/BSA), the BSA burst release percentage in the first 2 hours was reduced nearly by half, and the total release time was extended to 30 h. At pH 6.8-7.2, BSA with an isoelectric point of 4.7 carries a net negative charge (Foster, 1977). For this reason, the positively charged PDADMAC outer layer provides an electrostatic attraction which prompts and enhances the adsorption of negatively charged BSA on the modified PLA surface. These effects clearly have a determining effect on both the burst and overall release time of BSA from the device. For the 100% open cell porous PLA loaded with 5 layers of polyelectrolyte (PLA/PDADMAC/PSS/PDADMAC//PSS/PDADMAC/BSA), the release profile was improved even more significantly. The BSA release percentage after the first 2 hours was reduced to one-third that of the open cell, unmodified L0 sample. Furthermore the total release time of the L5 sample is extended to approximately 96 h, as shown in Figure 4.8a. These results indicate that the number of polyelectrolyte layers also plays a very important role. Note that in both the 3 layer and the 5 layer system, PDADMAC is the outer layer, nevertheless, the release performance of these

two systems is very different. This can be explained by the uniformity of the charge of the outer PDADMAC layer. It is well known in the LbL process that increasing the number of layers results in a more organized structure and more well-defined charges associated with each layer. The results of that are clearly seen in these release studies. Thus the increased BSA affinity for the 5-layer modified PLA surface results in a significantly increased release time and much lower burst release values. Other groups (Gergely et al. 2004) have also reported that hydrophobic and electrostatic interactions are the main factors governing the affinity between BSA and polyelectrolytes (Kaibara et al. 2000). It should also be noted in Figure 4.8a that the 5-layer system results in the somewhat lower overall release percentage of 92% at the plateau value as compared to 97% for the unmodified system. Clearly in the case of the 5-layer system, some of the BSA becomes immobilized within the device. Since significant quantities of BSA are present in this device, one would also expect that as the BSA is located farther from the PDADMAC surface layer, in the normal direction, it would behave more as free BSA. Hence, in the case of these devices with a modified PLA surface, one could classify the BSA as being in three possible categories: free, interacting and bound. The free BSA would constitute the principal component of the burst release, while the bound BSA can be determined by the plateau value at complete release. The case of the completely open-cell, unmodified PLA release profile is essentially a study of the release of free BSA since the interactions with PLA would be expected to be minimal..

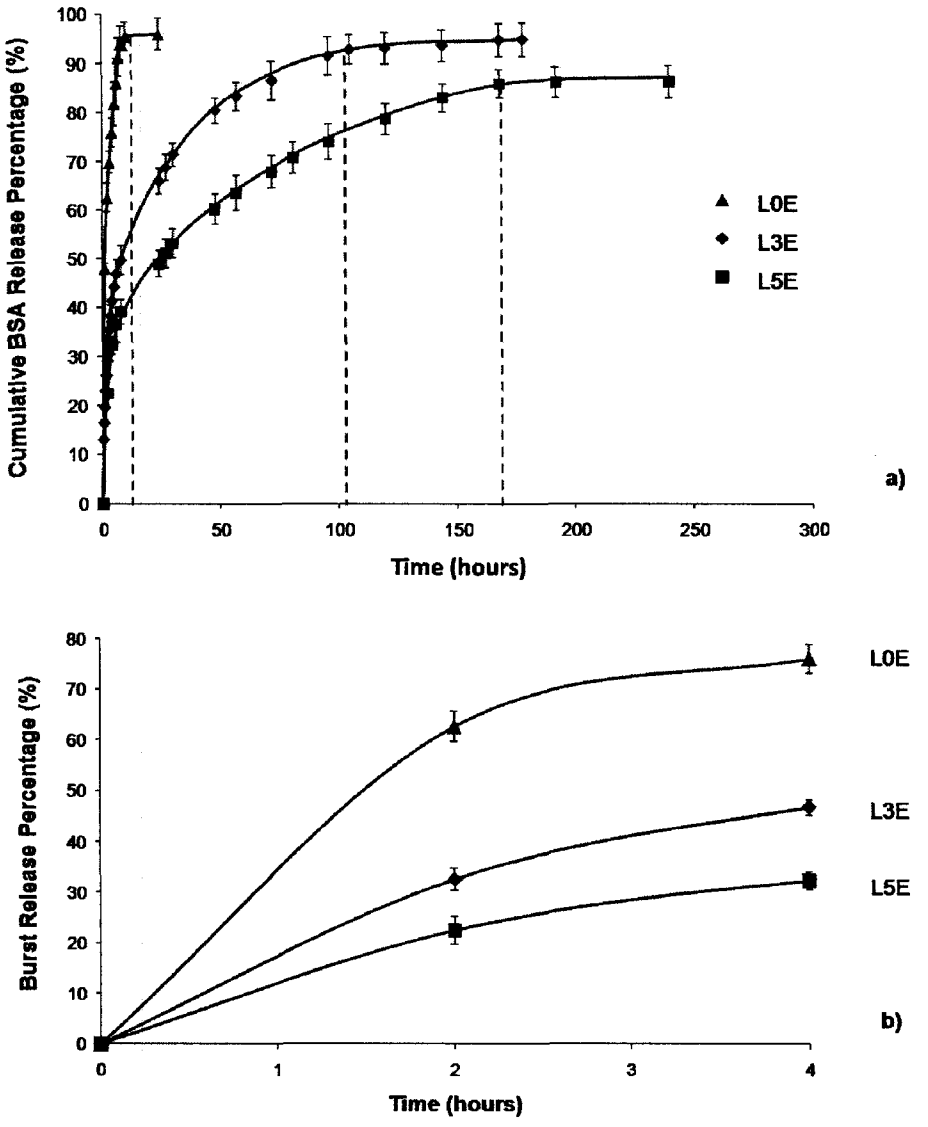

Figure 4.9 Effect of a Partially Closed-cell Structure (One-end Open) on the Drug Release for Modified Porous PLA Samples

L0E, L3E and L5E stand for one-end opened samples with 0, 3 and 5 layers pof polyelectrolytes surface deposition, respectively.

In this part the focus is on the influence of the surface modification of the porous PLA device in association with partially closed structures. Figure 4.9a showed the BSA release profile from open-end samples with a surface modification of 0, 3 and 5 layers of polyelectrolyte, respectively (samples L0E, L3E and L5E).

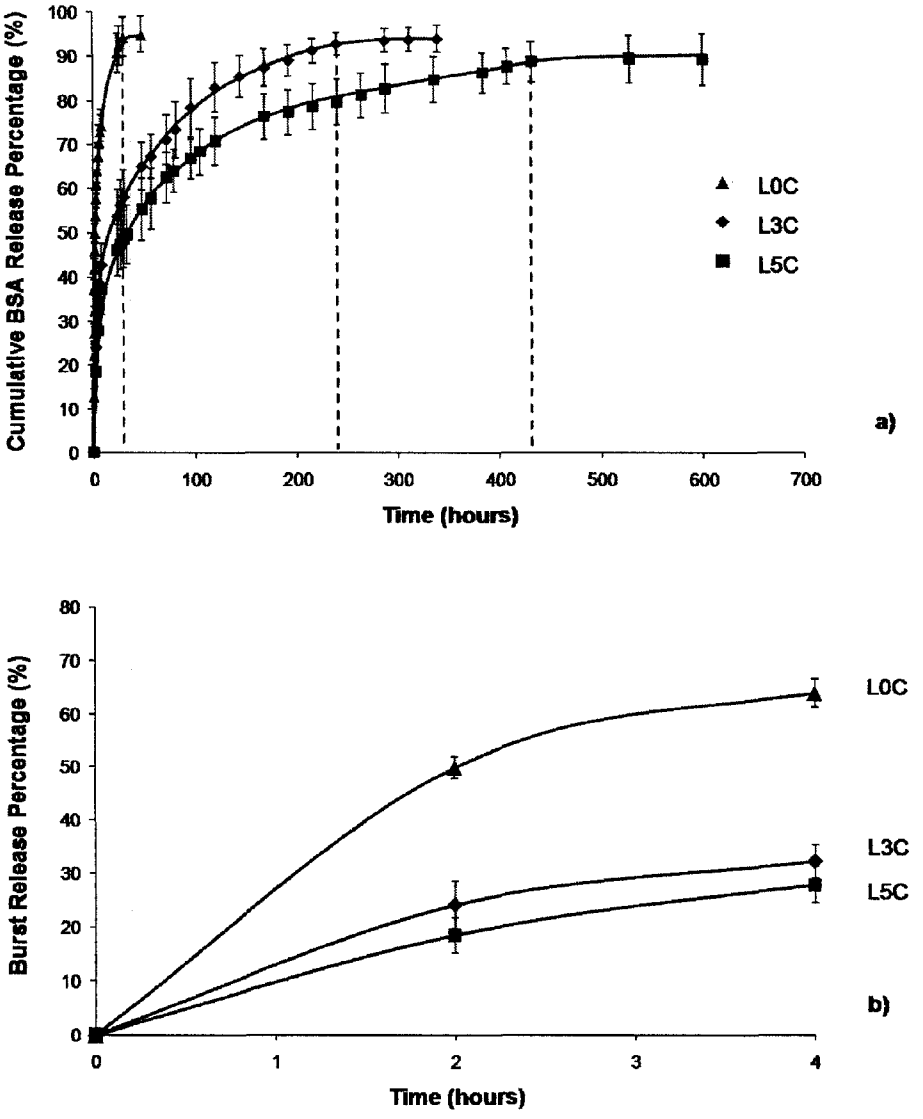

Figure 4.10 Effect of a Partially Closed-cell Structure (One-corner Open) on the Drug Release for Surface Modified Porous PLA Samples

L0C, L3C and L5C stand for one-corner opened samples with 0, 3 and 5 layers pof polyelectrolytes surface deposition, respectively.

Figure 4.10a shows the BSA release profile from the open-corner samples also with 0, 3 and 5 layers of polyelectrolyte, respectively (samples L0C, L3E and L3C). Since sample L5C (5 layers of polyelectrolyte and the open-corner) produced the best performance in terms of reduced burst and extended release times. Figure 4.11 was plotted to show the separate effects of surface modification and partially-closed cell strategies (L5 and L0C), and also their effect in combination (L5C).

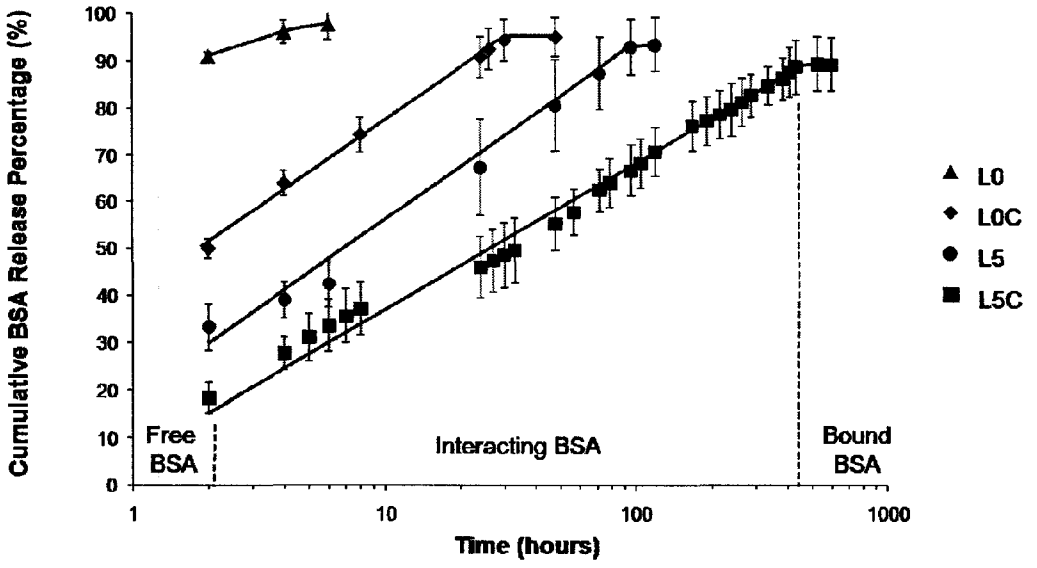

Figure 4.11 Effect of Surface Modification and Partially Closed-cell Strategy

Clearly both PLA surface modification and partially-closed structures result in remarkable effects and, in combination, dramatically reduce the burst release and significantly extend the total release times. The L5C sample shows a cumulative BSA burst release percentage after 2 hours which is 18.5%, as compared to 91.1% for the surface unmodified 100% open-cell PLA substrate(L0 sample) (Figure 4.11). Furthermore, the L5C sample demonstrates a total release time extending up to 18

days as compared to 3.5 h for the baseline L0 sample. In the release profile of the sample with 5 layers of polyelectrolyte and open-corner, three stages for the release can be defined; 1) burst release which shows a relative strong and fast release of BSA in the first 2 hours, 2) steady state release in which the BSA gradually achieves a much more stable and almost sustained release (3.5 hours to 17 days); and 3) a leveling-off part after 18 days where the BSA within the device is almost depleted. Although an upturn in the late stages of release due to the matrix degradation has been reported elsewhere, this was not observed in our case, confirming that the PLA device remains stable within the time scale of these experiments as expected.

4.2.4.7 Study of Protein Distribution inside the Sample via XPS

In this part of the work, the BSA distribution throughout the porous sample is examined for both the L0 and L5E sample at various release percentages in order to understand the underlying mechanism of release.

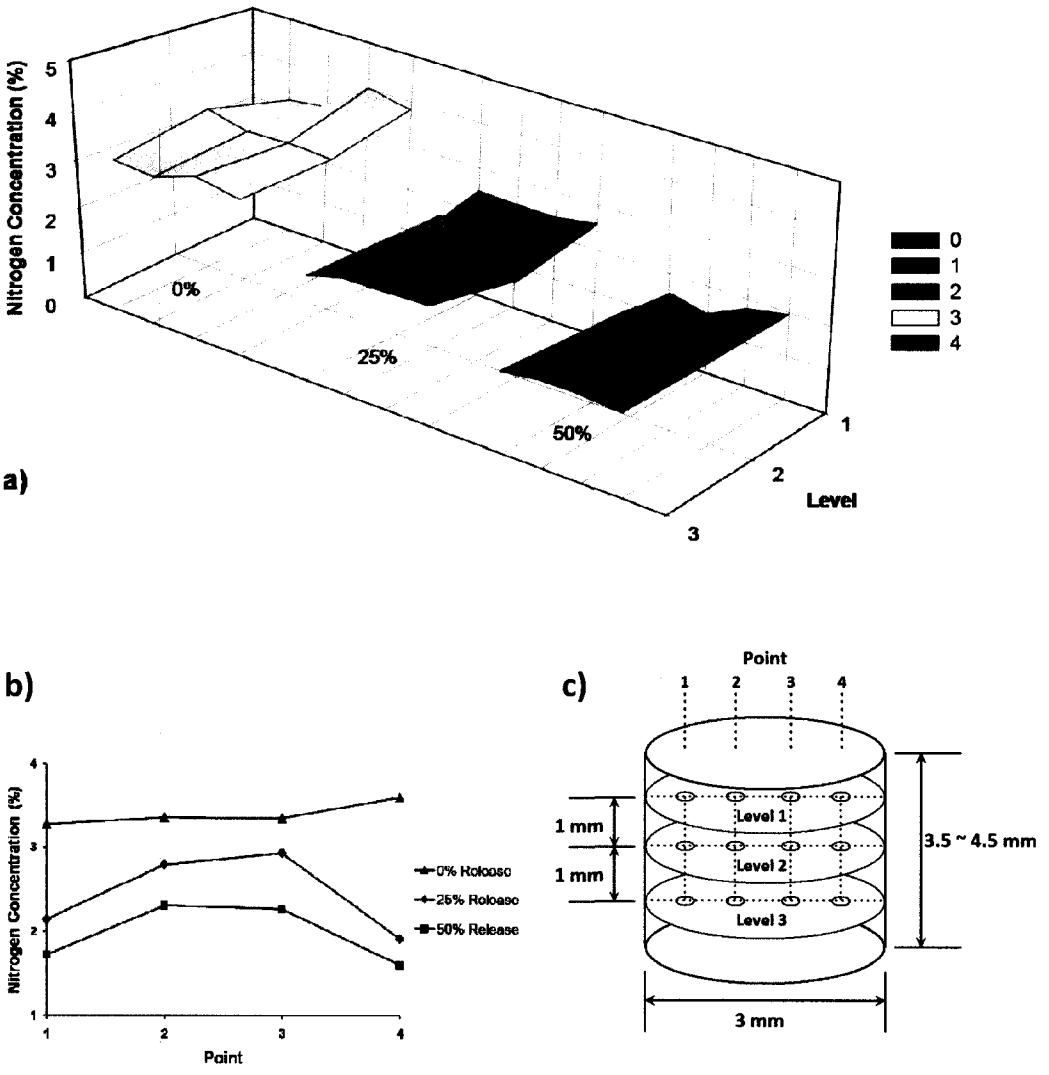

Figure 4.12 BSA Distribution inside the Unmodified Porous Template with Open-cell

a) BSA distribution of unmodified PLA substrate with open-cell, BSA release in all directions

b) Nitrogen concentration from sample center to surface at level 2 shown in c), when 0%, 25% and 50% cumulative BSA released.

c) Schematic image of a cylinder sample, showing the points where the XPS data was collected. Dash lines show the inner porous region of a one-end-open closed-cell strategy, and the arrow on top surface shows the opening.

The BSA solution loading efficacy study (Figure 4.2) shows that the protein distribution was homogeneous along the axial direction of the cylinder porous PLA substrate. For further confirmation of the BSA distribution, X-ray photoelectron spectroscopy (XPS) measurements were carried out to measure the surface composition inside the cylinder porous samples. In this study, a standard cylindrical sample was sectioned to create three internal surfaces classified as levels 1, 2 and 3 (Figure 4.12c). Also, the surface atom composition at four different points across the diameter of these internal surfaces was examined (Figure 4.12c). The nitrogen concentration, which represents the protein concentration inside the sample, was used as the probe for BSA since PLA does not contain any nitrogen atoms in its structure. The polyelectrolytes do contain nitrogen atoms, however, during their addition to the porous PLA, they were subjected to a vigorous four hour water wash after the addition of each layer in order to remove any unbound polyelectrolyte (20 hours total wash time for 5 layers). Furthermore, the polyelectrolyte layers are held together by very high electrostatic attraction effects. For these reasons, the levels of polyelectrolyte lost during BSA release are expected to be negligible.

The results for the 100% open cell, non-surface modified L0 sample loaded with BSA are shown in 3-D in Figure 4.12a. The results at 0% BSA release demonstrate a flat surface clearly indicating a homogeneous BSA distribution inside the cylinder, from top to bottom and from side to center. Also shown in this figure are BSA distributions inside the L0 sample, with 25% and 50% BSA released, respectively. The results after release clearly demonstrate a concentration gradient from the center of the device to the outer walls. This concentration gradient in the L0 sample is also shown in Figure 4.12b where the nitrogen concentrations at four points across level 2 for 0%, 25% and 50% cumulative BSA released are shown. At 25% BSA released, the overall nitrogen concentrations have dropped as compared to 0% released and a concentration gradient showing a higher concentration in the center of the device is evident. At 50% BSA released, the nitrogen concentration in the sample further deceases as expected and again a clear higher concentration of BSA in the center of the porous device is observed.

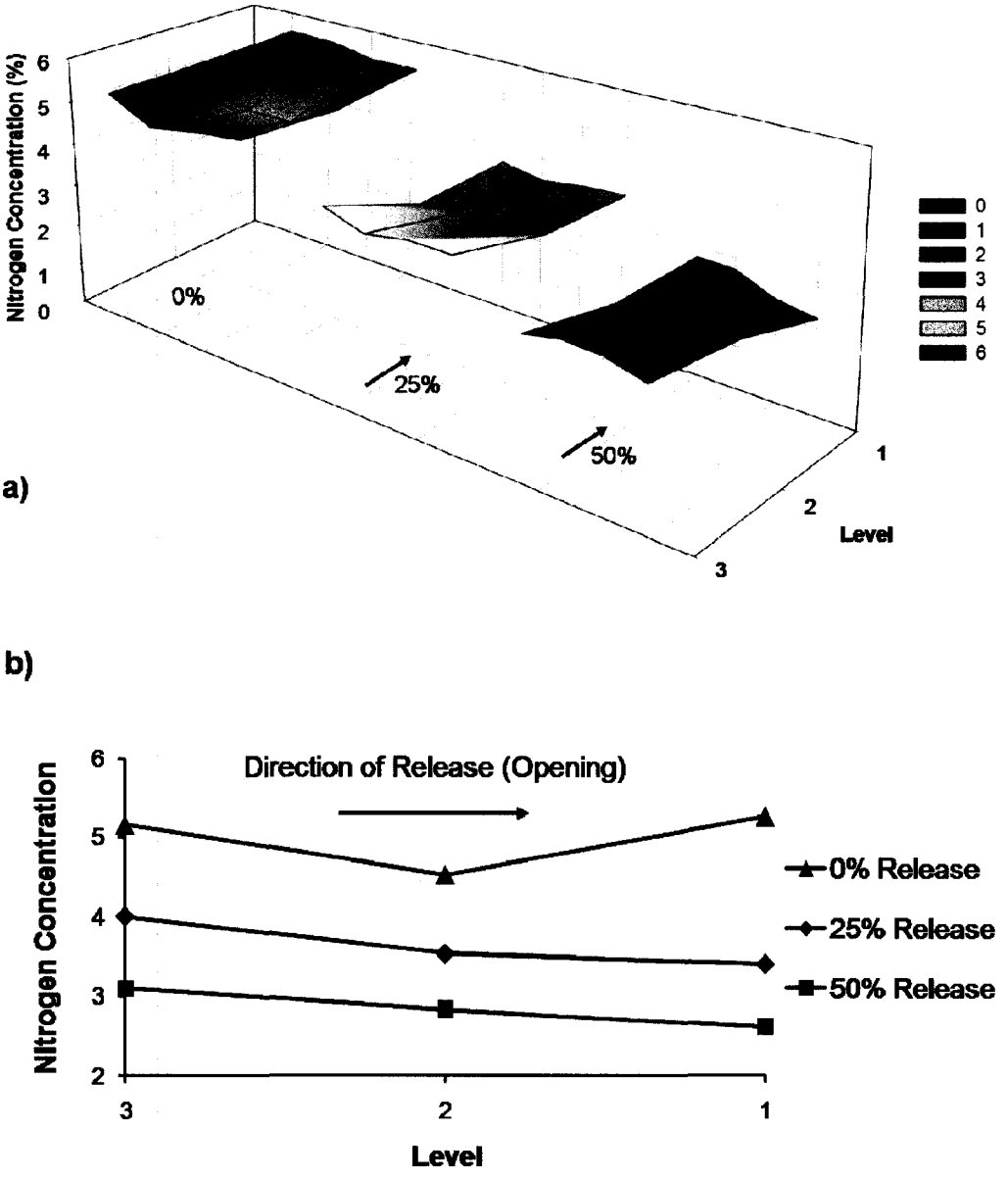

Figure 4.13 BSA Distribution inside the One-end Opened Porous Template with 5 Layers of Polyelectrolyte Surface Deposition

a) BSA distribution of close-cell with one end PLA substrate, preloaded with 5 layers of polyelectrolyte. Arrows show the direction of the opening.

b) Nitrogen concentration from sample bottom to opening along point 2 at all levels shown in Figure 12 c), when 0%, 25% and 50% cumulative BSA released.

Figures 4.13a and b, show the BSA concentrations inside the L5E sample (partially closed-cell sample with one-end open and 5 layers of polyelectrolyte) for 0%, 25% and 50% BSA released. Note the higher nitrogen concentrations for the 0% released sample as compared to the L0 sample in Figure 4.12b. This is due to the nitrogen contribution of the polyelectrolyte layers as discussed above.

It is interesting to note in Figure 13b that the nitrogen distribution inside the L5E sample with 0% BSA released is slightly lower in the center of the porous device. It may be that the surface modification makes it somewhat more difficult to load BSA in the center of the device. Nevertheless, the values are not that different and for the most part indicate that both the loading of BSA and the surface modification of the porous PLA was quite even throughout the sample. For the L5E samples subjected to 25% and 50% release, the trends are clear. There is a clear drop in nitrogen concentration when progressing from 25% released to 50% released, which closely corresponds to the BSA concentration released as measured by UV spectroscopy. Furthermore, a concentration gradient following the direction of release is evident for both the 25% and 50% released samples. Clearly in those cases, the lowest BSA concentration is at the open end.

4.2.4.8 Mechanism of Release

The mechanism of release in this system is clearly diffusion controlled with well defined concentration gradients observed in the direction of release for both the 100% open cell system (L0) and the partially closed sample with one end open (L5E). Clearly the diffusion of BSA out of the device is significantly reduced both by modifying the surface charge of the porous device and by modifying the device to be partially closed cell. The most dramatic results are observed when both of these effects are combined in the L5C sample with a 123 times increase in the total release time as compared to the L0 sample. These effects point towards a diffusion mechanism combined with a sorption/desorption interaction of the BSA with the modified PLA surface.

The BSA released in the first 2 hours of the L0 sample can be defined as an "apparent free BSA". These BSA molecules largely do not interact with the hydrophobic PLA surface. In the case of the unmodified PLA sample (L0), the entire release pattern can be attributed to an apparent free BSA. We use the term apparent since the L0 sample is only being used as a reference point here. Strictly speaking, due to the porous network morphology in the L0 sample, the BSA is not able to experience unrestricted free diffusion. Nevertheless, it provides a good baseline with which to compare the other data. It is interesting to note that the burst period in the L5C sample is about 2 hours which is very similar to the total release time for the L0 baseline reference sample. Thus, we will also define the principal component of the

burst effect (initial two hours of release) for all other samples as being an "apparent free BSA" fraction. In all those cases it is assumed that the BSA molecules released in that time range were either distant enough from the modified surface, or sufficiently close to the outer portion of the device to not be significantly affected by the surface or any partial closing effects. For the L5C sample the $(\text{free BSA})_{app}$ constitutes approximately 18% of the total BSA.

Some of the BSA does not diffuse out of the sample even after long times as seen in the final release plateau for the L5C sample. This BSA will be defined as "bound BSA". The L5C sample shows a final release percentage of 89% as compared to 97% in the L0 reference (see Figure 4.11). This indicates that about 8% of the BSA in the L5C sample is bound BSA.

All the rest of the BSA released from the samples in this study can be defined as an "interacting BSA". In the case of the L5C sample, the interactions come from a combination of both a surface modification of the PLA surface and a partially closed cell structure. These two effects combined create a much longer pathway over which the BSA molecules can interact with the negatively charged modified PLA surface. The result is a dramatic two-order of magnitude effect on the release rate.

Figure 4.11 allows one to separate out the relative contributions of surface modification and the partially closed cell approach. Comparing L0 with L0C and L5 in Figure 4.11 clearly demonstrates that, while both contributions are important, surface modification of the PLA is the more dominant effect in controlling the

release rate than the partially closed cell protocol. The first two hour burst release for L0, L0C and L5 is 91.1, 49.9 and 24.7% respectively. The release percentage ratio at 10 hours release for L0C/L0 is 0.8 and that for L5/L0 is 0.6. The total release time is extended by 9 times for the L0C sample and by 27 times for the L5 sample as compared to the reference L0. When both surface modification of the PLA and a partially closed cell approach are combined, in the L5C sample, the synergy is dramatic with a 5 times reduction in the two hour burst release, a release percentage ratio at ten hours for L5C/L0 of 0.35 and a total release time which is extended by 123 times as compared to the L0 sample. The L5C sample ultimately releases 89% of the total BSA loaded demonstrating the high level of interconnectivity of the micro channels in the porous PLA.

4.2.5. Conclusion

This work has demonstrated that it is possible to exercise a wide range of control over both the initial burst release and the final drug release times from porous PLA devices derived from co-continuous polymer blends. Two strategies were used, a layer-by-layer polyelectrolyte surface deposition approach on the porous PLA surface and the application of a partially closed-cell protocol. Porous PLA substrates with 0, 3 and 5 layers of polyelectrolyte and with open areas of 100%, 12% and 2% were studied both separately and in combination. It is shown that, while both are important, surface modification is more dominant in controlling the release rate than

the partially closed cell approach. When a 5 polyelectrolyte layer surface modification of the PLA and a partially closed cell approach (2% open area) are combined, in the L5C sample, the synergy is dramatic with a 5 times reduction in the first two hour burst release amount and a total release time which is extended by 123 times as compared to the 100% open cell, surface unmodified, reference sample. The L5C sample ultimately releases 89% of the total BSA loaded demonstrating the high level of interconnectivity of the micro channels in the porous PLA. The mechanism of release in this system is clearly diffusion controlled with well defined concentration gradients, as measured by XPS, observed in the direction of release for both the 100% open cell system (L0) and the surface modified, partially closed sample with one end open (L5E). These effects point towards a diffusion mechanism combined with a sorption/desorption interaction of the BSA with the modified PLA surface.

CHAPTER 5

GENERAL DISCUSSION AND CONCLUSIONS

5.1 General Discussion

5.1.1 Effect of Partially Closed-Cell Strategy on BSA Release Profile

The porous polymer substrates can be modified via a partially closed-cell strategy, by dipping the PLA porous device in its solvent to create a skin structure on the external surface, followed by cutting to open part of the surface. This strategy is able to prepare porous devices with only 12% and 2% open surface area, compared to unmodified devices. The reduction of the open surface of the porous device limits diffusion pathway and leads to a better control of the burst release and also extended total release time span from BSA *in vitro* release tests. Compared to the unmodified sample (L0), samples with one end open (L0E, 12% open surface) and those with one corner open (L0C, 2% open surface) reduced the BSA burst release by 29 and 42%, respectively. The total release times were also extended from 3.5 h for the unmodified device to 9 h and 30 h, respectively. This demonstrates that limiting open surface area available for the release medium to diffuse in and the drug molecule to diffuse out is a route to control the BSA burst release and total release time from a porous PLA device.

5.1.2 Effect of LbL Surface Modifications on BSA Release Profile

The porous polymer substrates were modified via a layer-by-layer surface deposition technique with different numbers of polyelectrolyte layers. Keeping positively charged polycation PDADMAC as the outmost layer, 3 and 5 layers of polyelectrolytes were loaded and deposited into the porous PLA in order to modify its surface properties and increase its affinity to proteins. The BSA *in vitro* release from surface modified porous devices shows that with 5 layers of polyelectrolyte (L5) the BSA burst release was reduced by 66% and the total release time was expanded to 96 h, compared to 3.5 h for the unmodified sample. The result of the 3 polyelectrolyte layers deposited porous PLA (L3) was a 48% reduction in BSA burst release and total release time of 30 h. Our observations suggest that 5 layers of polyelectrolyte give uniformly surface modification layer and stronger electrostatic attraction to the protein.

5.1.3 Combined Effect of Two Modification Strategies

The partially closed-cell and surface modification were applied together to study their combined effect on the BSA release profile. When a 5 polyelectrolyte layer surface modification of the PLA and a partially closed cell approach (2% open area) are combined, in the L5C sample, the synergy is dramatic with a 5 times reduction in the first two hour burst release amount and a total release time which is extended by

123 times as compared to the 100% open cell, surface unmodified, reference sample (L0). Our investigations suggest that there are three kinds of BSA in the porous PLA: free BSA, interacting BSA and bound BSA, respectively, responsible for burst release, sustained release and the residual BSA left inside the porous PLA device after the release test.

5.1.4 Release Mechanism Study

XPS was used in this study to examine the BSA distribution inside the porous PLA devices during different release stages. The mechanism of release in this system is clearly diffusion controlled with well defined concentration gradients, as observed in the direction of release for both the 100% open cell system (L0) and the surface modified, partially closed sample with one end open (L5E). These effects point towards a diffusion mechanism combined with a sorption/desorption interaction of the BSA with the modified PLA surface.

5.1.5 Future Work

There are many factors affecting BSA release from a porous PLA. LbL surface modification and partially closed-cell strategies have shown their potential to control the BSA burst release and total release time. Based on the references and our studies, we suggest some points for future work to follow, in order to gain a thorough understanding of this technique and to prepare an effective drug delivery device:

1. In order to increase drug loading efficiency of the porous PLA we developed, a BSA solution with higher concentration can be used to prepare BSA-loaded samples. Due to the higher viscosity with increasing BSA concentration, the loading device may also need to be improved to meet the needs. Higher loading pressure can be an option. However, there are several points to notice. Firstly, higher concentration and higher loading pressure both affect the BSA conformation in the aqueous state, which then affects the bioactivity of BSA. Secondly, although higher BSA concentration may lead to a higher drug loading efficiency, it may not necessarily improve the BSA release profile. Since the amount of BSA affected by electrostatic field generated by the polyelectrolyte is limited, once the polyelectrolyte surface is covered and occupied by BSA molecules, the excess BSA can be free to diffuse, which results in a burst release. The strategy of a partially closed-cell is still effective in this case.

2. Compared to the BSA dimension, the pore-size of the device (1.5 μm) is still too large to give enough physical restriction and tortuosity inside the porous sample for BSA molecule to diffuse out. Porous samples with an even smaller pore dimension can be introduced to improve the protein release. A smaller pore-size can increase the difficulty of the release medium to penetrate into the porous sample. Smaller pore-size gives more surface area for BSA to adsorb and, using polyelectrolyte surface deposition, even BSA diffusing in the middle of the channels can be affected by the electrostatic attraction, hence leading to less burst and release

in a more sustained manner. However, a smaller pore size will increase the difficulty of loading, which may requires a higher pressure for loading and the associated problems discussed above.

3. Theoretically the release medium (water) penetration will also be affected by the sample dimension, possibly the sample shape will also affect the release profile. A study of water uptake of the porous sample and its relationship with the burst release should be examined.

4. The degradation time of PLA used in our study is much longer than the release times. Also its natural affinity to the protein is poor. Other polymers with shorter degradation time and stronger hydrophilicity can be used as candidates to prepare porous device used in our study. However, it should be considered that the degradation and collapse of the drug carrier matrix can also contribute to the drug release.

5. The PLA surface lacks functional groups, which can limit the amount of the first polyelectrolyte layer deposited onto the surface, and consequently the amount and the structure of the following polyelectrolyte layers. Considering the porous nature of the samples we use, nitrogen-plasma surface treatment can be an option to add functional groups and modify the PLA surface properties such as wettability prior to LbL surface deposition. This may lead to a stronger interaction between the PLA surface and the first layer of polyelectrolyte and better structure of the

polyelectrolyte layers. This may contribute to attract more BSA molecules to the surface and reduce the burst and prolong the release.

6. BSA release from porous PLA mainly undergoes a sorption/desorption-diffusion process. Once leaving the substrate surface, BSA protein diffusion in the release medium (water) is very fast due to its high diffusion coefficient in water. Some other techniques can be considered to prolong the BSA diffusion through the torturus channels. For example, a dilute polymer solution can be mixed together with protein, loaded into the porous sample and finally form a hydrogel containing proteins inside. The low diffusion coefficient of protein in hydrogel can extend the total release time. However, the polymer solution system should be carefully chosen as the use of organic solvent is unfavorable to the protein bioactivity. Besides, the loading of even a dilute polymer solution into the pores can be another issue to consider.

7. In order to understand the protein interaction with the polymer surface, a study should be carried out to gain knowledge of adsorption and desorption of the protein on the PLA surface, and its role in controlled drug release.

8. These polymer scaffolds can provide mechanical strength, interconnected porosity, surface area, varying surface chemistry and unique geometries to direct tissue regeneration (Hutmacher, 2001). A biodegradable porous material with a highly controllable morphology and pore dimensions extending from about 1 micron to hundreds of microns could also be a good candidate to be used as a scaffold in

tissue engineering. As typical cell sizes range from a few to a hundred micrometers, it is not only macro-geometry that matters in tissue engineering, but also micro-geometry that affects the survival, proliferation, and differentiation of cells in the macro-geometry (Kim and Mooney, 1998).

5.2 Conclusions

1. Both modification strategies, LbL surface deposition of polyelectrolytes and partially closed-cell, can be effective in improving the release profile of BSA from porous drug carriers. Our observations indicate that the number of polyelectrolyte layers and the open surface area are controlling factors in the controlled drug release.

2. It was shown that the modified samples with 5 layers of polyelectrolytes and 2% open surface area give the best result for the controlled BSA release with less burst and a longer release time.

3. BSA distribution in the unmodified sample after loading is homogeneous while for the samples modified with LbL, polyelectrolytes may restrict the penetration of the BSA solution during loading.

4. The release of BSA from our porous PLA devices is diffusion controlled, with clear concentration gradients observed. The mechanism of release is diffusion controlled combined with a sorption/desorption interaction of the BSA with the modified PLA surface.

REFERENCE

ADAMSON, A.W., GAST, A.P. Physical Chemistry of Surfaces, 6th eds. 1997, New York, Wiley.

AHMED, A., BONNER, C. DESAI, T.A. (2002). "Bioadhesive microdevices with multiple reservoirs: a new platform for oral drug delivery." *J. Controlled Release.* **81**, 291-306.

ALDERBORN, G. (2002). Tablets and compaction. In Pharmaceutics: The Science if Dosage Form Design. London, Churchill Livingstone.

ALEM, H., BLONDEAU, F., GLINEL, K. DEMIUSTRIER-CHAMPAGNE, S., JONAS, A.M. (2007). "Layer-by-layer assembly of polyelectrolytes in nanopores." *Macromolecules.* **40**, 3366-3372.

ANDERSON, J.M. (1997). "Biodegradation and biocompatibility of PLA and PLGA microspheres." *Adv, Drug Deliv. Rev.* **28**(1), 5-24.

ARIGA, K., LVOV, Y., KUNITAKE, T. (1997). "Assembling alternate dye-polyion molecular films by electrostatic layer-by-layer adsorption." *J. American Chem. Society.* **119**, 2224-2231.

ARYS, X., LASCHEVSKY, A., JONAS, A.M. (2001). "Ordered polyelectrolyte multilayer: I. Mechanisms of growth and structure formation: a comparison with classical fuzzy multilayers." *Macromolecules.* **34**, 3318-3330.

AURAS, R., HARTE, B., SELKE, S. (2004). "An overview of polylactides as packaging materials." *Macromol. Biosci.* **4**, 835-864.

AVGEROPOULOS, G.N., WEISSERT, F.C., BIDDISON, P.H., BOHM, G.C.A. (1975). "Heterogeneous blends of polymers. Rheology and morphology." *Rubber Chemistry and Technology.* **49**, 93-104.

BALAKRISHNAN, B., MOHANTY, M., FERNANDEZ, A.C., MOHANNAN, P.V., JAYAKRISHNAN, A. (2006). "Evaluation of the effect of incorporation of dibutyryl cyclic adenosine monophosphate in an in situ-forming hydrogel wound dressing based on oxidized alginate and gelatin." *Biomaterials.* **27**, 1355-1361.

BARRY, J.A.B., SILVA, M.M.C.G., SHAKESHEFF, K.M., HOWDLE, S.M., ALEXANDER, M.R. (2005). "Using plasma deposits to promote cell population of the porous interior of three-dimensional poly(D,L-lactic acid) tissue-engineering scaffolds." *Adv. Func. Mat.* **15**, 1134-1140.

BERSMA, J, E, DE BRUIJIN, W.C., ROZAMA, F.R., BOS, R.R.M. BOERING, G. (1995). "Late degradation tissue response to poly(l-lactide) bone plates and screws." *Biomaterials.* **16**(1), 25-31.

BOURRY, D., FAVIS, B.D. (1998). "Continuity and phase inversion in HDPE/PS blends: influence of interfacial modification and elasticity." *J. Polym. Sci. Part B: Polym. Phys.* **36**, 1889-1899.

BRANNON-PEPPAS, L., BIRNBAUM, D.T., KOSMALA, J.D. (1997). "Polymers in controlled release." *Polymer.* **22**(9), 316

BRASH, J.L., Davidson, V.J. (1976). "Adsorption on glass and polyethylene from solutions of fibrinogen and albumin." *Thrombosis Research.* **9**, 249-259.

BRAUNAUER, S., EMMETT, P. H., TELLER, E. (1938). Journal of the American Chemical Society, 60, 309.

BREIMER, D.D. (1999). "Future challenges for drug delivery." *J. Controlled Release.* **62**, 3-6.

BRYANT, S.J., ANSETH, K.S. (2001). "The effects of scaffold thickness on tissue engineered cartilage in photocrosslinked poly(ethylene oxide) hydrogels." *Biomaterials.* **22**, 619-626.

BRYNE, P.D., MULLER, P., SWAGER, T.M. (2006). "Conducting metallopolymers based on azaferrocene." *Langmuir.* **22**(25), 10596-10604.

CAI, K. YAO, K., CUI, Y., YANG, Z., LI, X., Xie, H., GAO, L. (2002). "Influence of different surface modification treatments on poly(D,L-lactic acid) with silk fibroin and their effects on the culture of osteoblast in vitro." *Biomaterials.* **23**, 1603-1611.

CAM, D., HYON, S.H., IKADA, Y. (1996). "Degradation of high molecular weight poly(L-lactide) in alkaline medium." *Biomaterials.* **16**, 833-843.

CANNO, G.P., JACOB, J.S., MATHIOWITZ, E. (2000). "Nanosphere based oral insulin delivery." *J. Controlled Release.* **65**, 261-269.

CHANDRA, T., RUSTGI, R. (1998). "Biodegradable polymers." *Prog. Polym. Sci.*

23, 1273-1335.

CHASIN, M., LANGER, R. S. (1990). Biodegradable Polymers as Drug Delivery Systems. Marcel Dekker. New York, US.

CHEN, W., MCCARTHY, T.J. (1997). "Layer-by-layer deposition: a tool for polymer surface modification ." *Macromolecules.* **30**, 78-86.

CHEN, X.X., FERRIGNO, R., YANG, J., WHITESIDES, G.M. (2002). "Redox Properties of cytochrome C adsorbed on self-assembled monolayers: a probe for protein conformation and orientation." *Langmuir.* **18**(18), 7009-7015.

CHUANG, H.Y.K. (1987). "Interaction of plasma proteins with artificial surfaces." *Blood Compat.* **1**, 87-102.

CIMA, L.J., VACANTI, J.P., VACANTI, C., INGBER, D., MOONEY, D., LANGER, R. (1991) "Tissue engineering by cell transplantation using degradable polymer substrates." *J. Biotech. Eng.* **113**, 143-151.

COOK, W.D., ZHANG, T., MOAD, G., VAN DEIPEN, G., CSER, F., FOX, B., O'SHEA, M. (1996) "Morphology-property relationships in ABS/PET blends. I. compositional effects." *J. Appl. Polym. Sci.* **62**, 1699-1708.

DAVID, B., KOZLOWISKI, M., TADMOR, Z. (1993). Polym. Eng. Sci. **33**, 227.

DECHER, G., HONG, J.D., SCHMITT, J. (1992). "Buildup of unltrathin multilayer films by a self-assembly process: III Consequently alternating adsorption of onionic

and cationic polyelectrolytes on charged surfaces." *Thin Solid* Films. **210**, 831835.

DECHER, G. (1997). "Fuzzy nanoassemblies: toward layered polymeric multicomposites ." *Science*. **277**, 1232-1237.

DRUMRIGHT, R.E., GRUBER, P.R., HENTON, D.E. (2000). "Polylactic acid technology." *Advanced Materials*. **12**(23). 1841-1846.

DUBAS, S.T., SCHLENDOFF, J.B. (1999). "Factors controlling the growth of polyelectrolyte multilayer." *Macromolecules*. **32**, 8153-8160.

EDLUND, U., ALBERTSSON, A.C. (2002). "Degradable polymer microspheres for controlled drug delivery." *Advances in Polymer Sci.* **157**, 67-112.

EDWARDS, D.A., JANES, J., CAPONETTI, G., MINTZES, J., GRKACG, J., LOTAN, N. LANGER, R. (1997). "Large porous particles for pulmonary drug delivery." *Science*. 276, 1868-1871.

ELEMANS, P.H., JANSSEN, J.M., MEIJER, H.E.H. (1990). "The measurement of interfacial modifier in polymer/polymer systems: the breaking thread method." *J. Rheol.* **34**, 1311-1326.

ELWING, H. (1998). "Protein adsorption and ellipsometry in biomaterial research." *Biomaterials*. **19**, 397-406.

FAVIS, B.D., CHALIFOUX, J.P. (1988). "Influence of composition on the morphology of polystyrene /polycarbonate blends." *Polymer*. **29**, 1761-1767.

FAVIS, B.D. (1990). "Effect of processing parameters on the morphology of an

immiscible binary blend." J. Appl. Polymer Sci. **39**(2), 285-300.

FAVIS, B.D., SARAZIN, P., Li, J., YUAN, Z. (2004). U.S. Patent Application, 10/552,357 and WIPO (PCT) WO 2004/087797.

FERREIRA, M., RUBNER, M.F. (1995). "Molecular level processing of conjugated polymers. I. Layer-by-layer manipulation of conjugated polyions." *Macromolecules.* **28**, 7107-7114.

FOSTER, J.F., Albumine structure, function and uses. Pergamon: Oxford, 1977, 48-53.

GARLOTTA, D. (2002). "A literature review of poly(lactic acid)." *J. Polymers and the Environment.* **12**(23), 1841-1846.

GERGELY, C., BAHI, S. SZALONTAI, B., FLORES, H., SCHAAF, P., VOEGEL, J.C., CUISINIE, F.G. (2004). "Human serum albumin self-assembly on weak polyelectrolyte multilayer films structurally modified by pH changes." *Langmuir.* **20,** 5575-5582.

GILDING. D.K., REED, A.M. (1979). "Biodegradable polymers for use in surgery - poly(glycolic)/poly(lactic acid) homo- and copolymers: 1." *Polymer.* **20**(12). 1459-1464.

GOPFERICH, A. (1996). "Polymer degradation and erosion: mechanisms and applications." *European J. Phar. Biopharmaceutics.* **42(1)**, 1-11.

GOPFERICH, A. (1997). "Mechanisms of polymer degradation and elimination."

Handbook of Biodegradable Polymers. Hardwood Acad. 451-471.

GRAYSON, A., CHIO, I.S., TYLER, B., WANG, P., BREM, H., CIME, M., LANGER, R. (2003). "Multi-pulse drug delivery from a resorbable polymeric microchip device." *Nature Mater.* **2**, 767-772.

GREGEN, W.P., LUTZ, G.G., DAVISON, S. (1996). "Hydrogenated block copolymers in thermoplastic elastomer interpenetrating polymer networks." Hanser Publication, Munich.

GUAN, J. FUJIMOTO, K.L., SACKS, M.S., WANGER, W.R. (2005). "Preparation and characterization of highly porous, biodegradable polyurethane scaffolds for soft tissue applications." *Biomaterials*, **26**, 3961-3971.

GUBBELS, F., JEROME, R., TEYSSIE, P., VANLATHEM, E., DELTOUR, R., CALDERONE, A., PARENTE, V., BREDAS, J.L. (1994). "Selective localization of carbon black in immiscible polymer blends: a useful tool to design electrical conductive composites." *Macromolecules.* **27**, 1972-1974.

GURSEL, I., KORKUSUZ, F., TURESIN, F., AAEDDINOGLU, N.G., HASURCU, V. (2002). "In vivo application of biodegradable controlled antibiotic release systems for the treatment of implant-related osteomyelitis." *Biomaterials.* **22**, 73-80.

HACKER, M., TESSMAR, J., NEUBAUER, M., BLAIMER, A., BLUNK, T., GOPFERICH, A., SCHULZ, M.B. (2003). "Towards biomimetic scaffolds: anhydrous scaffold fabrication from biodegradable amine-reactive diblock copolymers." *Biomaterials.* **24**, 4459-4473.

HARLAND, R.S., GAZZANIGA, A., SANGALLI, M.E., COLOMBO, P., PEPPAS, N.A. (1988). "Drug –polymer matrix swelling and dissolution." *Pharmaceutial Res.* **5**, 488-494.

HARRIS, J.J., BRUENING, M. L. (2000). "Electrochemical and in situ ellipsometric investigations of the permeability and stability of layered polyelectrolyte films." *Langmuir.* **16**, 2006-2013.

HARRIS, L.D., KIM, B., MOONEY, D.J. (1998). "Open pore biodegradable matrices formed with gas foaming." *J. Biomed. Mater. Res.* **42**, 396-402.

HEILMANN, K. (1984). "Therapeutic systems: rate-controlled drug delivery: concept and development." Thieme-Stratton Inc. New York, US, second edition.

HEUBERGER, R., SUKHORUKOV, G., VOROS, J., TEXTOR, M., MOHWALD, H. (2005). "Biofunctional polyelectrolyte multilayers and microcapsules: Control of non-specific and bio-specific protein adsorption." *Adv. Func. Mat.* **26**, 357-366.

HIROTSU, T., NAKAYAMA, K., TSUJISAKA, T., MAS, A., SUCHE, F. (2002). "Plasma surface treatments of melt-extruded sheets of poly(L-lactic acid) ." *Polymer Eng. and Sci.* **42**(2), 299-306.

HO, R.M., WU, C.H., SU, A.C. (1990). "Morphology of plastic/rubber blends." *Polym. Eng. Sci.* **30**, 511-518.

HOLY, C.E., DANG, S.M., DAVIES, J.E., SHOICHET, M.S. (1999). "In vitro degradation of a novel poly(lactide-co-glycolide) 75/25 foam." *Biomaterials.* **29**, 1177-1185.

HOOK, F., VOROS, J., RODAHL, M., KURRAT, R. BONI, P., RANSDEN, J.J.,TEXTOR, M., SPENCER, N.D., TENGVALL, P. Gold, J., KASEMO, G. (2002). "A comparative study of protein adsorption on titanium oxide surfaces using in situ ellipsometry, optical waveguide lightmode spectroscopy, and quartz crystal microbalance/dissipation." *Colloids and Surfaces B-Biointerfaces.* **24**(2), 155-170.

HSIEH, M.C., FARRIS, R.J., MCCARTHY, T.J. (1997). "Surface `priming' for layer-by-layer deposition: Polyelectrolyte multilayer formation on allylamine plasma-modified poly(tetrafluoroethylene)." *Macromolecules.* **30**, 8453-8458.

HSU, Y.Y., GRESSER, J.D., TRANTOLO, D.J., LYONS, C.M., GANGADHARAM, P.R., WISE, D.L. (1997). "Effect of polymer foam morphology and density on kinetics of in vitro controlled release of isoniazid from compressed foam matries." *J. Biomed. Mater. Res.* **35**, 107-116.

HSU, W.Y., WU, S. (1993). "Percolation behavior in morphology and modulus of polymer blends." Polymer. Eng. Sci. **33**, 293-302.

HUA, F.J., KIM, G.E., LEE, J.D., SON, Y.K., LEE, D.S. (2002). "Macroporous poly(l-lactide scaffold 1. Preparation of a macroporous scaffold by liquid-liquid phase separation of a PLLA-dioxane-water system." J. Biomed. Mater. Res. **63**, 161-167.

HUTMACHER, D.W. (2001). "Scaffold design and fabrication techniques for engineering tissues – state of the art and future perspectives." *J. Biomat. Sci. Polym. Ed.* **12**, 107-124.

INAGAKI, N., NARUSHIMA, K., TSUTSUI, Y., OHYAMA, Y. (2002)." Surface modification and degradation of poly(lactic acid) films by Ar-plasma." *J. Adhesion Sci. Technol.* **16**(8), 1041-1054.

INAGAKI, N., NARUSHIMA, K., LIM, S.K. (2003). "Effects of aromatic groups in polymer chains on plasma surface modification ." *J. Applied Polym. Sci.* **89**, 96-103.

JAMSHIDI, K., HYON, S.H., IKADA, Y. (1988). "Thermal characterization of polylactides." *Polymer.* **29(12)**, 2229-2234.

JAIN, R.A. (2000). "Manufacturing techniques of various drug loaded biodegradable poly(lactide-co-glycolide) (PLGA) devices." *Biomaterials.* **21**(23), 2475-2490.

JIANG, W., SCHWENDEMAN, S.P. (2000). "Formaldehyde-mediated aggregation of protein antigens: comparison of untreated and formalinized model antigens." Biotechnology and Bioengineering. **70**(5), 507-517.

JORDHAMO, G.M., MANSON, J.A., SPERLING, L.H. (1986). "Phase continuity and inversion in polymer blends and simultaneous interpenetrating networks." *Polym. Eng. Sci.* **26**, 517-524.

KAIBARA, K., OKAZAKI, T., BOHIDAR, H.B., DUBIN, P.L. (2000). "pH-induced coacervation in complexes of bovine serum albumin and cationic polyelectrolytes." *Biomacromolecules.* **1**, 100-107.

KEYES-BAIG, C., DUHAMEL, J., FUNG, S.Y., BEZAIRE, J., CHEN, P. (2004). "Self-assembling peptide as a potential carrier of hydrophobic compounds." *J.Am.Chem.Soc.* **123**, 7522-7532.

KIM, B., MOONEY, D.J. (1998). "Development of biodegradable synthetic extracellular matrices for tissue engineering." *Trends in Biotechnology*. 16, 224-230.

KIM, K. YU, M., ZONG, X., CHIU, J., FANG, D., SEO, Y., HSIAO, B.S., CHU, B., HADJIARGYROU, M. (2003). "Control of degradation rate and hydrophilicity in electrospun non-woven poly(D,L-lactide) nanofiber scaffolds for biomedical applications." *Biomaterials*. **24**, 4977-4985.

KIM, S.S., KIM, H., KOSKI, J.A., WU, B.M., CIMA, M.J., SOHN, J., GRIFFITH, L.G., VACANTI, J.P. (1998). "Survival and function of hepatocytes on a novel three-dimensional synthetic biodegradable polymer scaffolds with an intrinsic network of channels." *Annals of Surgery*. **228**(1), 8-13.

KLOSE, D., SIEPMANN, F., ELKHARRAZ, K., KRENZLIN, S., SIEPMANN, J. (2006). "How porosity and size affect the drug release mechanisms from PLGA-based microparticles." *International J. of Pharm.* **314**(2), 198-206.

KOHN, J., LANGER, R. Bioresorbable and Biorodible Materials. Academic Press, San Diego, CA, 1996.

KONDO, A.F., MURAKAMI, F., HIGASHITANI, K. (1992). "Circular dichroism studies on conformational changes in protein molecules upon adsorption on ultrafine polystyrene particles." *Biotech. And Bioeng*. **40**(8), 889-894.

KOSTARELOS, K. (2003). "Rational Design and engineering of delivery systems for therapeutics: biomedical exercises in colloid and surface science." *Advances in*

Colloids and Interface Science. **106**, 147-168.

KULKARNI, R.K., PANI, K.C., NEUMAN, C., LEONARD, F. (1996). "Polylactide acid for surgical implants." *Archives of Surgery.* **93**, 839-843.

KUMAR, N., RAVIKUMAR, M.N., DOMB, A.J. (2001). "Biodegradable block copolymers." *Adv. Drug. Deliv. Rev.* **53**, 23-44.

LADAM, G., CERGELY, C., SENGER, B., DECHER, G., VOEGEL, J-C., SCHAAF, P., CUISINIER, F.J.G. (2000). "Protein interactions with polyelectrolyte multilayers: Interactions between human serum albumin and polystyrene sulfonate/polyallylamine multilayers." *Biomacromolecules.* **1**(4), 674-487.

LAI, C.Y., JEFTINIJA, B.G., XU, K., LIN, V.S. (2003) "A mesoporous silica nanosphere-based carrier system with chemically removable CdS nanaparticle caps for stimuli responsive controlled release of neutrotransmitters and drug molecules." *J.Am.Chem.Soc.* **125**, 4451-4459.

LANGER, R, PEPPAS, N.A. (1983). "Chemical and physical structure of polymers as carriers for controlled release of bioactive agents: a review." *J. Macromolecular Sci.* **23**, 61-126.

LANGER, R. (1990). "New methods of drug delivery." *Science.* **249**, 1527-1533.

LANGER, R, PEPPAS, N.A. (2003). "Advances in biomaterials, drug delivery and bionanotechnology." *AIChE Journal.* **49**(12), 2990-3006.

LEWIS, D.H. (1990). "Biodegradable polymers as drug delivery systems." New York, Marcel Dekker. 1-41.

LEVON, K., MARGOLINA, A., PATASHINSKY, A.Z. (1993). "Multiple percolation in conducting polymer blends." *Macromolecules.* **26**(15), 4061-4063.

LI, J., FAVIS, B.D. (2001) "Characterizing co-continuity high density polyethylene/polystyrene blends." Polymer, **42**, 5047-5053

LI, J. (2001) "Co-continuous polymer blends." Thèse de Doctorat, École Polytechnique de Montréal.

LI, J., MA, P., FAVIS, B.D. (2002). "The role of the blend interface type on morphology in co-continuous polymer blends." *Macromolecules.* **35**, 2005-2016.

LI, W., LAURENCIN, C.T., TUAN, R.S., KO, F.K. (2002). "Electrospun nanofibrous structure: A novel scaffold for tissue engineering." *J. Biomed. Mat. Res.* **60**, 613-621.

LVOV, Y., ARIGA, K., KUNITAKE, T. (1994). "Layer-by-layer assembly of alternate protein/polyion ultrathin films." *Chemistry Letters.* **12**, 2323.

LVOV, Y., ARIGA, K., ICHINOSE, I., KUNITAKE, T. (1995). "Assembly of multicomponent protein films by means of electrostatic layer-by-layer adsorption." *J.Am.Chem.Soc.* **117**(22), 6117-6123.

LUNDSTORM, I. (1985). "Models of protein adsorption on solid surfaces." *Pro Colloid & Polymer Sci.* **70**, 76-82.

MA, Z., GAO, C., JIAN, J., SHEN, J. (2002a). "Protein immobilization on the surface of poly-L-lactic acid films for improvement of cellular interactions." *European Polymer Journal.* **28**, 2279-2284.

MA, Z., GAO, C., YUAN, J., JI, J., GONG, Y., SHEN, J. (2002b). "Surface modification of poly-L-lactide by photografting of hydrophilic polymers towards improving its hydrophilicity." *J. Applied Poly.Sci.* **85**(10), 2163-2171.MALMSTEN, M., BURNS, N., VEIDE, A. (1998). "Electrostatic and hydrophobic effects of oligopeptide insertions on protein adsorption." *J. Colloid and Interface Sci.* **204**(1), 104-111.

MATOS, M., FAVIS, B.D., LOMELLINI, P. (1995). "Interfacial modification of polymer blends: the emulsification curve. Part I: influence of molecular weight and chemical composition of the interfacial modifier." *Polymer.* **36**, 3899-3907.

MATSUMOTO, A., MATSUKAWA, Y., SUZUKI, T., YOSHINO, H. (2005). "Drug release characteristics of multi-reservoir type microspheres with poly(dl-lactide-co-glycolide) and poly(dl-lactide)." *J. Controlled Release.* **106**, 172-180.

MCALONEY, R.A., SINYOR, M., DUDNIC, V., GOH, C. (2001). "Atomic force microscopy studies of salt effects on polyelectrolyte multilayer film morphology." *Langmuir.* **17**, 6655-6663.

MEHIER-HUMBERT, S. GUY, R.H. (2005). "Physical methods for gene transfer: improving the kinetics of gene delivery into cells." *Adv. Drug Deliv.Rev.* **57**,733-753.

MEKHILEF, N., FAVIS, B.D., CARREAU, P.J. (1997). "Morphological stability, interfacial tension, and dual-phase continuity in polystyrene-polyethylene blends." *J. Polym. Sci. Part B: Poly. Phys.* **35**, 293-308.

MIAO, Z., CHENG, S., ZHANG, X., ZHUO, R. (2005). "Synthesis, characterization, and degradation behavior of amphiphilic poly-α,β-[N-(2-hydroxyethyl)-L-aspartamide]-g- poly(ε-caprolactone)." *Biomacromolecules.* **7**, 2020-2026.

MIDDLETON, J.C., ARTHUR, J.T. (1998). "Synthetic biodegradable polymers as medical devices." *Medical Plastics and Biomater Mag.* **Match**, 30.

MIDDLETON. J.C., ARTHUR, J.T. (2000). "Synthetic biodegradable polymers as orthopedic devices." *Biomaterials.* **21**, 2335-2346.

MIKOS, A.G., BAO, Y., CIMA, L.G., INGBER, D.E., VACANTI, J.P., LANGER, R. (1993). "Preparation of poly(glycolic acid) bonded fiber structures for cell attachment and transplantation." *J. Biomed. Mater. Res.* **27**, 183-189.

MIKOS, A.G., LYMAN, M.D., FREED, L.E., LANGER, R. (1994). "Wetting of poly(l-lactic acid) and poly(d,l-lactic-co-glycolic acid) foams for tissue engineering." *Biomaterials.* **15**, 55-58.

MIKOS, A.G., THORSEN, A.J., CZERWONKA, L.A., BAO, Y., LANGER, R., WINSLOW, D.N., VACANTI, J.P. (1994). "Preparation and characterization of poly(L-lactic acid) foams." *Polymer.* **26**, 1068-1077.

MILES, I.S., ZUREK, A. (1998). "Preparation, structure, and properties of two phase co-continuous polymer blends." *Polym. Eng. Sci.* **28**, 796-805.

MO, X., WEBER, H. (2004). "Electrospinning P(LLA-CL) nanofiber: A tubular scaffold fabrication with circumferential alignment." *Macromolecular Symposia.* **217**,

413-416.

MOIOLI, E.K., CLARK. P.A., XIN, X., LAI, S., MAO, J.J. (2007). "Matrices and scaffolds for drug delivery in dental, oral and craniofacial tissue engineering." *Adv. Drug Deliv.Rev.* **59**, 308-324.

MOONEY, D.J., KAUFMANN, P.M., SANO, K. MCNAMARA, K.M., VACABTI, J.P., LANGER, R. (1994). "Transplantation of hepatocytes using porous biodegradable sponges." *Transplant. Proc.* **26**, 3425-3426.

MOONEY, D.J., MAZZONI, C.L., BREUER, C., MCNAMARA, K., HERN, D. VACANTI, J.P., LANGER, R. (1996a). "Stablized polyglycolic acid fiber-based tubes for tissue engineering." *Biomaterials.* **17**, 115-124.

MOONEY, D.J., BALDWIN, D.F., SUH, N.P., VACANTI, J.P., LANGER. R. (1996b). "Novel approach to fabricate porous sponges of poly(d,l-lactic-co-glycolic acid) without the use of organic solvents." *Biomaterials.* **17**, 1417-1422.

Müller, M. (2001). "Orientation of α-helocal poly(L-lysine) in consecutively adsorbed polyelectrolyte multilayers on texturized silicon substrates." *Biomacromolecules.* **2**(1), 262-269.

NAM, Y.S., PARK, T.G. (1999). "Biodegradable polymeric microcellular foams by modified thermally induced phase separation method." *Biomaterials.* **20**, 1783-1790.

NORDE, W., LYKLEMA, J. (1991). "Why proteins prefer interfaces." *J.Biomater.Sci.Polym.Ed.* **2**(3), 183-202.

NORDE, W. (1996). "Driving forces for protein adsorption at solid surfaces."

Macromolecular Symposia. **103**, 5-18.

OKADA, H. (1997). "One-and three-month release of injectable microspheres of the LH-RH superagonist leuprorelm acetate." *Adv Drug Deliv Rev.* **28** , 43-70.

OLABISHI, L., ROBESON, M., SHAW, M.T. (1979) Polymer-Polymer Miscibility. Academic Press. New York.

OSTUNI, E., CHAPMAN, R.G., HOLMLIN, R.E., TAKAYAMA, S., WHITESIDES, G.M. (2001). "A survey of structure-property relationships of surfaces that resist the adsorption of protein." *Langmuir.* **17**(18), 5605-5620.

PARK, T.G., LU, W.Q., CROTTS, G. (1995). "Importance of in-vitro experimental conditions on protein release kinetics, stability and polymer degradation in protein encapsulated poly(D,L-lactic acid-co-glycolic acid) microspheres." *J. Controlled Release.* **33**(2), 211-222.

PAUL, D.P., BUCKNALL, C.B. (2000). Polymer Blends. Vol. 1 and 2, Wiley-Interscience, New York.

PAUL, D.R., MCSPADDEN, S.K. (1976). "Diffusional release of a solute from a polymer matrix." *J. Membrane Sci.* 33-48.

PRAUSNITZ, M.R., MITRAGOTRI, S. LANGER, R. (2004). "Current status and future potential of transdermal drug delivery." *Nat Rev Drug Discov.* **3**, 115-124.

QUIRK, R.A., DAVIES, M.C., TENDLER, S.J.B., CHAN, W.C., SHAKESHEFF, K.M. (2001). "Controlling biological interactions with poly(lactic acid) by surface entrapment modification." *Langmuir.* **17**, 2817-2820.

RAHMAN, N.A., MATHIOWITZ, E. (2004). "Localization of bovine serum albumin in double-walled microspheres." *J. Controlled Release*. **94**, 163-175.

RHINE, W.D., SUKHATME, V., HSIEH, D.S.T., LANGER, R.S. (1980). "A new approach to achieve zero-order release kinetics from diffusion-controlled polymer matrix systems." Controlled Release of Bioactive Materials, Academic Press, New York, 177-187.

RHTEZAZI, T. (2000). "Controlled release of macromolecules from PLA microspheres: using porous structure topology." *J. Controlled Release*. **68**(3), 361-372.

ROBERT, P.L., LANGER, R., VACANTI, J.P. (2000). Principles of Tissue Engineering. Second Edition.

ROY, X. SARAZIN, P., FAVIS, B.D. (2006), "Ultraporous nanosheath materials by layer-by-layer deposition onto co-continuous polymer blend templates." *Advanced Materials*. **18**, 1015-1019.

ROY, X. SARAZIN, P., FAVIS, B.D. (2007). WIPO (PCT) WO 2007/053955.

SAKELLARIOU, P., EASLMOND, G.C., MILES, I.S. (1989). Interfacial activity of polycarbonate/polystyrene graft copolymers in polycarbonate/polystyrene blends." *Polymer*. **34**, 30307-3047.

SALEHI, P., SARAZIN, P., FAVIS, B.D. (2008). "Porous devices derived from co-continuous polymer blends as a route for controlled drug release."

Biomacromolecules. **9**, 1131-1138.

SANTINI, J.T., CIMA, M.J., LANGER, R. (1999). "A controlled-release microchip." *Nature*. **397**(6716), 335-338.

SANTINI, J.T. (2000). « Microchips as controlled drug-delivery devices." *Angew. Chem. Int. Ed.* **39**, 2396-2407.

SARAZIN, P., FAVIS, B.D. (2003). "Morphology control in co-continuous poly(L-lactide)/polystyrene blends: a route towards structured and interconnected porosity in poly(L-lactide) materials." *Biomacromolecules*. **4**, 1669-1679.

SARAZIN, P., ROY, X., FAVIS, B.D. (2004). "Controlled preparation and properties of porous poly(L-lactide) obtained from a co-continuous blend of two biodegradable polymers." *Biomaterials*. **25**(28), 5965-5978.

SARAZIN, P., FAVIS, B.D. (2005) "Influence of temperature-induced coalescence effects on co-continuous morphology in poly(3-caprolactone)/polystyrene blends." *Polymer*. **46**, 5966-5978.

SARAZIN, P., VIRGILIO, N., BASIL, B.D. (2006). "Influence of the porous morphology on the in vitro degradation and mechanical properties of poly(L-lactide) disks." *J. Appl. Polym. Sci*. **100**, 1039-1047.

SHAH, S.S., CHA, Y., PITT, C.G. (1992). "Poly(glycolic acid-co-dl-lactic acid): diffusion or degradation controlled drug delivery." *J. Controlled Release*. **18**, 261-270.

SIEPMANN, J., FAISANT, N., AKIKI, J., RICHARD, J. BENOIT, J. (2004). "Effect of the size of biodegradable microparticles on drug release experiment and theory." *J. Controlled Release*. **96**(1), 123-134.

SLOWING, I., TREWYN, B.G., GIRI, S., LIN, V.S. (2007). "Mesoporous silica nanoparticles gor drug delivery and biosensing applications." *Adv. Funct. Mater.* **17**(8), 1225-1236.

SU, T.J., LU, J.R., THOMAS, R.K., CUI, Z.F., PENFOLD, J. (1998). "The conformation structure of bovine serum albumin layers adsorbed at the silica-water interface." *K. Phys. Chem. B.* **102**(41). 8100-8108.

SUH, H., HWANG, Y., LEE, J., HAN, C.D., PARK, J. (2001). "Behavior of osteoblasts on a type I atelocollagen grafted ozone oxidized poly-L-lactic acid membrane ." Biomaterials. **22**, 219-230.

SZYK, L., SCHAAF, P., GERGELY, C., VOEGEL, J.C., TINLAND, B. (2001). "Lateral mobility of proteins adsorbed on or embedded in polyelectrolyte multilayers." *Langmuir*. **17**, 6248-6253.

TAN, W., DESAI, T.A. (2004). "Layer-by-layer microfluidics for biomimetic three-dimensional structures." *Biomaterials*. **25,** 1355-1364.

TANG, Z., WANG, Y., PODSIADLO, P., KOTOV, N.A. (2006). "Biomedical applications of layer-by-layer assembly: From biomimetics to tissue engineering." *Adv. Mat.* **18**, 3203-3224.

TAO, S.L., LUBELEY, M.W., DESAI, T.A. (2003). "Bioadhesive poly(methyl

methacrylate) microdevices for controlled drug delivery." *J. Controlled Release.* **88**, 215-228.

TCHOUDAKOV, R., BREUER, O., NARKIS, M. SIEGMANN, A. (1996). "Conductive polymer blends with low carbon black loading: Polypropylene/polyamide." *Polym. Eng. Sci.* **36**(10), 1336.

THEEUWES, F. (1975). "Elementary osmotic pump." *J. Pharmaceutical Sci.* **64**(12), 1987-1991.

TSUJI, H., SASAKI, H., GOTOH, Y., ISHIKAWA, J. (2002). "Neuron attachment properties of carbon negative-ion implanted bioabsorbable polymer of poly-lactic acid ." *Nuclear Instruments and Methods in Physics Research, Section B.* **191**, 815-819.

TSUJI, H., SOMMANI, T., MUTO, T., UTAGAWA, Y., SASAKI, H., SATO, Y., GOTOH, Y., ISHIKAWA, J. (2005). "Immobilization of extracellular matrix on polymeric materials by carbon-negative-ion implantation ."*Nuclear Instruments and Methods in Physics Research, Section B.* **237**, 459-464.

UHRICH, K.E., CANNIZZARO, S.M., LANGER, R.S., Shakesheff, K.M. (1999). "Polymeric systems for controlled drug release." *Chemical Rev.* **99**: 3181-3198.

UTRACKI, L.A. (1989). Polymer Alloys and Blends. Hanser Publishers, New York, 180.

VERHOOGET, H., VAN DAM, J., POSTHUMA DE BOER, A. (1994). "Morphology-processing relationship in interpenetrating polymer blends." American

Chemical Society. Washington.

WAGENAAR, B.W., MULLER, B.W. (1994). "Piroxicam release from spray-dried biodegradable microspheres." *Biomaterials.* **15**(1), 49-54.

WAKE, M.C., GUPTA, P.K., MIKOS, A.G. (1996). "Fabrication of pliable biodegradable polymer foams to engineer soft tissues." *Cell Transplant.* **5**, 465-473.

WANG, L.W., VENKATRAMAN, S., KLEINER, L. (2004). "Drug release from injectable depots: Two different in vitro mechanisms." *J. Controlled Release.* **99**, 207-216.

WENDORF, J.R., RADKE, C.J., BLANCH, H.W. (2004). "Reduced protein adsorption at solid interfaces by sugar excipients." *Biotech. and Bioeng..* **87**(5), 565-573.

WERTZ, C.F., SANTORE M.M. (1999). "Adsorption and relaxation kinetics of albumin and fibrinogen on hydrophobic surfaces: single-species and competitive behavior." *Langmuir.* **15**(26), 8884-8894.

WERTZ, C.F., SANTORE, M.M. (2001). "Effects of surface hydroophobicity on adsorption and relaxation kinetics of albumin and: single-species and competitive behavior." *Langmuir.* **17**(10), 3006-3016.

WHANG, K., THOMAS, H., HEALY, K.E., NUBER, G. (1995). "Novel method to fabricate bioabsorbable scaffolds." *Polymer.* **36**, 837-842.

WILLEMSE, R.C. (1999). "Co-continuous morphologies in polymer blends: Stability." *Polymer.* **40**(8), 2175-2178.

WILLIS, J.M., FAVIS, B.D., LUNT, J. (1990). "Reactive processing of polystyrene-co-maleic anhydride/elastomer blends: processing-morphology-property relationships." *Polym. Eng. Sci.* **30**, 1073-1084.

WINZENBURG, G. et al. (2004). "Biodegradable polymers and their potential use in parental veterinary drug delivery systems." *Adv. Drug Deliv. Rev.* **56**, 1453-1466.

XIE, B., PARKHILL, R.L., WARREN, W.L., SMAY, J.E. (2006). "Direct writing of three-dimensional polymer scaffolds using colloidal gels." *Adv. Func. Mat.* **16**, 1685-1693.

YANG, J., SHI, G., BEI, J., WANG, S., YAO, Y., SHANG, Q., YANG, G., WANG, W. (2002). "Fabrication and surface modification of macroporous poly(L-lactic acid) and poly(L-lactic-co-glycolic acid) (70/30) cell scaffolds for human skin fibroblast cell culture." *J. Biomed. Mat. Res.* **62**(3), 438-446.

YANG, J., WAN, Y., YANG, J., BEI, J., WANG, S. (2003). "Plasma-treated, collagen-anchored polylactone: Its cell affinity evaluation under shear or shear-free conditions." *J. Biomed. Mat. Res.* **67**(4), 1139-1147.

YANG, K., HAN, C.D. (1996). "Effects of shear flow and annealing on the morphology of rapidly precipitatedimmiscible blends of polystyrene and polyisoprene." *Polymer.* **37**, 5795-5805.

YANG, Y., PORTE, M., MARNEY, P., HAJ, A.E., AMEDEE, J., BAQUEY, C. (2003). "Covalent bonding of collagen on poly(L-lactic acid) by gamma irradiation." *Nuclear Instruments and Methods in Physics Research Section B.* **207**, 165-174.

YANNAS, I.V., BURKE, J.F., GORDON, P.L., HUANG, C., RUBENSTEIN, R.H. (1980). "Design of an artificial skin. Part II. Control of chemical composition." *Biomaterials*. **14**, 107-131.

YOLLES, S., SARTORI, M.F. (1980). Degradable polymers for sustained release. Oxford University Press. New York, US.

YOON, B.J., LENHOFF, A.M. (1992). "Computation of the electrostatic interaction energy between a protein and a charged surface." *J.Phys.Chem.* **96**(7), 3130-3134.

YOON, J.J., SONG, S.H., LEE, D.S., PARK, T.G. (2004). "Immobilization of cell adhesive RGD peptide onto the surface of highly porous biodegradable polymer scaffolds fabricated by a gas foaming/salt leaching method." *Biomaterials*. **25**, 5613-5620.

YOSHIMOTO, H., SHIN, Y.M., TERAI, H. VACANTI, J.P. (2003). "A biodegradable nanofiber scaffold by electronspinning and its potential for bone tissue engineering." *Biomaterials*. **24**, 2077-2082.

YUAN, Z., FAVIS, B.D. (2004). "Macroporous poly(L-lactide) of controlled pore size derived from the annealing of co-continuous polystyrene/poly (L-lactide) blends." *Biomaterials*. **25**, 2161-2170.

VOZZI, G., FLAIM, C.J., BAINCHI, F., AHLUWALIA, A., BHATIA, S. (2002). "Microfabricated PLGA scaffolds: a comparative study for application to tissue engineering." *Materials and Engineering, C, Biomimetic Materials, Sensors and Systems*. **20**, 43-47.

ZACHARIA, N.S., DELONGCHAMP, D.M., MEDESTINO, M., HAMMOND, P.T. (2007). "Controlling diffusion and exchange in layer-by-layer assemblies." *Macromolecules*. **40**, 1598-1603.

ZHU, H., JI, J., SHEN, J. (2003). "Surface Engineering of Poly(DL-lactic acid) by Entrapment of Biomacromolecules." *Macromol. Rapid Commun*. **23**, 819.

ZHU, H., JI, J., TAN, Q., BARBOSA, M.A., SHEN, J. (2003). "Surface Engineering of Poly(DL-lactide) via Electrostatic Self-Assembly of Extracellular Matrix-like Molecules." *Biomacromolecules*. **4**(2), 378-386.

ZHU, H., JI, J., SHEN, J. (2004). "Biomacromolecules electrostatic self-assembly on 3-dimensional tissue engineering scaffold." *Biomacromolecules*. **5**, 1933-1939.

ZHU, Y., GAO, C., HE, T., LIU, X., SHEN, J. (2003). "Layer-by-layer assembly to modify poly(L-lactic acid) surface toward improving its cytocompatibility to human endothelial cells." *Biomacromolecures*. **4**, 446-452.

ZIEN, I., HUTMACHER, D.W., TAN, K.C., TEOH, S.H. (2002). "Fused deposition modeling of novel scaffold architectures for tissue engineering applications." *Biomaterials*. **23**(4), 1169-1185.

ZOUNGRANA, T., HINDENEGG, G.H., NORDE, W. (1998). "Structure, stability and activity of adsorbed enzymes." *J. Colloid and Interface Sci*. **190**(2), 437-447.

APPENDIX A

LOADING BSA AND POLYELECTROLYTES INTO POROUS DEVICE

Loading Protocol

- Wash, clean and dry the test tube
- Weigh and record the mass of the sample
- Prepare the solution[1]
- Fill the test tube with solution till half high
- Place the sample into the sample holder
- Immerse the sample holder into the solution in the test tube
- Place the test tube into the loading device
- Apply the vacuum for 30 minutes
- Gradually release the vacuum and keep the system in atmosphere for 2 min
- Stir the sample together with the test tube
- Apply the pressure (80 atm) for 15 min
- Gradually release the vacuum and keep the system in atmosphere for 2 min
- Stir the sample together with the test tube
- Apply the pressure (80 atm) for 15 min
- Gradually release the vacuum and keep the system in atmosphere for 2 min
- Stir the sample together with the test tube

- Apply the vacuum for 30 minutes
- Gradually release the vacuum and keep the system in atmosphere for 2 min
- Stir the sample together with the test tube
- Apply the pressure (80 atm) for 15 min
- Gradually release the vacuum and keep the system in atmosphere for 2 min
- Stir the sample together with the test tube
- Apply the pressure (80 atm) for 15 min
- Gradually release the vacuum and keep the system in atmosphere for 2 min
- Stir the sample together with the test tube
- Apply the vacuum for 60 minutes
- Gradually release the vacuum and keep the system in atmosphere for 2 min
- Stir the sample together with the test tube
- Apply the pressure (80 atm) for 15 min
- Gradually release the vacuum and keep the system in atmosphere for 2 min
- Stir the sample together with the test tube
- Apply the vacuum for 30 minutes
- Gradually release the vacuum
- Take the sample out from the sample holder
- Rinse the sample surface with deionized water
- Dry the sample under vacuum at 37°C till constant weight[2]
- Weigh and record the mass of the sample

- Calculate the mass increase

Preparation of BSA solution and polyelectrolyte solutions are discussed in detail in Chapter 3. Experimental Methodology.

In the case of loading polyelectrolytes, the sample is washed by deionized water with agitation for 4 hours before drying. Details are discussed in Chapter 3. Experimental Methodology.

APPENDEX B

SAMPLE SERIES

In this study, there are 9 different samples prepared for in vitro BSA release test in total, with different numbers of polyelectrolyte (PE) layers and various open surface area. They are listed as follows:

Table B.1 Sample series

Closed-cell / LbL	All Open	End Open	Corner Open
No PE	L0	L0E	L0C
3 Layers of PE	L3	L3E	L3C
5 Layers of PE	L5	L5E	L5C

L0: Samples with no PE layers and 100% open surface area, loaded with BSA

L0E: Samples with no PE layers and 12% open surface area, loaded with BSA

L0C: Samples with no PE layers and 2% open surface area, loaded with BSA

L3: Samples with 3 PE layers and 100% open surface area, loaded with BSA

L3E: Samples with 3 PE layers and 12% open surface area, loaded with BSA

L3C: Samples with 3 PE layers and 2% open surface area, loaded with BSA

L5: Samples with 5 PE layers and 100% open surface area, loaded with BSA

L5E: Samples with 5 PE layers and 12% open surface area, loaded with BSA

L5C: Samples with 5 PE layers and 2% open surface area, loaded with BSA

APPENDEX C

EXPLANATION OF BURST RELEASE

Burst release of BSA was observed in all the *in vitro* drug tests we carried out. The explanation of this effect can help to understand its formation and find the way to control it. The reason of the burst release of BSA could be as follows:

(1) Some BSA loosely trapped or not attached onto the PLA surface in the pores could be easily liberated and release out at the beginning of the test;

(2) A small amount of BSA, which adsorbed on the outer surface of PLA could not be avoided even by surface washing after BSA loading, easily desorbed from the outer surface at the beginning of the release test;

(3) BSA is hydrophilic and highly soluble in water, and the concentration of BSA in release medium is zero at the very early stage of the release test, the high concentration gradient between BSA in porous PLA and in release medium would promote the fast release of BSA;

(4) Hydrophobicity of PLA was another driving force for the fast release of BSA from the porous polymer devices, especially for the unmodified porous PLA substrate.